# Orthogonal Frequency Division Multiplexing Modelling

*by*

**Noah Kudakwashe Katsiru**

MSc Materials Physics / BSc Hons (Telecommunications) /

Submitted to the University of Cape Town in partial fulfilment of the requirements for the degree

**Master of Engineering in Telecommunications**

Supervisor:

Dr Simon Winberg

Department of Electrical Engineering

Faculty of Engineering and the Built Environment

**UNIVERSITY OF CAPE TOWN**




10 August 2021

# Declaration

I declare that this dissertation is my own, unaided work. I know the meaning of plagiarism and declare that all the work in the document, save for that which is properly acknowledged, is my own. This thesis/dissertation has been submitted to the Turnitin module (or equivalent similarity and originality checking software) and I confirm that my supervisor has seen my report and any concerns revealed by such have been resolved with my supervisor. It is being submitted for the degree of Master of Engineering in Telecommunications in the University of Cape Town. It has not been submitted before for any degree or examination in any other university.

Signature of Author: . . Signed by candidate

Cape Town

Date……10 August 2021……..

# Dedication

To my loving and caring wife Cathrine for her enthusiastic and energetic willing help that was consistent.

# Abstract

This work is motivated by the need to understand the performance of Orthogonal Frequency Division Multiplexing (OFDM) and Filterbank Multicarrier (FBMC). Multicarrier techniques are widely being considered for the development of the telecommunication systems such as the Long Term Evolution (LTE) networks, 5th Generation (5G) and beyond. One of the modulation strategies for upcoming 5G mobile communication technologies is FBMC. When compared to OFDM, which is utilised in Fourth Generation (4G) mobile communications technology, it employs multicarrier techniques that are immune to fading produced by transmission of more than one route at a time and also resistant to intersymbol interference. OFDM is one of the popular and highly recommended modulation schemes for LTE applications. OFDM is used for communications and is found in modern digital communication systems (e.g. WiFi, 4G, etc.). OFDM transmits streams of data in many orthogonal sub-carrier frequencies at varying data rates. These carriers do not interfere with each other and thus mitigate inter-symbol interference (ISI) and inter-carrier-interference (ICI). The simulation of an OFDM modulation technique, as well as the performance of OFDM in contrast to an FBMC modulation scheme in terms of delivering the same quantities of data, will be investigated using an ideal communication channel and replicated in a multipath fading channel. Using OFDM modulation techniques, a multipath channel was investigated for realistic simulations. In MATLAB, a picture was used as the input signal to identify the OFDM modulation method with the lowest bit error rate (BER). Quadrature amplitude modulation (QAM) was examined using 16QAM, 32QAM and 64QAM, Binary phase shift keying (BPSK), eight phase shift keying (8PSK), quadrature phase shift keying (QPSK), 16QAM, 32QAM and 64QAM OFDM modulation techniques were used. Channel noise is modelled by adding a white Gaussian noise (AWGN). The channel noise variance decreases with an increase in signal to noise ratio (SNR). 10dB SNR and 20dB SNR inputs were used in the simulations to obtain the BER of the recovered image. QPSK modulation scheme in a multipath fading system produced bit error rates which are higher than BER produced in BPSK modulation scheme. 8PSK modulation scheme produced a higher BER compared to BER of BPSK modulation scheme at the same input SNR. As the modulation order increased the BER increased. 64QAM has the highest BER. Frequency and Phase offsets resulted in symbol error

rates increasing as the channel impairments increased in FBMC. The spectral efficiency of OFDM is higher than FBMC spectral efficiency at low burst durations. High burst duration results in FBMC spectral efficiency getting higher than OFDM spectral efficiency. Mild impairments rarely caused symbol recovery errors, but the harsh impairments caused multiple symbol errors. To reduce and eliminate the effects of multipath fading, the least squares channel estimation method is used.

# Acknowledgements

Firstly, I would like to thank God for giving me the strength and good health to complete my dissertation written during the trying times of COVID 19, without Him I would not have been able to complete my dissertation, and without Him l would not have made it through my master's degree. I convey my sincere gratitude to my supervisor Dr. Simon. Winberg, whose guidance, patience, insight and knowledge into the subject matter steered me throughout. My biggest thanks, to my wonderful, caring and loving parents Mrs Letwin Muriva-Makombe and Dr. Shadreck. Muriva-Makombe, Mrs Esther Ruredzo and Mr Fredrick John Katsiru for the support and encouragement, which kept me going with late night calls of hope because of the distance. Mr Phinias Muriva Makombe and Advocate Melissa Muriva Makombe for their unending support.

# Nomenclature

| | |
|---|---|
| 4G | Fourth Generation |
| 5G | Fifth Generation |
| BPSK | Binary Phase Shift Keying |
| 8PSK | Eight Phase Shift Keying |
| CDMA | Code Division Multiple Access |
| CMT | Cosine Modulated Multitone |
| CP | Cyclic Prefix |
| C-RAN | Cloud Radio Access Network |
| DAB | Digital Audio Broadcasting |
| DSB-SC | Double Side band Suppressed Carrier |
| DSP | Digital Signal Processing |
| dTTb | Digital Television Terrestrial Broadcasting |
| FBMC | Frequency Band Multi Carrier |
| FFT | Fast Fourier Transform |
| FMT | Filtered Multitone |

| | |
|---|---|
| GFDM | Generalized Frequency Division Multiplexing |
| IFFT | Inverse Fast Fourier Transform |
| LTE | Long Term Evolution |
| MIMO | Multiple Input Multiple Output |
| OFDM | Orthogonal Frequency Division Multiplexing |
| PAM | Pulse Amplitude Modulation |
| PAPR | Peak to Average Power Ratio |
| 16QAM | 16 Quadrature Amplitude Modulation |
| 32QAM | 32 Quadrature Amplitude Modulation |
| 64QAM | 64 Quadrature Amplitude Modulation |
| QPSK | Quadrature Phase Shift Keying |
| SNR | Signal to Noise Ratio |
| SMT | Staggered Multitone |
| TDMA | Time Division Multiple Access |
| UFMC | Universal Frequency Multi Carrier |
| VSB | Vestigial Sideband |

# Contents

# List of Figures

# List of Tables

# Chapter 1

# Introduction

The motivation for this work is to have an understanding of the differences in the performance of Orthogonal Frequency Division Multiplexing (OFDM) and Filter Bank Multicarrier systems (FBMC). OFDM is a single carrier modulation scheme whilst FBMC is a multicarrier modulation scheme. OFDM and FBMC methods are being explored extensively for the development of telecommunications systems as in long term evolution LTE to 5th Generation (5G) networks and beyond. A system model for OFDM is created in this work, based upon the simulation in MATLAB performed with BER calculations for digital modulations BPSK, QPSK, 8QAM, 16QAM, 32QAM and 64QAM. Channel noise is modelled by adding a white Gaussian noise (AWGN) and an AWGN multipath fading channel noise. The channel noise variance decreases with an increase in signal to noise ratio (SNR). In MATLAB, a picture was used as the input signal to identify the OFDM modulation scheme with the lowest bit error rate (BER) per input SNR For 10dB and 20dB input SNR, and the OFDM signal was sent through the channel. The received signal was demodulated for each SNR level, and the obtained data were compared to the original information to evaluate the performance. The results of the simulation present BER plots that are compared to SNR, which gives system performance. The OFDM signal was sent through the AWGN channel, and then the experiment was repeated in an AWGN multipath fading channel. FBMC simulations using modulation parameters for communications systems was conducted in experiments in an ideal communication system and repeated in multipath fading channels.

Energy per bit to noise power spectral density ratio (Eb/N0) is a normalised signal-to-noise ratio (SNR) metric, often known as the "SNR per bit" in digital communication or data transfer. It is notably handy for evaluating the bit error rate (BER) performance of different digital modulation methods without accounting for bandwidth. A comparison of Eb/No and SNR is presented to show the effects of increase in SNR on the decrease in BER for theoretical calculations and experimental

differences. This is then evaluated against the experimental outcomes of this study for OFDM modulation systems in AWGN channels and AWGN multipath fading channels.

## 1.1 Problem Statement

In this study we investigate the effects of multipath and fading on OFDM and FBMC communication systems. A number of research questions needed to be answered in order to evaluate the performance of multicarrier modulation schemes, OFDM and FBMC.

i. How does a communication system having multipath fading behave?
ii. Does the spectral efficiency of OFDM modulation scheme differ from the spectral efficiency of FBMC modulation scheme?
iii. Does the phase of an oscillator in the transmitter have any effect if it is not known and if it is assumed incorrectly in the receiver [10]?
iv. What happens if the frequency at the transmitter oscillator is off from specifications [10]?

These questions were investigated through a number of experiments which required modifications to ideal communications systems simulations. The simulations brought about the fact that in a time varying channel gain, small violations often can be tolerated but as operational conditions increase or become severe, the receiver system must be adjusted to increase its robustness [10]. Performance of FBMC transmission system has many advantages and improvements to the performance of OFDM modulation scheme and these were laid out by the modelling in this research project. Improvements in BER and spectral efficiency were investigated in FBMC modulation scheme in comparison to OFDM modulation scheme [11].

## 1.2 Research objectives

This research identifies a series of research objectives emanating from the effects of multipath fading channels in a communication system. Assumptions that were made during the construction of a communication system focused on the degradations that were caused by the multipath fading

loss causing distortions in both OFDM and FBMC transceiver systems. The research objectives were:

1. Evaluation of BER of OFDM modulation schemes using BPSK, QPSK, 16QAM, 64QAM at 10dB and 20 dB input SNR values.
2. Use of least squares estimation method for channel estimation.
3. Spectral efficiency evaluation of OFDM modulation scheme in comparison with FBMC modulation scheme.

## 1.3 Motivation

Performance evaluation of the simulations of OFDM modulation scheme and FBMC modulation scheme is essential to determine the differences that exist between the two multicarrier modulation schemes such that a better performance between them can be chosen for future mobile communications [11]. Inter-symbol-interference (ISI) and inter-channel-interference (ICI) are removed in FBMC due to the use of vestigial sidebands. ISI and ICI are minimised due to the use of cyclic prefix in OFDM modulation scheme [7].

An ideal communication system has no noise and that condition is unlikely to hold in practice. The assumptions that there is no interference and noise from the communication system and also that the gain is assumed to be unity in an ideal system will result in the signal that leaves the transmitter being exactly the same signal which is received at the receiver. These assumptions are very limited and violated in practice. There is noise which is encountered in a real communication system and this is examined in this study on OFDM and FBMC performance evaluation. There is a possibility That the channel gain varies with time due to multipath fading [10]. These non-idealities that were encountered in real systems caused the channel gain to drop [4]. If the communication system cannot react to changes, it suffers from errors during the reconstruction of the message.

## 1.4 Terms of Reference

The research requirements and expected functionalities are given in this section to achieve the desirable deliverables as shown in Table 1. The research requirements were to address the research objectives whereby the functionalities of the requirements were the expected solutions.

### 1.4.1 The main requirements:

R1. Does the channel have noise? What happens if the channel has fading and multipath interference causing significant in-band distortions that tend to deteriorate BER performance?

R2. Performance evaluation of BER of OFDM modulation schemes using BPSK, QPSK, 16QAM, 64QAM at different SNR values.

R3. Reduction of spectral efficiency.

R4. The use of least squares estimation method for channel estimation. What happens when the phase of an oscillator in the transmitter was not known or if it was assumed incorrectly in the receiver?

The first requirement was first considered for an ideal communication for OFDM and FBMC simulations. Simulations were then implemented in a multipath fading channel for OFDM whereby channel estimation was implemented using different input signal to noise ratios (SNR).The third requirement was then investigated whereby spectral efficiency of OFDM against FBMC was expected to vary over given time frames. In FBMC simulations, transmitter phase and frequency offset in a multipath fading channel were investigated addressing the fourth requirement.

### 1.4.2 The functionality needed to achieve these requirements:

These are the research functionalities answering and providing the solutions to the research requirements thereby addressing the research objectives.

These functionalities are subsequently addressed in Chapter 5, where the results of the simulations are discussed.

F1. Multipath slow fading channel requires channel estimation in the receiver for adequate performance, so the least squares estimation method was implemented [10].

F2. The BER of OFDM modulation schemes using BPSK, QPSK, 16QAM, 64QAM were examined using various SNR values [4, 10].

F3. Variations in spectral efficiency were achieved on OFDM against FBMC.

F4. Different phases were investigated in the simulations to asses the phases at the signal will not be recovered [10].

The first functionality was first considered for an ideal communication system for OFDM and FBMC simulations to obtain a solution for the first requirement, thereby addressing the multipath fading channel effects objective. The second functionality states the functionality of improved BER on using different input SNR values in a multipath fading channel in a communication system that had channel estimation methods implemented and also repeated in a system without channel estimation. The third functionality shows the significant changes in spectral efficiency that were achieved on OFDM against FBMC modulation schemes [10].

## 1.5 Project Scope

The goal of this research project was to obtain a performance evaluation of the OFDM modulation scheme in comparison with FBMC modulation scheme with a specific focus on cosine modulated multitone (CMT) synthesis and analysis filters for implementation in a communication system [8].

Table 1: Breakdown of the sub-tests that were performed in acceptance testing.

| **Test Number** | **Description** | **Functions Checked** | **Requirements Tested** |
|---|---|---|---|
| T1 | Performance analysis on OFDM and FBMC with an ideal channel | Least squares channel estimation<br>BER<br>SE | Least squares channel estimation<br>BER<br>SE |
| T2 | Performance analysis on OFDM and FBMC with a fading, multipath with AWGN channel | Least squares channel estimation<br>BER<br>SE | Least squares channel estimation<br>BER<br>SE |

The multicarrier CMT makes use of pulse amplitude modulation (PAM). The modulated symbols have vestigial sideband modulation, in which the subcarrier band was minimally spaced and maximally overlapped. Hence CMT, with the use of PAM, has better spectral efficiency than other FBMC schemes [13].

## 1.6 Project Limitations

FBMC was limited to cosine modulated multitone modulation scheme since CMT makes use of pulse amplitude modulation technique. Other frequency band multicarrier modulation techniques such as Staggered Multitone (SMT) and Filtered Multitone (FMT) were not examined in this simulation study because they are not based on pulse amplitude modulation and also because they are complex which results in high power consumption in the transceiver leading to low energy efficiency. OFDM was limited to digital modulation schemes using BPSK, QPSK, 16QAM, 64QAM at input SNR values of 0dB, 10dB, and 20dB. Spectral efficiency of FBMC and OFDM was limited to a range of 30 seconds. The number of cyclic prefix extensions and lengths of filers

used were limited to be equal in the simulations for OFDM and FBMC to vary over the range of bursts.

## 1.7 Document Outline

This section brings out the structure that was followed for this dissertation. A brief summary of each of the chapters is given below.

Chapter 1 gives the background behind OFDM and FBMC modulation techniques. The section disscused the research objectives which were to be achieved in this study. A motivational discussion behind what led to the drive for research in this area was presented together with the problem statements that were adrressed. A research scope was then defined for this study giving mention on the areas of focus for research. Research limitaions were stated giving out the limitations to the research.

Chapter 2 provides a review of OFDM and FBMC modulation techniques current research work in the telecommunications field. Principles of OFDM modulation detailing the transmission signal structures and how cyclic prefix (CP) was added and removed and also how an OFDM signal attains non inter-symbol-interference and inter-channel interference to improve bandwidth spectral efficiency. A brief OFDM system used for modelling OFDM is presented giving out how subcarriers are distributed and how guard bands infuse in them. Timing recovery which involves the identification of CP and non-CP extensions on OFDM symbols was discussed and how it affects a communication system when there are offsets was also analysed. Carrier acquisition and tracking as delt with in current research studies was presented together with the effects of PAPR and how to eradicate high PAPR effects in order to increase OFDM system efficiency. FBMC in-depth review was presented dealing with the vestigial sideband modulation which was used in the CMT filters when implementing PAM.

In Chapter 3 we have a description of how the design methodology was done in the OFDM and FBMC modelling using MATLAB simulations. The research methodology was structured in such a way as to answer the research objectives and also answering the research questions stated in Chapter 1. OFDM modelling using different modulation schemes in this case 16QAM, BPSK, 8PSK, QPSK, 32QAM, 64QAM, were implemented in MATLAB. FBMC system using the PAM modulation scheme in CMT was also implemented in MATLAB. Spectral efficiency of OFDM against FBMC was simulated for 30s burst duration whilst considering the level of spectral efficiency achieved for OFDM against FBMC systems. Properties of shaping filters were discussed and how to achieve a Nyquist solution was analysed. Raised cosine filters were briefly discussed and how finite impulse windowing deisgn was achieved. FBMC and OFDM eperiments for ideal channels and multipath fading channels and the experiments for spectral efficiency of OFDM against FBMC were done.

Chapter 4 brings out the results of the simulations of OFDM and FBMC. The results were shown for different input parameters of an ideal channel simulation and repeated for multipath fading channel simulations of OFDM and FBMC modulation techniques. Spectral efficiency of OFDM against FBMC for the burst duration of 30ms were shown depicting how OFDM and FBMC vary as the burst duration increases.

Chapter 5 presents the conclusions that were drawn from the outcomes of the research. In this chapter a re-look into the research objectives and research requirements given in Chapter 1 to what magnitude they had been achieved was addressed. Each objective results are laid out making it clear on how the results differ from the experiments conducted. The chapter states clearly the results obtained as having met the required objectives outlined for the research. Insights which were achieved through this study were presented. Lastly the future works which can be done from this research were proposed.

# Chapter 2

# Literature Review and Requirements

## 2.1 Introduction

Global interconnectivity has been achieved by wireless communications, but this has come with several challenges such as multipath fading that is associated with the wireless channels [2]. Sklar [3] states that due to Moore's law of electronics, there has been a rise of mobile devices recently due to the large increase in demand of voice and data communications. The long term evolution (LTE) technology brought in significant advancements in data rates, spectral efficiency, energy efficiency, latency and reliability. Orthogonal frequency division multiplexing modulation scheme that is being used for LTE, LTE Advanced and LTE Advanced Pro has proven to be reliable in providing high data rates of 1 Gbps, but not as high as fifth generation (5G) demands [4]. Use of cyclic prefixes (CP) to avoid unnecessary side lobes, has resulted in tremendous reduction in spectral efficiency in comparison to some theoretical existing performance evaluations of multicarrier modulation schemes [5]. OFDM has been a great telecommunications achievement for many years [6]. It has been discovered that no single waveform, of the known waveforms, can provide all the required advantages and their solutions which are much sought after for building future communication technologies [6, 7].

Introduction of the Digital Audio Broadcasting (DAB) which was based on OFDM [13], successful tests on OFDM for the Digital Television Terrestrial Broadcasting (dTTb) and the research on OFDM on HIPERLAN type II and Wireless ATM projects has put a major interest towards research on OFDM over the past years [14] . Since the 1960s, concepts of using frequency multiplexing and parallel data transmission was established [6]. After years of research and development, OFDM became widely implemented in very high speed digital communications. Advances in digital signal processing (DSP) led to the obstacles that are experienced by OFDM implementation being eradicated [11]. The use of fast Fourier transforms (FFT) algorithms eliminated arrays of the

sinusoidal signal generators and the requirement of coherent demodulation in the parallel data systems making the implementation of the OFDM system to be cost effective [5] .

Transmission in mobile communications is impaired by Doppler shift and delay. OFDM system performance is severely degraded due to the time variations that are caused by the increase in symbol duration. The increase of symbol duration will introduce Inter-Carrier-Interference (ICI) which causes loss of orthogonality among carriers. Channel variations on an OFDM symbol introduce ICI which leads to degradation of system performance. capacity-interference (ISI) is the due to the increase in symbol duration thereby affecting an adjacent symbol [7]. Therefore, for the performance of an OFDM system improvement, there is a need for mitigation of ICI and ISI.

Channel equalizer combats ISI, but it results in complexity of the receiver. Channel equalizer also introduces noise enhancements over the communication portion of the communication frequency band in which the channel gain is small. This noise enhancement results in what is achieved as a significant degradation to the communication link. ISI decreases as the symbol rate decreases [11, 15, 16]. In a mobile communication system, the relative mobility between receiver and transmitter causes Doppler shifts and fading. The subcarriers cannot be perfectly synchronised leading to random frequency errors in an OFDM system which distorts the orthogonality between the subcarriers leading to occurrence of inter-carrier interference [15]. In an OFDM system, orthogonality of the subchannels can be maintained making a complete separation of individual subchannels by fast Fourier transform at the receiver module when there appears no ISI and ICI introduced by distortions of the transmission channel. OFDM is robust against ISI due to the increase in the symbol duration. However, for mobile applications, channel variations during one OFDM symbol introduce ICI which degrades the performance. This gets more severe as mobile speed, carrier frequency or OFDM symbol duration increases.

OFDM makes it possible to achieve high data rates in mobile communications. The application principle of OFDM to the high data rate transmission in mobile communication has led to many

researches in this area and further investigations are helping to come up with a completely new paradigm shift in communications networks leading to the evolvement of the current 5G communications. Cellular radio systems that made use of pilot based correction mechanisms have been developed and these have provided vast improvements in the BER performance in a fading environment [16]. The introduction of OFDM in cellular mobile communications was largely driven by flexibility and equalization capabilities. With flexibility, the transceivers had access to subcarriers that were within the cell layer. Easy equalization is possible when OFDM symbols are much longer than the maximum delay spread [10, 17].

The benefit of OFDM is that in a wireless communication system, a receiver does not necessarily need to be constantly adapting an equalizer as would a single carrier system. OFDM communication system shows favourable properties such as high spectral efficiency, resistance to the channel fading, impulse interference immunity and a high capability to handle multipath fading, thus handling strong echoes [5]. Mobile communications channel suffers from multipath propagation in a time-variant channel, usually depending on Doppler shift [11]. Forward error-correcting mechanisms are employed in OFDM systems to improve performance. Appropriate coding schemes applied to an OFDM system provides a diversity effect due to exploitation of the multipath nature of the channel [18]. Another limitation of an OFDM system is that it is sensitive to the frequency errors that are caused by the frequency differences between local oscillators in receivers and transmitters [10]. OFDM concept involves spreading data to be transmitted over a number of carriers whereby each carrier is modulated at a low rate. Appropriate choice of frequency spacing between carriers ensures orthogonality between them. Making contrast to Frequency Division Multiplexing (FDM), spectral overlapping amongst OFDM subcarriers is possible since there exists orthogonality which ensures subcarrier separation of the receiver module and by so doing thereby providing a better spectral efficiency eliminating the use of steep band-pass filter [15, 17].

OFDM modulation system offers an advantage over single-carrier systems in that it spreads out frequency selective fading over a number of symbols [6]. This randomises the burst errors that are caused by impulse interference or fading such that instead of having several adjacent symbols completely destroyed, many of the symbols are slightly distorted allowing successful reconstruction to the majority of symbols in cases when there is no forward error correction. Due to the division of the entire bandwidth of the signal into narrow sub-bands, there is a flat frequency response over the individual sub-bands because sub-bands are smaller than the coherence bandwidth of the channel. Equalisation is much simpler in such a case in than in a single carrier system, if there is differential encoding implemented, the equalization may be avoided completely [19].

The spectrum in OFDM signals is not band limited which allows linear distortions known as multipath propagation causing each of the sub-channels to spread out their energy into the adjacent channels causing ISI. A way of preventing ISI is the creation of a cyclically extended guard interval in which each symbol is preceded by an extension of an OFDM signal itself. When the guard extension is slightly longer than multipath delay or channel impulse response, ISI is eliminated in the system [4, 6]. OFDM system provides a way to transmit information in a frequency selective channel by using frequency diversity and time diversity[20]. Fading itself is not suppressed. Individual sub-channels can be affected by fading depending on where they are positioned in the frequency domain. Channel coding is required to protect further the transmitted information. Time and frequency interleaving combined with coded OFDM are considered most effective means for a channel with frequency selective fading [15].

## 2.2 Important Terminology

Important terminology that were used in this research for simulations of OFDM and FBMC in an ideal channel and repeated in a multipath fading channel are defined in this section. A multipath fading channel implementation was done to achieve a realistic communications transmission system characteristics.

**Spectral Efficiency (SE).**

In this document, 'SE' refers to spectral efficiency of a signal [1].

**Cosine Modulated Multitone (CMT).**

'CMT' refers to an FBMC scheme which implements PAM scheme [22].

## 2.3 Background

The way in which wireless communications have evolved has led to the provision of multiple services and a broad variety of applications to the user. A number of requirements which have been established as basic requirements for 5G technology are: end-to-end latency of 1 millisecond; 1-10 Gbps connections; 99.999% availability; high bandwidth per unit area; 100% coverage; low network energy usage; and ability to support a large number of connected devices [4]. These requirements cover a broad range of requirements and many researchers believe that they cannot be satisfied through a single modulation scheme [7]. This research proposes FBMC modulation scheme to achieve these requirements and a performance evaluation is done in MATLAB and validated with a comparison to OFDM modulation scheme. The challenges that are faced in wireless communications are magnified as a result of the fact that they are based on radio spectrum which is a scarce and finite resource [4]. Access protocols and standardization of waveforms, including the use of network frequency spectrum were the mandatory steps in order to establish and facilitate the development of reliable and efficient mobile radio communication systems. The journey to 5G communications has initiated drastic changes in orientation and objectives of wireless networks evolution [4, 7, 11, 23]. 5G will be an incorporation of a number of emerging applications and services some of which will deviate from development steps that are conventional in cellular networking [4, 24]. 5G will be a transition to the machine-type communications. Vehicular communications and device-to-device communications will allow connectivity to millions of artificial intelligent machines making it possible for monitoring and remote control as well as the unmanned coordination and operation. Tactile Internet will also be enhanced as a technology which is 5G-enabled. Extremely low-latency communications delivers a number of

services ensuring real-time control cyber systems and remote sensing for example unmanned surface/aerial/ground vehicles, automated machinery, robots and other applications [7].

OFDM and OFDM-based transmission technologies have taken a leading role and dominated the current wireless network communications standards which includes Long Term Evolution (LTE) and LTE Advanced [5]. OFDM took dominance because of specific advantages which include: robustness to frequency; selective fading due to division of data symbols that are in parallel narrowband channels; overlapping transmission for parallel channels that are orthogonal leading to an efficient use of the spectrum; low-complexity implementation of the transmission system making use of FFT; non-complex channel equalization in comparison with the single carrier transmission; high resistance to impulse noise; high ability to make integration with adaptive coding and modulation techniques in efforts to exploit and making full use of a radio channel [9, 25-28]. These reasons have given a boost and rise to the evolution of wireless communications. As the demands of the requirements became high, the OFDM disadvantages became a stumbling block in the route to the new 5G technology. OFDM technology exhibits a high PAPR which means that it is not recommended for use in low-cost mobile user equipment (UE) in which poor power amplifier performance together with low digital-to-analogue converter resolution leads to OFDM signal distortion [9, 28].

Higher data rates will be achieved by 5G mobile communications to satisfy the ever-increasing demand for higher throughput for mobile user devices and their emerging applications and to make efficient use of the available spectrum and the limited resources of these radio systems (e.g. battery power). For maximum utilization of spectrum resources, 5G makes use of composite network system structures that differentiate from standard conventional cellular networks [1]. Massive multiple input multiple output (MIMO), Cloud Radio Access Network (C-RAN) system, coordinated multipoint and full-duplex are part of the major technology concepts that have been adopted for the design of the 5G communications systems [7]. This, therefore, brings out the fact that 5G communications aim for a design system of a radio network that is tolerant and robust to interference, maximises frequency spectral efficiency, able to synchronise accurately over a large

diversity of radio and network conditions and be able to harmoniously coexist with mobile users that have varying requirements and objectives [6].

Generalized Frequency Division Multiplexing (GFDM) is a modulation method which yields high spectral efficiency and energy efficiency [6]. It is not orthogonal on each subcarrier but subcarriers can interleave with each other. There is good spectral efficiency and good outer band emission. GFDM can support MIMO and has good flexibility [29]. GFDM does not have control of inbound emissions which means that the spectral efficiency is not as improved from that of FBMC multicarrier techniques.

MIMO systems are grouped into Network MIMO and Massive MIMO. Network MIMO also called co-operative MIMO is whereby a user is serviced by all Base Stations (BS) within its range of operation. In non-cooperative MIMO systems, BS has antennas which are simultaneously serving a small number of users [30, 31]. Pilot contamination is a problem in time division duplexing (TDD) non-cooperative MIMO systems [16]. CMT which is a form of frequency band multicarrier corrects this pilot contamination problem thereby increasing the spectral efficiency of the system [32]. In massive MIMO network systems, CMT has a blind equalization capability which is used for pilot decontamination. Channel estimation errors which are caused by these contaminated pilots have been analysed to check on how blind equalization of CMT can be used to remove them [10].

Massive MIMO network system is a multiple user technology that has the same concepts as those of spread-spectrum systems. The massive MIMO network system has a BS made up of multiple antenna arrays that simultaneously serve tens of mobile user terminals (UT) with each UT having a single antenna [22, 30, 31, 33]. MIMO makes use of the wireless channel to provide seamless communication between the transmitter and receiver that are reliable and having high data rates due to the help of multiple service antennas. Massive MIMO is an advancement from MIMO and it exploits high speed electronics to enhance data rates [33]. Multiple antennas focus the reception

and transmission of signals into very small regions leading to high throughput and turning away of antennas from undesired direction also results in low latency levels due to beamforming [30]. In massive MIMO, the linear combinations of various signal components from independent channels from each other smoothens the channel distortion thereby improving on channel bandwidth. This property in massive MIMO is as a result of CMT filter banks and it is called self-equalization [32].

Out-of-band leakage signal as depicted in Figure 2.1 below shows a result of channel estimation errors and ISI [11].

The number of subcarriers is reduced in a CMT network system. This leads to an improvement in system latency and a reduction in system complexity thereby improving energy efficiency of the system. This is achieved by use of synthesis filter banks in CMT transmitter together with corresponding analysis filter banks in the receiver section of the communication system leading to high bandwidth efficiency as a result of linear combinations of signal components which equalize the channel gain on each subcarrier band [7].

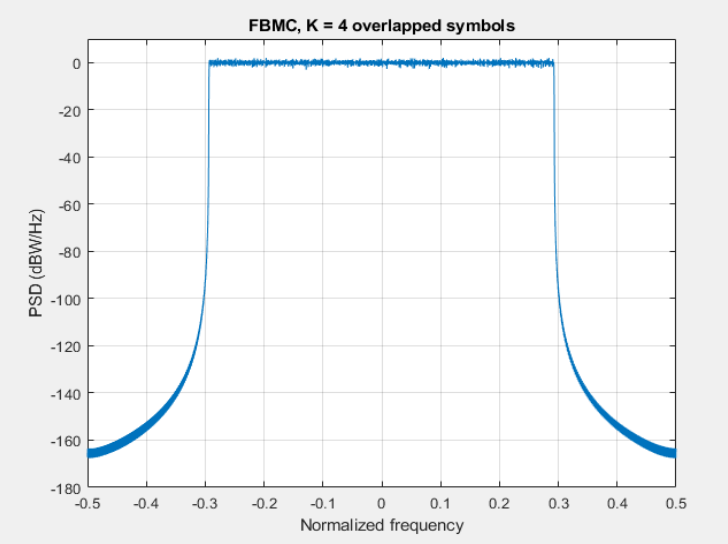


Figure 2.1: Power spectral density of CMT signal [17].

Capacity is dependent on bandwidth as shown by [6],

$$C = B \log (1 + SNR) \tag{2.1}$$

Where C (bps) is the achievable capacity, and B (Hz) is bandwidth and $SNR$ is the signal to noise ratio [5]. Sensitivity in CMT to carrier frequency offset will be reduced by increasing subcarrier spacing [7]. Spectral or carrier aggregation using non-contiguous frequency bandwidths of the available spectrum for transmission becomes insignificant because each subcarrier will be confined to a specific range assigned to it and having negligible ISI with other frequency bands. This is not available in OFDM systems [7].

Difference of OFDM and FBMC lies in the choice of filter $\rho_\tau$ which is commonly called the prototype filter. Each subcarrier needs to be filtered by this prototype filter in OFDM [7]. OFDM is a sum of windowed modulated exponential functions and it does not have maximum bandwidth efficiency.

$$\eta = \frac{T_{sym}}{T} \tag{2.2}$$

The symbol $\eta$ is bandwidth efficiency and $T_{sym}$ represents the transmission rate and $T$ is the bandwidth of a symbol. In wireless network systems, signals can reach an intended receiver using multiple paths and a delay exists. This combined effect causes multipath fading [6].

$$h(t) = \sum_{n=1}^{N} a_n \delta(t - \tau_n) \tag{2.3}$$

where $h(t)$ represents the equivalent multipath model impulse response, $N$ represents number of received communication signal impulses which are equivalent to the number of multiple paths. $\tau_n$ represents the time delay of an $n^{th}$ electromagnetic signal, and $a_n$ is the complex magnitude and phase of the received electromagnetic signal.

## 2.4 Signal to noise ratio

The signal-to-noise ratio (SNR) is a scientific and engineering statistic that compares the strength of the desired signal to the strength of background noise. The SNR is frequently given in decibels

and is defined as the ratio of signal power to noise power. A signal-to-noise ratio larger than 1:1 (more than 0 dB) shows that there is more signal than noise.

## 2.5 Multipath

Cyclic prefix (CP) makes a transformation of classical channel convolution onto a cyclic convolution that makes way for easy demodulation just after FFT. To avoid ICI, a portion of last part of the symbol is copied to the front of a symbol [5]. Multipath propagation causes the duration of a symbol to be extended causing interference with the next symbol which results in crosstalk. In OFDM system guard bands avoid ICI [34]. Signals with a bandwidth that is higher than its coherence bandwidth face a variable attenuation of the signal at different frequencies as shown below in Figure 2.2 causing a distortion on the signal in time and frequency domain giving rise to what is known as frequency selective fading which is undesirable in a communications system [10]. Channel equalization techniques are used in the receiver to reduce this effect. To avoid ICI, guard band frequencies are put between channels. Multipath fading, frequency selective fading, delay spread and ICI gave rise to multiple access techniques [4]. Complex hardware and high power consumption would have left OFDM to just a theoretical idea and difficult to implement, it was made possible by adjustments and manipulations in digital signal processing. Inverse fast Fourier transforms (iFFT) solves this problem by converting the parallel frequency signals into signal samples of composite time domain that are much easier to formulate at the transmitter side [10].

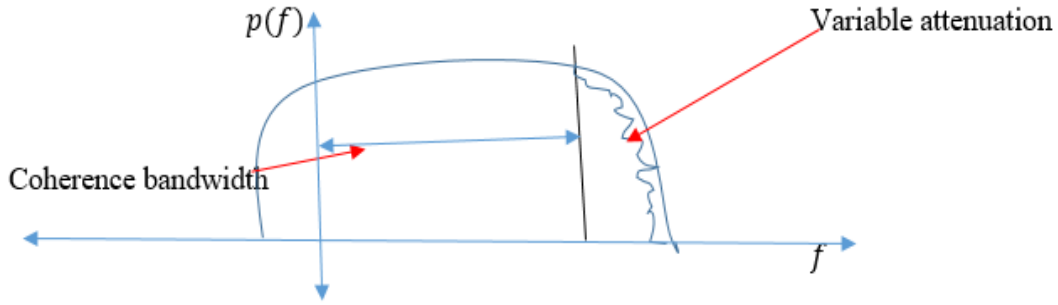


Figure 2.2: Variable attenuation [7].

The time domain signal is transmitted at radio frequencies. As the signals are sampled by iFFT, they must be taken above the Nyquist frequency for efficient reproduction of the signal in receiver module [10].

IFFT summation of multiple parallel subcarriers results in high PAPR that results in high power being consumed during signal generation [28]. Portable handheld devices have a limited power capability because of battery life. This results in OFDM system being unfavorable for uplink transmission in handheld devices [9]. Overcoming this LTE makes use of SC-FDMA in uplink and OFDM in downlink. SC-FDMA is a single carrier that has short symbol duration in comparison to OFDM. This is possible due to carrier aggregation. SC-FDMA introduces an N-point FFT after the serial to parallel shifter in the receiver of OFDM system. FFT converts the parallel sequence of symbols to different frequency points. SC-FDMA makes a reduction in PAPR by reducing subcarriers used in uplink. There are also problems in single carrier transmission. Side effects are reduced by ensuring that the transmission bandwidth is not too high. This high PAPR is overcome by the implementation of FBMC at the transmitter [11].

## 2.6 Principles of OFDM

In the following OFDM system derivation, channel noise is ignored whose presence in a communication system results in the inaccuracy of the transmit symbol estimates. At the receiver, noisy estimates are obtained. It is also assumed that the receiver was made aware of an exact carrier frequency in a signal that is received that is to say that the received OFDM symbols are free of carrier offset [35]. It was assumed that the channel had a finite duration $L + 1$ samples which matched the corresponding length of cyclic prefix equalling to *L.* The channel **h** was made known at the receiver side making it possible for perfect equalization. An assumption that CP position could be identified by the receiver was made. These are all ideal situations of a communication system receiver [8].

The transmitter module begins with generating a complex baseband signal vector x[$n$] by taking the iFFT of the multiplexed data symbol vector [5].

$$s[n]=[s_0[n]\ s_1[n]\ldots s_{N-1}[n]]^T \qquad (2.4)$$

It follows that,

$$\mathrm{x}[n] = \mathcal{F}^{-1}s[n] \tag{2.5}$$

Where $\mathcal{F}$ is the FFT matrix and thus $\mathcal{F}^{-1}$ is the iFFT matrix and the transpose of a matrix is denoted by **T** . Noting that,

$$\mathcal{F}^{-1} = \frac{1}{N}\begin{bmatrix} 1 & 1 & 1 & \cdots & 1 \\ 1 & e^{j\frac{2\pi}{N}\times 1} & e^{j\frac{2\pi}{N}\times 1} & \cdots & e^{j\frac{2(N-1)\pi}{N}\times 1} \\ 1 & e^{j\frac{2\pi}{N}\times 2} & e^{j\frac{2\pi}{N}\times 2} & \cdots & e^{j\frac{2(N-1)\pi}{N}\times 2} \\ \vdots & \vdots & \vdots & \ddots & \vdots \\ 1 & e^{j\frac{2\pi}{N}\times (N-1)} & e^{j\frac{2\pi}{N}\times (N-1)} & \dots & e^{j\frac{2(N-1)\pi}{N}\times (N-1)} \end{bmatrix} \tag{2.6}$$

It then follows that

$$\mathrm{x}[n] = \sum_{k=0}^{N-1} \mathrm{x}_k[n] \tag{2.7}$$

where

$$\mathrm{x}_k[n] = \frac{1}{N}s_k[n]f_k \quad \text{,for } k = 0,1,2,\dots,N-1 \text{ and}$$

$$\mathrm{f}_k = \begin{bmatrix} 1 \\ e^{j\frac{2\pi}{N}\times 1} \\ e^{j\frac{2\pi}{N}\times 2} \\ \vdots \\ e^{j\frac{2\pi}{N}\times (N-1)} \end{bmatrix} \tag{2.8}$$

Then $\mathrm{x}_k[n]$ shows that the $k$th symbol characterized by the symbol $s_k[n]$ modulates a complex carrier at the frequency $f_k = \frac{2Nk}{N}$ [36] . The scale factor $\frac{1}{N}$ emerges from the definition of the inverse Fast Fourier Transform and can be removed without causing any major disruptions on the outcomes from the transmitter section. $f_k$ are the modulator vectors, $\mathrm{x}[n]$ is the $n$th OFDM symbol. From the above equations it is noted that $s_0[n]$ does modulate any carrier with frequency $f_0 = 0$. Between the carriers is a frequency spacing $\frac{2\pi}{N}$. Since

$$e^{j\frac{2(N-k)}{N}} = e^{-j\frac{2\pi k}{N}} \tag{2.9}$$

The higher carrier frequencies can be counted, with $f_k > \pi$ , as the negative frequencies. With this in mind, an example would be

$$f_{N-k} = \frac{2(N-k)}{N} \tag{2.10}$$

May in an instance be replaced by

$$f_{-k} = -\frac{2\pi k}{N} \tag{2.11}$$

The iFFT operation is the modulation process in which the symbol $s_0[n]$ modulates carrier 0, the symbol $s_1[n]$ modulates carrier $\frac{2\pi}{N}$, the symbol $s_{N-1}[n]$ modulates carrier $-\frac{2\pi}{N}$, the symbol $s_2[n]$ modulates carrier $\frac{4\pi}{N}$, the symbol $s_{N-2}[n]$ modulates the carrier $-\frac{4\pi}{N}$, and so on [10, 21].

To fight the channel effect in OFDM, the following principles are put in place. The modulator vectors $f_k$ are orthogonal vectors, for $k = 0,1,2, \dots, N-1$ [36]. This implies that all the transmitted symbols $\mathrm{x}_k[n]$ are orthogonal with respect to each other. Transmit symbols $s_k[n]$ are obtained by pre-multiplying $f_k^H$ with $\mathrm{x}[n]$ ,

$$s_k[n] = f_k^H \mathrm{x}[n] \tag{2.12}$$

Where $f_k^H$ denotes the conjugate transpose of modulator vectors $f_k$. This produces same result as to applying FFT to $\mathrm{x}[n]$ and it is noted that application of FFT returns the once pre-iFFT data symbols [21]. After traversing through the channel, $\mathrm{x}[n]$ converts to

$$\mathrm{y}[n] = \mathrm{x}[n] \star \mathbf{h} \tag{2.13}$$

where **h** is the baseband impulse response of a communication channel and $\star$ denotes the linear convolution. The complex signal vector $\mathrm{x}[n]$ having a signal length of N and also assuming that the baseband impulse response has a length of $L + 1$, it then follows that $\mathrm{y}[n]$ has a length of

$L + N$. The signal sequence $x[n]$ is a result of concatenation of OFDM symbols x[$n$] as shown below in Figure 2.3.

The sequence y[$n$], the received signal sequence, is obtained from an overlap-and-add method that is shown above. This shows that concatenation of OFDM symbols x[$n$] leads to ISI amongst adjacent symbols. ISI occurs in overlapped intervals as shown in Figure 2.3 (b).

Demonstration of OFDM signal transmission with guard bands is depicted in Figure 2.4. The guard interval is consisted of either zero samples or of a copy of the last guard period $N_{cp}$ samples of each succeeding OFDM symbol, as shown in Figure 2.4 [15, 21]. To completely avoid ISI, a guard period, which is equivalent to

$$N_{cp} \geq L \tag{2.14}$$

samples of the signal $x[n]$ is inserted before and after each OFDM signal symbol as demonstrated by Figure 2.3a.

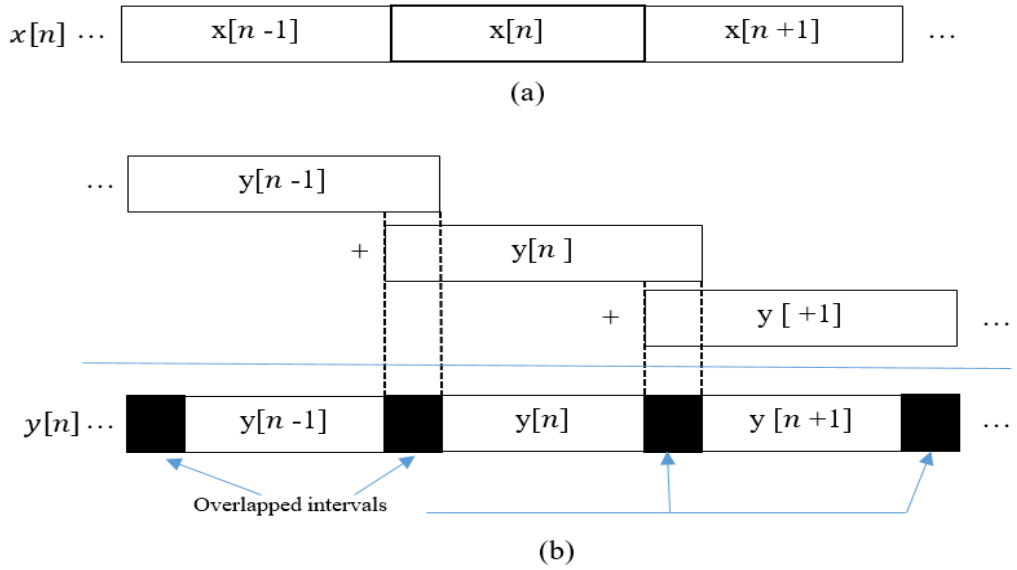


Figure 2.3: OFDM transmission without guard bands. (a) Transmitted signal x[n]. (b) Received signal y[n] [29].

Cyclic prefix use is beneficial in some aspects of communications, however CP has a major impact on the reduction of spectral efficiency [1]. There is high need of synchronisation accuracy in frequency and time domains in OFDM, errors can be extremely damaging in an OFDM signal since it leads to ICI [7].

In Figure 2.5, the copied portion of the symbol is called the cyclic prefix (CP) [15]. Cyclic prefix samples are used for guard intervals. The presence of these guard intervals in an OFDM signal results in removal of ISI amongst adjacent OFDM symbols. The contents of guard intervals are inserted before and after OFDM symbol by a copy of the $N_{cp}$ samples of succeeding OFDM symbol as depicted in Figure 2.4, this results in avoiding ISI.

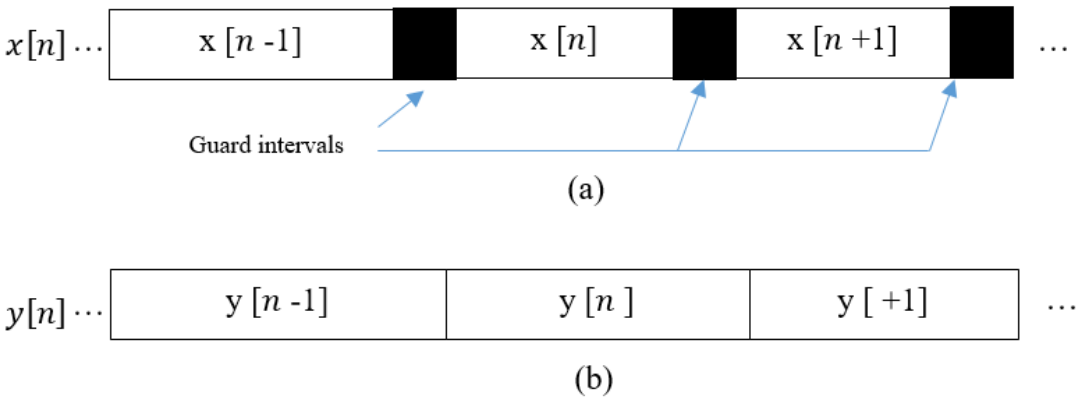


Figure 2.4: (a) Transmitted signal x[n] (b) received signal y[n] [29]

The transmitted and received signals are depicted in Figure 2.4 (a) and Figure 2.4(b) respectively.

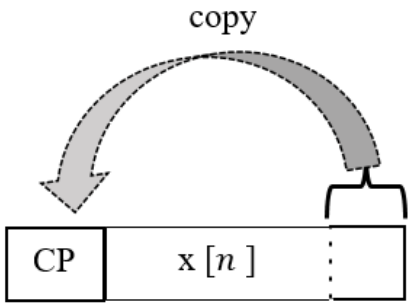


Figure 2.5: Cyclic prefix interval demonstration [25].

A notable advantage is that the use of CP restores orthogonality of the subcarrier channels by removal of ISI and thus allowing the recovery of transmitted symbols $s_k[n]$ by making use of the fast Fourier transform operation, at the receiver, and a single-tap equalizer per each subcarrier channel [10]. Considering the periodic signal

$$x_{k,p}[m] = \frac{1}{N} s_k[n] e^{j\frac{2\pi k}{N}m}, -\infty < m < \infty \tag{2.15}$$

And taking note of the fact that this is a cyclic prefix extension of the signal vector $\mathrm{x}_k[n]$. Subscript *p* denotes that the cyclic extension is a periodic sequence [15]. The cyclic extension is a pure tone with frequency

$$f_k = \frac{2\pi k}{N} \tag{2.16}$$

The CP is a complex-valued sine wave, and when it has been passed through a channel **c** where

$$\mathbf{c} = [c[0]\ c[1]\ \ldots\ c[L]]^T \tag{2.17}$$

It can only be scaled by a channel gain

$$C\left(e^{j\frac{2\pi k}{N}}\right) = \sum_{l=0}^{L} c[l]\, e^{-j\frac{2\pi k}{N}l} \tag{2.18}$$

Then channel output is

$$y_{k,p}[m] = \frac{1}{N} C\left(e^{j\frac{2\pi k}{N}}\right) s_k[n] e^{j\frac{2\pi k}{N}m} \tag{2.19}$$

Which is a product of the cyclic extension and the channel gain. If the input periodic signal $x_{k,p}[m]$ for $m < m_0$ is forced to zero, i.e., it starts from a considerably finite time $m = m_0$, then a steady state output which matches $y_{k,p}[m]$ of [21] will be attained at a stage after which a transition period that is equal to the duration of a channel impulse response. Passing a version of $x_k[n]$ that has cyclic prefixes through a channel **h** dropping all first L samples of the output results in the next N samples of the output being

$$\frac{1}{N} C\left(e^{j\frac{2\pi k}{N}}\right) s_k[n] e^{j\frac{2\pi k}{N} m}, \text{for } m = 0,1,2,\dots,N-1. \qquad (2.20)$$

At the receiver after dropping off the CP samples, a channel response to the input vector $\mathrm{x}_k[n]$ will be determined to be the output vector

$$\mathrm{y}_k[n] = C\left(e^{j\frac{2\pi k}{N}}\right) \mathrm{x}_k[n] \qquad (2.21)$$

The output vector $\mathrm{y}_k[n]$ is basically valid for $k = 0,1,2,\dots,N-1$ and also the channel is linear. It is noticed that in an OFDM cyclic prefixed system, the channel response to input signal $\mathrm{x}[n]$ is found to be [10, 15, 21]

$$\mathrm{y}_k[n] = C\left(e^{j\frac{2\pi k}{N}}\right) \mathrm{x}_k[n] \qquad (2.22)$$

Recalling the FFT operation $s_k[n]$, we obtain

$$\check{s}_k[n] = f_k^H \mathrm{y}[n]$$

$$= C\left(e^{j\frac{2\pi k}{N}}\right) \mathrm{x}_k[n], \text{ for } k=0,1,2,\dots,N-1 \qquad (2.23)$$

Where the $\check{s}_k[n]$ denotes the fast Fourier transform of $s_k[n]$ and $f_k^H$ denotes the conjugate transpose of $f_k$. The scaled replicas of transmitted signal symbols $s_k[n]$ are achieved by computing FFT of a received signal when the CP has been removed, viz., $\mathrm{y}[n]$. Rearranging $\check{s}_k[n]$, we obtain

$$s_k[n] = \frac{1}{C\left(e^{j\frac{2\pi k}{N}}\right)} f_k^H \mathrm{y}[n], \quad \text{for k} = 0,1,2,\dots,N-1 \ . \qquad (2.24)$$

Addition of a scaling factor $1/\, C\left(e^{j\frac{2\pi k}{N}}\right)$ to $s_k[n]$ is referred to as the single-tap equalizer [21].

### 2.6.1 Peak to Average Power Ratio

OFDM system has a number of properties which have made it a desirable modulation scheme for high speed transmission networks. However, a major difficulty to OFDM has been its high peak to average power ratio (PAPR) which lowers energy efficiency of a system [9]. These high peaks cause the power amplifiers to saturate which leads to intermodulation products amongst the subcarriers and a disturbance on out of band energy. It is desirable to reduce PAPR in an OFDM transmission system to get high energy efficiency. Several techniques have been proposed to reduce PAPR such as clipping, peak windowing, coding, tone injection and tone reservation. These methods are unable to simultaneously achieve a low PAPR with low coding overhead, less complexity, without transmitter receiver symbol handshake, and without performance degradation [9]. OFDM signal complex envelope consisting of *N* number of carriers as suggested by [21],

$$S_{total} = \sum_{k=-\infty}^{\infty} \sum_{n=0}^{N-1} a_{n,k}.\, g(t - kT).\, e^{jn\frac{2\pi}{T}t} \tag{2.25}$$

$g(t)$ represents the rectangular pulse of a duration *T* where *T* is the duration of an OFDM symbol. PAPR is defined by [21],

$$PAPR = \frac{\underset{t \in [0,T]}{max}[S(t)]^2}{\varepsilon[S(t)]^2} \tag{2.26}$$

Using the central limit theorem for values of *N* which are large, $S(t)$ real and imaginary values become Gaussian distributed. The OFDM signal amplitude will therefore have a Rayleigh distribution that has a zero mean with a variance that is one complex sinusoid. PAPR is the crest-factor and peak envelope that are defined as the PAPR square root. IFFT outputs that are symbol spaced sampling values miss some of OFDM signal peaks. Calculating the PAPR using sample values from this will result in the calculated PAPR being lower than the actual value of PAPR which should be obtained. The real situation will not be illustrated as the result is optimistic, but enough for OFDM signal reconstruction. To combat this issue, oversampling is done on the signal

by passing the IFFT signal through a low pass filter and then sampling at a higher sampling rate. This results in increased samples being close to real analog signal making a calculation of PAPR basing on these samples to give a true PAPR [19].

As the number of subcarrier increases so does the PAPR of a system. For baseband OFDM signal that has *N* subcarriers has

$$PAPR = \frac{N^2}{N} = N \tag{2.27}$$

A way to reduce PAPR is by reducing the subcarriers to be as low as possible regardless of a PAPR reduction scheme being employed. One of the simple ways to lower PAPR to a minimal level is by clipping an OFDM signal just before amplification [37] since there is a very low probability of occurrence of large peaks. Removal of peaks brings in slight self-interference. Clipping of a signal is nonlinear process that causes significant in-band distortions which tend to degrade BER performance, and the out of band noise that reduces spectral efficiency. Spectral platter can be reduced by filtering soon after clipping. This is one of the techniques which is so promising in the reduction of PAPR [9]. Clipping with forward error correcting codes is another approach to reduce PAPR. Improved PAPR performance and significant improvements in spectral efficiency is achieved when clipping is used on a signal together with forward error correcting code [37].

Another approach is the use of peak windowing in which signal peaks that are large are multiplied by a window function that has desirable spectral properties. In an ideal situation, the window is expected to be as narrowband as possible and being not long in time domain. Kaiser, Cosine and Hamming windows are good examples. The signal will no longer be composed of the orthogonal carriers after the multiplication of the windowing function and the OFDM signal. This results in an increase in the BER and the out of band radiation [21, 25, 37].

## 2.7 Principles of Frequency Band Multicarrier

Overlapping subcarriers in frequency domain namely CMT provides the highest bandwidth efficiency [2]. There are two types of implementations in FBMC systems based on polyphase networks (PPN) and frequency spreading concepts respectively. In CMT, a set of pulse amplitude modulation (PAM) baseband streams are vestigial sideband (VSB) modulated and placed at different subcarriers [38].

### 2.7.1 Double Sideband Suppressed Carrier Modulation (DSB-SC)

The signal $x(t)$ is a low frequency message signal and $c(t)$, a high frequency carrier modulating signal, are fed to the product modulator to get double side band single carrier (DSB-SC) output after multiplication of the two signals [38], [39].

$$y(t) = x(t) * c(t) \tag{2.28}$$

The frequency $Y(f)$

$$Y(f) = \frac{A_c}{2}[x(t_c - t_o) + x(t_c + t_o)] \tag{2.29}$$

The product $Y(f)$ has two frequency components, the lower side band (LSB) frequency and the upper side band (USB) frequency components. In DSB-SC amplitude modulation scheme the carrier wave signal $c(t)$ is independent of the message signal $m(t)$ component meaning that the carrier wave transmission is a waste of transmission power [41]. A small amount of transmitted power signal is for propagating the message signal. To overcome this shortcoming effect, the carrier component is suppressed from the modulated wave which then gives rise to double sideband suppressed carrier modulation [40].

By superimposing message signal with carrier signal we obtain a DSB-SC amplitude modulated (AM) signal [39].

$$
\begin{aligned}
s(t) &= c(t) * m(t) \\
&= A_c \cos(\omega_c t) * A_m \cos(\omega_m t) \\
&= A_c A_m \cos(\omega_c t) * \cos(\omega_m t) \\
&= A_c A_m [\cos(\omega_c - \omega_m)t + \cos(\omega_c + \omega_m)t] * \frac{1}{2}
\end{aligned}
\tag{2.30}
$$

The generation of the DSB-SC modulated signal consists of a superimposition of the message signal with the carrier wave signal. A product modulator also known as the straightforward multiplier is the device required for this modulation to take place. Figure 2.6 depicts modulation which results in USB and LSB from double sideband suppressed carrier.

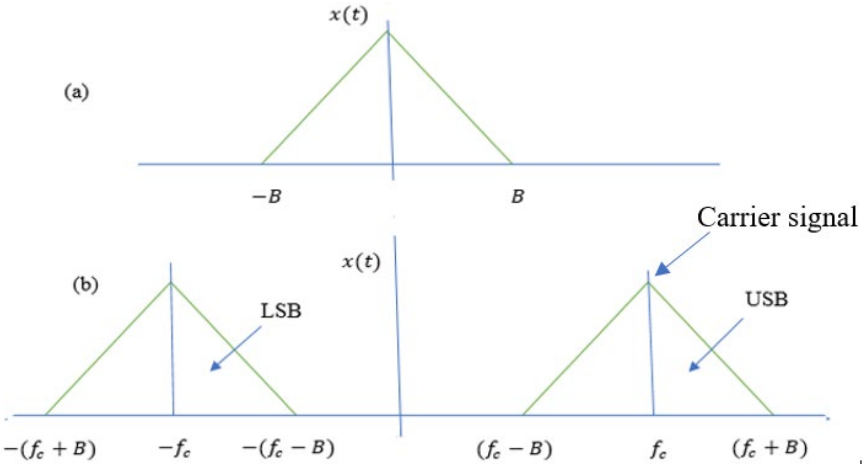


Figure 2.6:(a) Double Side band Suppressed Carrier DSB-SC (b) USB and LSB [21].

The double side band suppressed carrier in Figure 2.6(a) is a combination of lower side band and upper side band. Figure 2.6 (b) shows the lower side band and the upper sideband separately during modulation [21].

### 2.7.2 Vestigial Sideband Modulation

In Vestigial Sideband (VSB) modulation, a vestige of the sideband is transmitted instead of completely removing a whole sideband as proposed by Chang [41]. Almost all of the second band is transmitted together with the vestige [42, 43].

Frequency response of vestigial sideband (VSB) modulation filter is $y(t)$ which is the convolution response of VSB with DSB-SC input [11]. Output of the VSB filter is given below as

$$Y(f) = \frac{A_c}{2}[x(t_c - t_o) + x(t_c + t_o)]H(F) \tag{2.31}$$

Whereby $H(f)$ is the frequency response of the VSB filter. When a signal is transmitted through a VSB filter, only one side band and a vestigial band are transmitted as shown in Figure 2.8.

***Generation of VSB side shaping filter***

We use a special filter called sideband shaping filter for the generation of VSB modulator using frequency discrimination method as depicted in Figure 2.7.

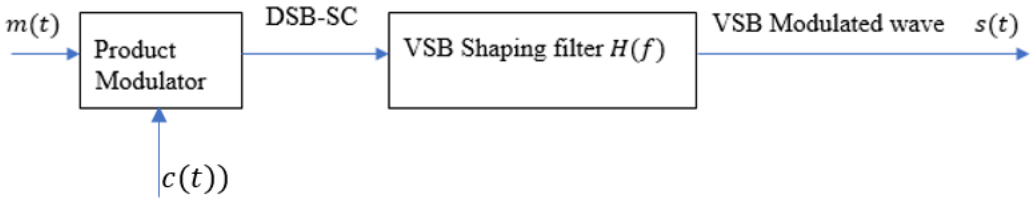


Figure 2.7: Vestigial sideband modulator using frequency discrimination [35].

A product modulator is used and it is followed by a bandpass filter which is a sideband shaping filter. Bandpass filter is a specially designed filter with transfer function is $H(f)$. The input signals are superimposed $c(t)$ and $m(t)$ signals to get a DSB-SC signal. By using a transfer function the DSB-SC is shaped into a VSB modulated wave $s(t)$ as depicted in Figure 2.7 to produce a raised cosine filter shown in Figure 2.8.

In Figure 2.8, an upper side band has a portion of bandwidth that a vestige is to occupy. When a vestige has occupied the USB upper part, the USB will be complete as depicted in Figure2.8.

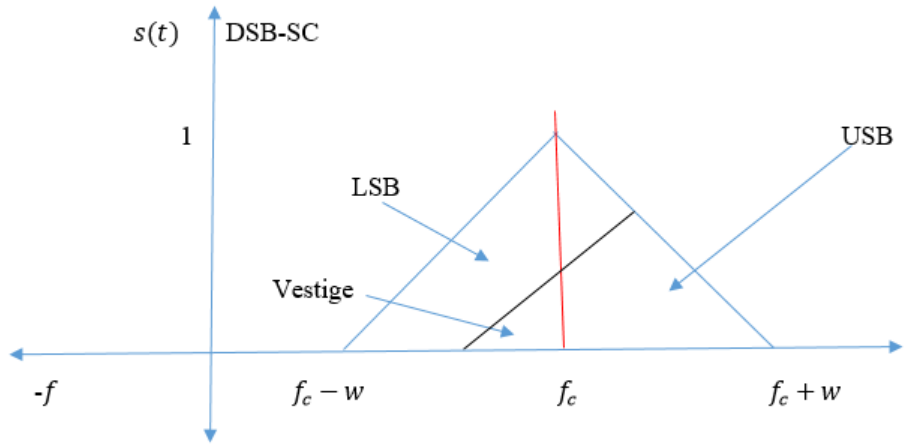


Figure 2.8: Upper Sideband positive frequency portion [9].

Assume the vestige of the VSB lies in a lower sideband of the DSB-SC modulated wave then $f_v$ is the vestige bandwidth, and $w$ is the message signal bandwidth.

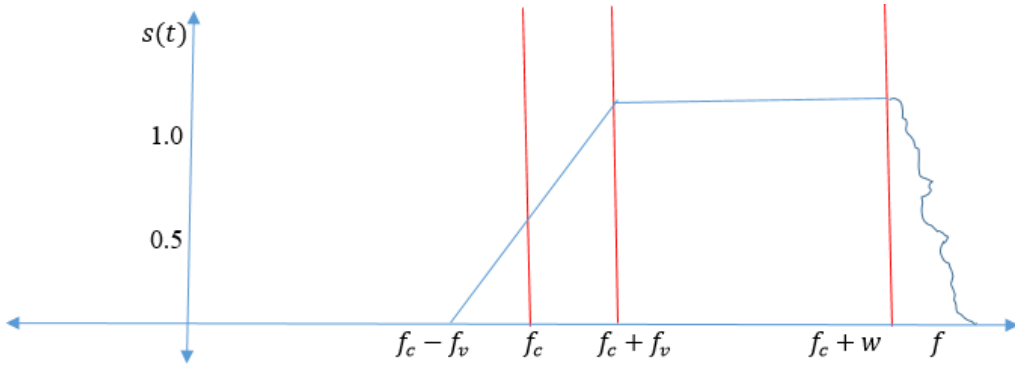


Figure 2.9: Amplitude response of the sideband shaping filter [9].

In the transfer function, the amplitude with respect to $f_c$ is 0.5 and the amplitude with respect to $f_v + w = 1$ . In order to determine the vestige bandwidth, we take the upper frequency as $f_c$ and

the lower frequency as $f_c - f_v$. With the help of amplitude response of sideband shaping filter we obtain the vestigial sideband [7, 39]. Figure 2.10 depicts that the vestige is found between $f_c + f_v$ and $f_c$. VSB only takes the positive portion of the frequency portion. Almost the USB is passed through the filter that is limited between $f_c$ and $f_c + f_v$. The transmission bandwidth for the VSB lies between $f_c + w$ and $f_c$. Bandwidth is $w$ for the USB and $f_v$ is vestige sideband that is from the LSB.

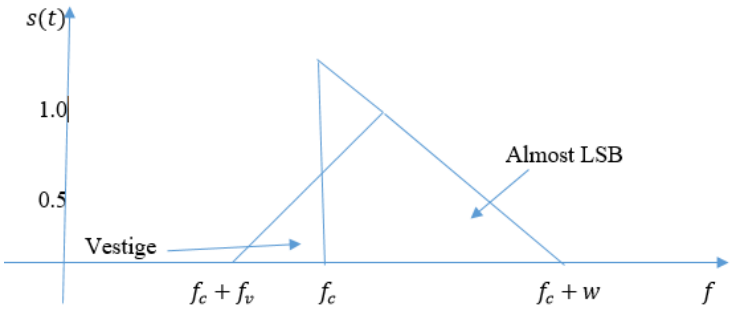


Figure 2.10**:** Vestigial sideband [3].

As far as the designing of the shaping filter is concerned, the requirement is that the transmitted vestige compensates the spectral portion missing from the USB as shown in Figure 2.10 [7].
To obtain this, the transfer function must satisfy the following condition.

$$H(f + f_c) + H(f - f_c) = 1 \tag{2.32}$$

$H(f + f_c)$ is the positive frequency part of $H(f)$ shifted to the left by $f_c$. $H(f - f_c)$ is the negative frequency part of of $H(f)$ shifted to the left by $f_c$ [10].

### 2.7.3 Properties of the side shaping filter

The transfer function of the sideband shaping filter exhibits odd symmetry about the carrier frequency $f_c$.

$$H(f) = u(f - f_c) - H_v(f - f_c) \tag{2.33}$$

it is given that

$$f - f_c < |f| < f_c + w \tag{2.34}$$

such that

$$u(f - f_c) = \begin{cases} 1, & f > f_c \\ 0, & f < f_c \end{cases} \tag{2.35}$$

This property is due to the consideration that $u(f)$ is the unit step frequency function as depicted in Figure 2.11 [21]35]. It follows that $H_v(f - f_c)$ is a frequency function which is shifted by carrier frequency $f_c$ and it represents a vestige as a part of the lower sideband. It is the frequency shifted function of a low pass transfer function $H_v(f)$ that is depicted in Figure 2.13, because we consider a vestige as part of the lower side band. It is completely determined by the vestige of the modulated wave [21, 42].

According to the first property, the transfer function of the sideband shaping filter must exhibit odd symmetry about the carrier frequency $f_c$. Odd symmetry is given by this second term $H_v(f - f_c)$ which depends upon the vestige of the modulated wave. The transfer function of the filter $H(f)$ is band limited between $f_c - f_v$ and $f_c + w$. $f_c + w$ is called the high frequency component and $f_c - f_v$ the lower frequency component .

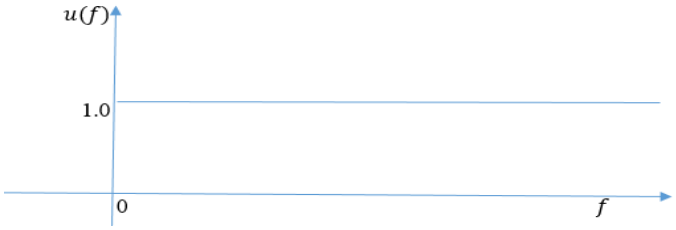


Figure 2.11: Frequency domain representation of the unit step function $u(f)$ [10].

Now we can determine the bandwidth of the transmission bandwidth of the sideband shaping filter and it is equal to $f_c + w$ from the difference of USB and LSB $(f_c + w) - (f_c - f_v)$ [21].

Frequency domain of the unit step frequency function $\boldsymbol{u(f)}$ is depicted in Figure 2.11.

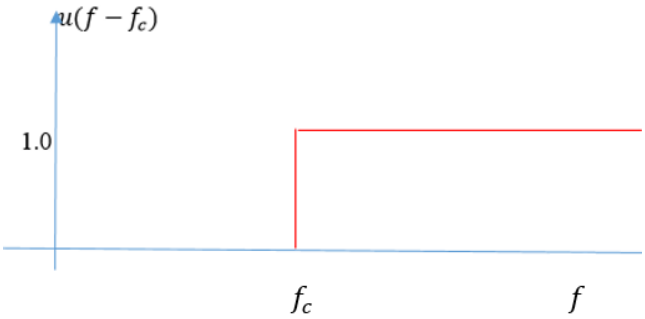


Figure 2.12: Frequency domain representation of $u(f-f_c)$ [10].

A translation of the unit step frequency function to give $\boldsymbol{u(f-f_c)}$ is depicted in Figure 2.12.

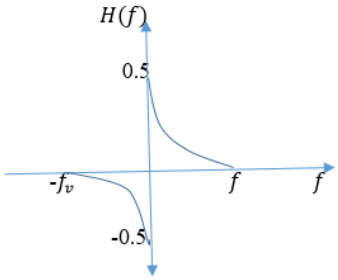


Figure 2.13: Frequency domain representation of $H(f)$ [44].

The transfer function $H(f)$ is depicted in Figure 2.13 is high when frequency is low at zero and when frequency increases, the transfer function decreases to a point where the transfer function gets to zero.

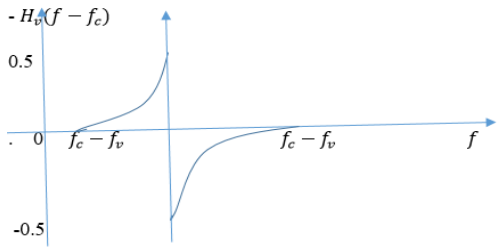


Figure 2.24: Frequency domain representation of $-H_v(f-f_c)$.

$H_v(f)$ represents odd symmetry function with negative amplitude. After shifting to the right by

the amount of $f_c$ we represent $-H_v(f - f_c)$ that is shown in the Figure 2.14.

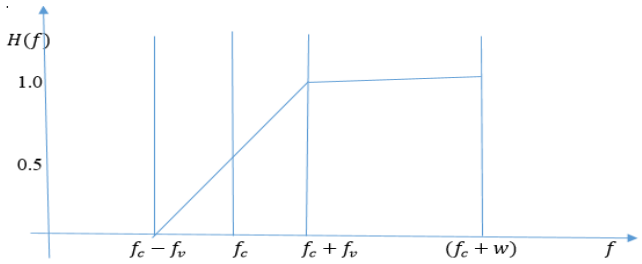


Figure 2.35: Transfer function of a vestigial sideband.

In order to represent the second term of the transfer function we first translate the amplitude. Figure 2.15 depicts a transfer function of a vestigial sideband. The second term exhibits odd symmetry about the carrier frequency. For the second term we consider an odd symmetric function that is used to determine the vestige of the VSB and it is determined by $H_v(f)$.

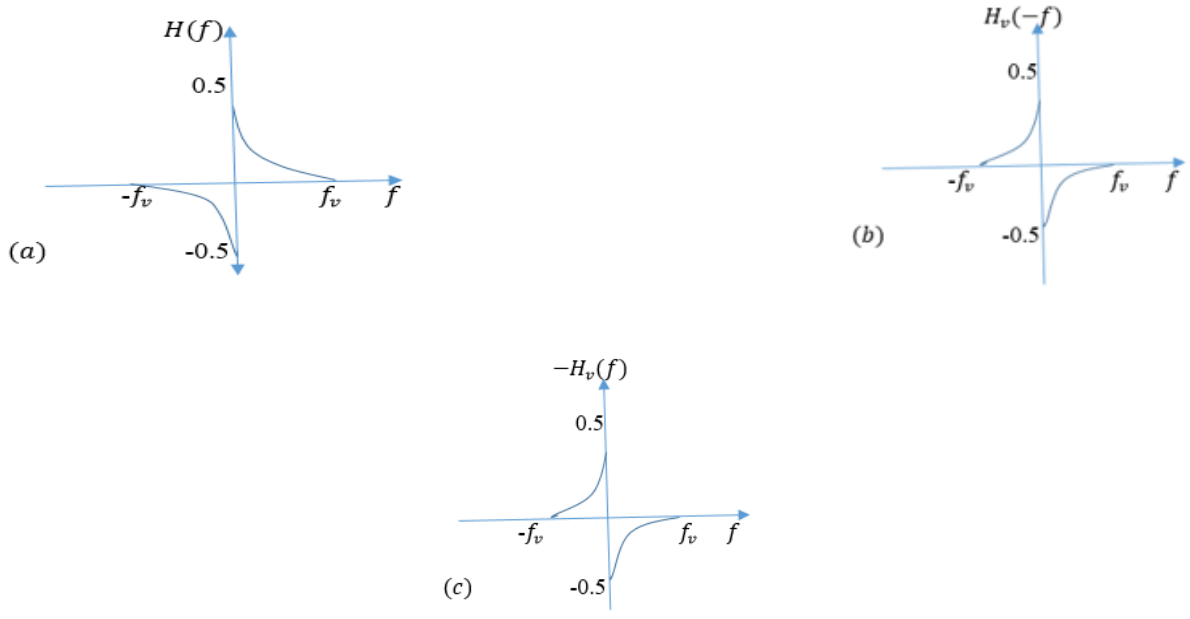


Figure 2.46: Odd symmetry of (a) is depicted in (b) and (c).

The transfer function $H_v(f)$ is required to satisfy the odd symmetry condition only for frequency interval $-w \leq f \leq w$. $H(f)$ has arbitrary specification for $|f| > f_c + w$. Vestigial bandwidth is about 25% to 33% of one sideband.

## 2.8 Chapter Summary

This Chapter discussed concepts of OFDM and FBMC. In FBMC, special focus was on CMT modulation scheme which implements PAM. Vestigial sideband modulation methods were presented for efficient bandwidth utilisation. Orthogonality of OFDM that this research was implementing was discussed showing how it comes to effect. Some background information to OFDM communication system was laid down and how it was vital for enhancement of modulation schemes for the removal of some impairments of OFDM in future technologies. The foundations in this research was taken from work which has already been done and was cited using distinct literature which called for further research in this area of telecommunications.

# Chapter 3

# Methodology

## 3.1 Introduction

This Chapter describes the methodology of the research which was implemented in this study. It is structured in such a way as to answer the research questions and to achieve the objectives of the study which were given in Chapter 1. MATLAB software was used for the simulations of OFDM using different modulation schemes in this case BPSK, 8PSK, QPSK, 32QAM and 64QAM. FBMC system using PAM modulation scheme for CMT multicarrier modulation technique was simulated using MATLAB. A structure for the spectral efficiency modelling of the communication systems of OFDM and FBMC was developed and performance analysis was done to establish which modulation scheme performed better than the other to ensure a good recommendation for future communications for a given duration. Simulation experiments were done for BER performance of AWGN channel and the experiments were repeated for BER performance of AWGN multipath fading channel of OFDM modulation schemes, BPSK, QPSK, 8QAM, 16QAM, 32QAM and 64QAM. FBMC modulation scheme simulations were carried out in an AWGN channel and repeated in an AWGN multipath fading channel. A comparison of Eb/No and SNR is presented to show the effects of increase in SNR on the decrease in BER for theoretical calculations and experimental differences. This is then evaluated against the experimental outcomes of this study for OFDM modulation systems in AWGN channels and AWGN multipath fading channels.

## 3.1 Tools and Resources

This research was based on the trust and reliability of MATLAB software [45]. MATLAB was used for the simulations of OFDM digital modulation schemes using BPSK, QPSK, 16QAM and 64QAM. Simulations of FBMC modulation scheme was done with the implementation of PAM modulation scheme in MATLAB. Spectral efficiency of OFDM against MATLAB was implemented using MATLAB software for the burst duration of 30ms.

## 3.2 Theoretical Model

This section provides theoretical modelling in order to validate the methods for OFDM and FBMC modulation schemes. Channel modelling, channel estimation and draft designs are discussed in this section to produce theoretical results which are used to validate the simulations of the multicarrier systems. Theoretical results are presented in this section.

### 3.2.1 Channel Modelling

In order to simulate a realistic communication system, the following channel model was used which includes Additive White Gaussian Noise (AWGN) and multipath fading.

$$y(n) = x(n) * g(n) + w(n) \tag{3.1}$$

Orthogonal frequency division multiplexing propagates through noisy channels with multipath fading effects. The Time-domain of an OFDM signal is represented by $x(n)$, and the channel impulse response is given as $g(n)$. AWGN is represented by $w(n)$ And the corrupted OFDM modulation signal is $y(n)$.

### 3.2.2 Channel Estimation

The communication channel used the least squares channel estimation approach to remove the effects of multipath fading. Since $w(n)$ is AWGN and having zero mean, It has been removed from equation (3.1),

$$y(n) = x(n) * g(n) \tag{3.2}$$

A fast Fourier transform of $y(n)$ in (3.1) yields,

$$Y(n) = X(\omega)G(\omega) \tag{3.3}$$

$X(\omega)$ is the known signal and the output signal is $Y(\omega)$. By measuring the response $Y(\omega)$ to a known input signal $X(\omega)$, the channel frequency response $G(\omega)$ is estimated

$$\hat{G}(\omega) = \frac{Y(\omega)}{X(\omega)} \tag{3.4}$$

Channel equalization in an OFDM system is carried out in frequency domain as,

$$\hat{X}(\omega) = Y(\omega)\hat{G}(\omega)^{-1} \tag{3.5}$$

This process is called the least Squares channel estimation method. The known signal $X(\omega)$ is the pilot signal. Block type pilot $X(\omega)$ spans the entire frequency range and it is transmitted periodically. Comb type pilot signal $X(\omega)$ spans selected frequencies and it is transmitted constantly the entire time range.

### 3.2.3 Draft designs

The communication system shown in Figure 3.1 shows the simulation of a digital system which is divided into two parts as the research simulation was based on such a system. The transmitter created a signal that was analogue. The data message signal was a character string in FBMC communication scheme. In ODFM communication system, a picture input signal was used [10]. The message signal was first translated into a 4-PAM symbol set and then a pulse train enters a synthesis filter for pulse shaping [10]. The sifting properties of the filter then produced an analogue signal which was modulated thereby forming the transmitted signal. An ideal system was first assumed and then a multipath fading channel together with noise was then examined on the communication system.

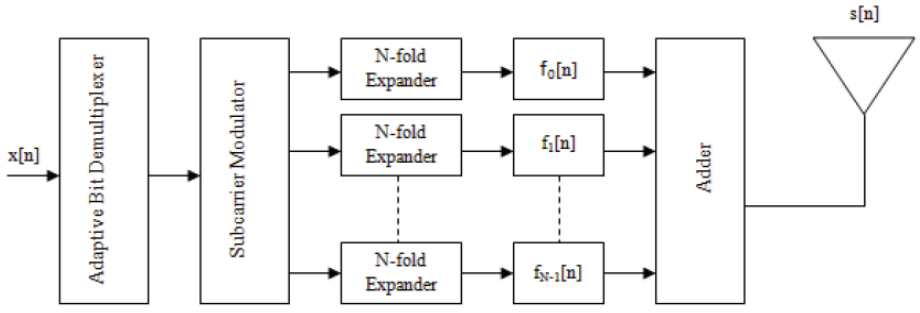


(a) The graphical illustration of the FBMC transmitter

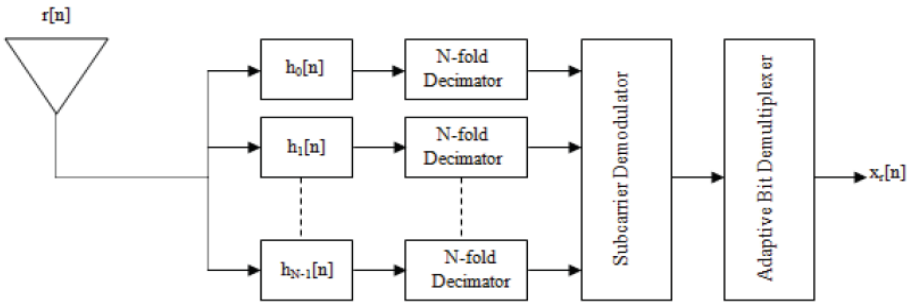


(b) The graphical illustration of a generic FBMC receiver

Figure 3.1: Ideal FBMC communication system block diagram [1].

The received signal was demodulated and filtered in the receiver. An Analysis filter was used in the receiver section. The signal from the filter was correlated and down-sampled after which it was quantized and decoded to produce a message signal which was evaluated for its BER and spectral efficiency.

***Decisions and Error Measures***

In an analogue communication system, transmitted waveforms attain any values. However in digital communication systems, the message which is transmitted should be one of a small number of the values which are defined by the symbol alphabet. This results in the received signal waves in the analogue communication system attaining any value, but in a digital communication system implementation, the message signal that is recovered is meant to be one of a small number of values which are from a source alphabet. Consequently, when the signal is demodulated to a symbol and when it does not belong to the alphabet, then the difference between the demodulated value which is called a soft decision and that nearest element of that alphabet (the hard decision) have a provision to provide the information that shows the performance of the system. When the transmitted message signal differs from the received signal, errors would have had occurred during the transmission process. The quality of a system is measured by symbol recovery errors. The difference between the message signal and the quantized output of the receiver is used to measure the “hard-decision error”.

The block diagram in Figure 3.2 shows an OFDM communication system used in this research. A stream of binary data bits was shifted to parallel blocks by a serial to parallel shifter. Then the parallel blocks of data, using a suitable modulation scheme, were mapped into symbols. IFFT changed the data stream from frequency domain to time domain. The signal was shifted to serial data in time domain, followed by the addition of a cyclic prefix to the OFDM signal for orthogonality and combating ISI. OFDM signal was then subjected to a multipath fading channel. Cyclic prefix was removed in the receiver and the data stream was shifted to parallel blocks for signal processing.

FFT was then used for shifting the data stream into the frequency domain after which channel estimation using least squares estimation method was applied. The data stream was then demodulated using a multicarrier scheme which was used for modulation and it was shifted from symbols to bits and finally the bit stream was shifted from the parallel blocks to serial binary data stream [5].

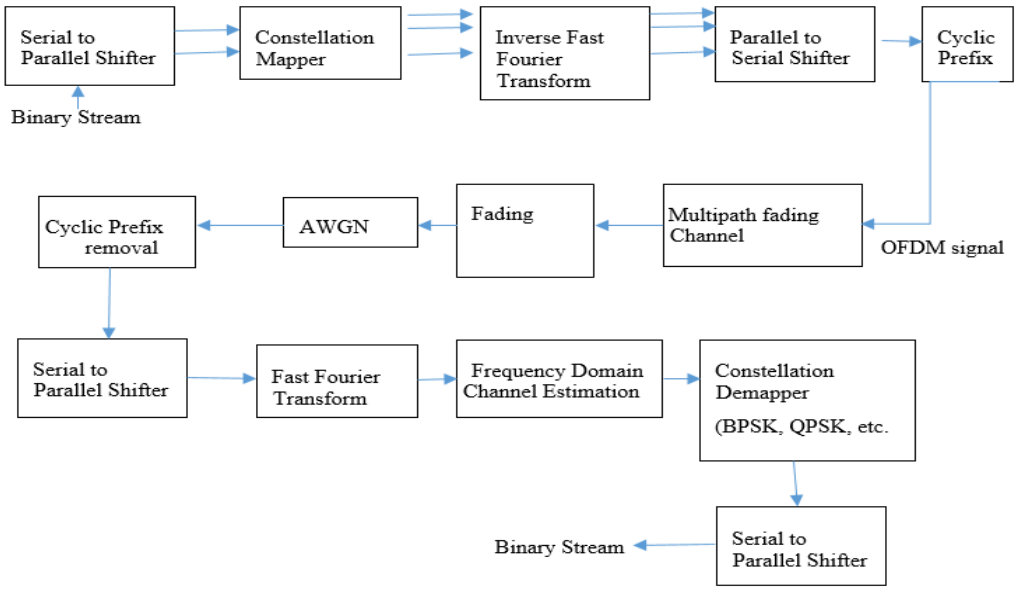


Figure 3.2: OFDM Block diagram [2].

The ideal communication systems of OFDM and FBMC modulation schemes were first evaluated taking note of the difference in the performances of these systems[11]. To achieve a realistic

practical communication scenario, both FBMC and OFDM communication systems were subjected tests using varying parameters of the transmitter, channel and the receiver section [10]. Performance evaluation was done on these multicarrier modulation schemes using simulations in MATLAB. Multipath fading in a communication channel required estimation methods for its removal in the receiver to achieve best performance. A multipath and fading channel for both OFDM and FBMC communication systems was evaluated while varying input parameters such as input signal to noise ratio for OFDM system and variations of frequency and phase impairments for FBMC system. Then a random noise was added to the communication channel noting all of the performances of the systems. Different modulation schemes were then investigated for OFDM in this case BPSK, QPSK, 16QAM, 32QAM, and 64 QAM to check on the BER after changing the input SNR of the system.

Simulation experiments of OFDM systems in MATLAB were first evaluated whereby multipath fading effects were disregarded. An FFT and iFFT of size 64 and cyclic prefix extension of length size 16 was used as initial parameters for the simulations. BER of the modulation techniques in OFDM were examined on how the system performs at different input SNR values [4], [10]. OFDM makes use of channel estimation to remove multipath fading. Block type frequency domain estimation method used in this research was the Least Squares method which was used for the simulations of OFDM in the frequency domain.

### 3.2.4 Theoretical Modelling

Effects of multipath fading were considered on these modulation schemes. Improvements on BER were expected when least squares estimation methods were used in the receiver. Least squares estimation methods are statistical procedures for finding the best fit for data points by use of minimising the sum of offsets of the points from a plotted curve.

Binary phase shift keying consists of two points on the in phase-axis opposite the quadrature axis and maps one bit to one symbol. For 10dB SNR a BER of 7.6% is achieved on the received image.

Increasing the SNR to 20dB results in BER of 0.55%. QPSK expands BPSK by adding additional two points along the unit circle. QPSK maps 2 bits to 1 symbol and for an input of 10dB SNR, a 21% BER is obtained on the received image. An input SNR of 20dB leads to a BER of 5.6%. 8PSK maps 3 bits to 1 symbol and an input of 10dB SNR leads to a 19% BER on the received image. Increasing the input SNR to 20dB leads to the BER decreasing to 5%. At simulations of higher order modulation schemes, the pattern continues. At these fixed SNR vales, the higher order modulation should have a higher BER. For 16 QAM which maps 4 bits to 1 symbol, the 10dB SNR achieves a 20% BER and for an input SNR of 20dB achieves a 20.1% BER. A 32QAM maps 5 bits to 1 symbol. For an input of 10dB SNR on 32QAM, a 20 % BER is obtained. It is expected that as modulation order increases, the constellations became dense and a high SNR is needed to preserve the BER.

## 3.3 Orthogonal Frequency Division Multiplexing Modelling

This section describes OFDM simulation. Maximum number of subcarriers in OFDM system is set to be equal to $N = 64$. This is equivalent to FFT/ iFFT length. 52 subcarriers are active. These are the subcarriers from numbers 1 through 26 and 38 to 63 [7, 21]. Higher frequencies in FFT/iFFT are counted as being negative frequencies which means that the subcarriers 38 through 63 corresponds to -26 through to -1. The first subcarrier in this case does not carry data therefore its associated symbol will always be set equal zero. The rest of those unused subcarriers appear at both sides of the transmission band, and are chosen in such a way as to allow guard bands between the adjacent OFDM frequency bands [21].

### 3.3.1 Timing recovery

In an OFDM system, identification of CP and non-CP extensions of each symbol is known as timing recovery [15]. This allows removal of the CP portion and extraction of the non-CP part which is the desired part of each of the OFDM symbol just before passing into the FFT module for demodulation. The length of a CP is greater than the period of a channel impulse response such that there is a range which may be chosen as a beginning of an OFDM symbol without having an effect on the receiver performance. A transmit signal $x[n]$ is achieved by making use of

concatenation of the cyclic prefixed portions of the IFFT outputs from $\mathrm{x}[n]$. The vector $\mathrm{x}_{\mathrm{cpd}}[n]$ denotes the cyclic prefixed version of $\mathrm{x}[n]$ and the sequence $x[n]$ is shown in Figure 3.3 below. Each cyclic prefixed version in Figure 3.3(a) is a signal vector of length $N + N_{cp}$. The lightly shaded area depicts the CP part while the darker shaded area depicts the ISI part [21]. After traversing the channel, each cyclic prefixed version of $\mathrm{x}[n]$ is given an extension by $L$ samples and it then overlaps with first $L$ samples of a next OFDM symbol, in which $L + 1$ is a duration of an impulse response of an equivalent baseband channel, $c[n]$.

Samples which are within these intervals usually suffer from ISI and due to this fact they cannot be the samples selected to be passed to an FFT block for the process of demodulation [11]. Any points within the lightly shaded regions of $\mathrm{y}_{\mathrm{cpd}}[n]$ can be a starting point for $N$ samples of $\mathrm{y}_{\mathrm{cpd}}[n]$ which may be passed to an FFT block.

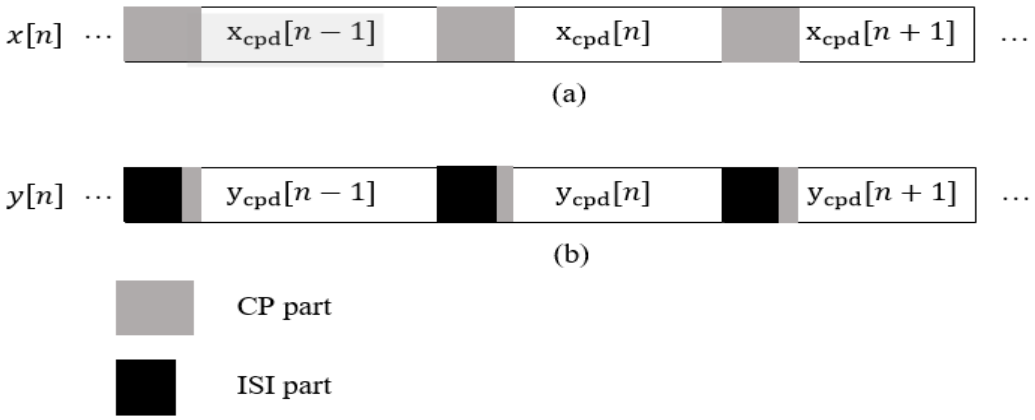


Figure 3.3: (a) ODFM transmitted signal with CP, (b) OFDM received signal with CP [15].

With this, it then follows that when the duration of $c[n]$ is much smaller than $N_{\mathrm{cp}} + 1$, there appears a range of the timing phase in which the OFDM receiver performance will remain insensitive to timing phase [21].

In Figure 3.3(b) when timing phase has been set such that the FFT window matches the non-shaded regions (white part), CP is deleted and FFT of selected samples followed by single-tap equalizers which were introduced in $s_k[n]$ [21] results in perfect recovery of transmitted data symbols $s_k[n]$. When there happens to be a timing offset, and also when starting points of selected samples are in the ISI free region of the CP portion of an OFDM symbol, single-tap equalization will be applicable [10]. To account for timing error which is a deviation from perfect timing phase, linear phase rotation is added to equalizer coefficients [5]. If the starting point specifically is $\Delta t$ samples before perfect timing phase, then there is effectively processing of samples that belong to $y[n-\Delta t]$. A time delay of $\Delta t$ samples in frequency domain is equal to linear phase $e^{-j2\pi\Delta t\ \mathrm{k/N}}$.

$$s_k[n] = \frac{e^{\frac{j2\pi\Delta t\ \mathrm{k}}{N}}}{C\left(e^{j\frac{2\pi k}{N}}\right)} f_k^H \mathrm{y}[n], \text{ for } k = 0,1,\dots,N-1 \tag{3.6}$$

This result will be significant in the tracking and fine tuning of the timing phase. $s_k[n]$ now implies that due to the timing phase offset $\Delta t$, the most effective transfer function of an OFDM channel changes to $e^{\frac{j2\pi\Delta t\ \mathrm{k}}{N}}/C\left(e^{j\frac{2\pi k}{N}}\right)$ from $C\left(e^{j\frac{2\pi k}{N}}\right)$. In time domain, this equals the delay of $c[n]$ by the $\Delta t$ samples. A positive value of the timing phase offset is the same as a right shift and a negative value of the timing phase offset relates to a shift to the left of $c[n]$. On an ideal situation, first non-zero samples of $c[n]$ start at $n = 0$. In case of a single carrier, sensitivity of a receiver module to timing phase is generally resolved by making use of a fractionally spaced equalizer [5]. OFDM effectively uses a fractionally spaced equalizer whereby the sampled signal does not suffer from any aliasing because of the existence of guard bands on all sides of a transmission band.

## 3.3.2 Carrier Acquisition and Tracking

Carrier acquisition and tracking are the two fundamental steps into carrier recovery. This section takes a brief insight into carrier offset impact, carrier acquisition and carrier tracking.

***Carrier offset impact.***

Recalling $\mathcal{F}^{-1}$ and $\mathrm{x}_k[n]$ after the removal of CP, an $n$th symbol in an OFDM received signal is obtained as

$$y_k[n] = \frac{1}{N}\sum_{k=0}^{N-1} C\left(e^{j\frac{2\pi k}{N}}\right) s_k[n]\boldsymbol{f}_k + \boldsymbol{v}[n] \tag{3.7}$$

where $\boldsymbol{v}[n]$ is the channel noise vector [21]. The data symbols $s_k[n]$ which are a set of random variables that have zero mean and $\sigma_v^2$ variance are uncorrelated to one another. It is assumed that $\boldsymbol{v}[n]$ is a Gaussian zero-mean symmetric complex random vector and that

$$E\left[\boldsymbol{v}[n]\boldsymbol{v}^H[n]\right] = \sigma_v^2\mathbf{I}. \tag{3.8}$$

The fast Fourier transform operation can be viewed as a filter bank whereby each of the filters is centred at the subcarrier symbols in which it has nulls at other symbols. The presence of frequency offset introduces a shift in the location of incoming subcarrier symbols such that a result of an attenuated gain on desired symbol and introduction of a significant level of ICI is present [33].

***Carrier acquisition***

Acquisition and tracking are the two fundamental steps into carrier recovery. In the acquisition step, an estimate of carrier frequency and an estimate of carrier frequency offset is achieved. An estimate of the offset is applied which then leads the OFDM receiver to enter into tracking mode where a phase locked loop is used for the fine tuning of the receiver carrier track variations [4].

***Carrier Tracking.***

IEEE 802.11a and other standards have now adopted use of pilot symbols in carrier tracking. An example is IEEE 802.11a subcarrier numbers 27, 57, 7 and 43 are continuously being filled in with the pilot symbols which are already known to a receiver [46]. The unused zero-th subcarrier and those subcarriers unused at both sides of an OFDM band are handled as subcarriers that have known null transmit symbols. They are known as the virtual subcarriers [1].

### 3.3.3 Orthogonality

In frequency division multiplexing (FDM), the sub channels are separated in the frequency domain to avoid interference between the subcarriers by guard bands. It results in loss of spectral efficiency because the guard bands do not carry data. OFDM allows removal of these frequency guard bands. The subcarriers determine the symbols that are sent at the same time. Orthogonality brings high spectral efficiency. If a sinusoidal signal into the time domain, it corresponds to a single spike in the frequency domain by fast Fourier transformation. The representation of a pure sinusoid in the frequency domain is the Dirac delta function. The width of a sinc function is inversely proportional to the duration of the square signal. Increasing the width of the square function shrinks the sinc function [5]. Convolution theorem states that under suitable conditions, the Fourier transform of a convolution of two signals is the pointwise product of their Fourier transform [10].

$$
\begin{aligned}
< e^{j2\pi fkt}, e^{j2\pi fkt^*} > &= \frac{1}{T}\int_0^T e^{j2\pi fkt} e^{-j2\pi fkt} dt \\
&= \frac{1}{T_{sym}}\int_0^{T_{sym}} e^{j2\pi \frac{k}{T_{sym}}t}\, e^{-j2\pi \frac{i}{T_{sym}}t} dt \\
&= \frac{1}{T_{sym}}\int_0^{T_{sym}} e^{j2\pi \frac{(k-i)}{T_{sym}}t}\, dt \\
&= \begin{cases} 1, if\ k = i \\ 0, otherwise \end{cases}
\end{aligned}
\tag{3.9}
$$

Where $T_{sym}$ is the period of a symbol and < > represents convolution. Orthogonality only holds in integration interval of $T_{sym}$ length.

$$
\frac{1}{T_{sym}}\int_0^{T_{sym}} e^{j2\pi \frac{(k-i)}{T_{sym}}t}\, dt = \int_{-\infty}^{\infty} \rho_\tau(t) e^{j2\pi \frac{(k-i)}{T_{sym}}t}\, dt\, \rho_\tau
$$

$$= \begin{cases} 1, & 0 \leq t \leq T_{sym} \\ 0, & otherwise \end{cases} \quad (3.10)$$

Equation (3.10) reveals that there is some windowing happening where $\rho_\tau$(t) is the pulse shaping signal or the windowing signal [4].

## 3.4 FBMC Modelling

This section gives detail on FBMC modulation scheme. Nyquist solution for zero ISI is discussed followed by the physical realization of the Nyquist channel. The sinc function time response is explained and the raised cosine filter bandwidth requirements are discussed for CMT multicarrier modulation scheme used in this study. Finite impulse response windowing design for FBMC cosine modulated multitone is discussed.

### 3.4.1 Nyquist solution for Zero Inter-symbol-interference

In digital signal processing, the transmission of digital data ISI is a problem and can be minimised by controlling the power spectrum $p(t)$ and $P(f)$ in the time and frequency domain respectively of the overall system including transmit filter channel and receive filter channels. In order to meet zero ISI, Nyquist criterion must be fulfilled for distortion-less baseband transmission [4]. For zero ISI we have

$$p(t) = sinc(2B_0 t) \quad (3.11)$$

$$B_0 = \frac{1}{2T_b} \quad (3.12)$$

$B_0$ is the Nyquist criterion minimum bandwidth for zero ISI, $p(t)$ is in time domain and it is the only function in which we get an ideal solution. It is the minimum bandwidth for ISI to be zero [26]. Equation (3.11) becomes

$$p(t) = sinc(\frac{t}{T_b}) \quad (3.13)$$

Whereby $T_b$ is the peak duration. The $sinc$ function is shown below in Figure 3.4 which characterize the impulse response of an ideal low pass filter (LPF). At $t = 0$ the magnitude is unity and $p(t)$ becomes zero at t =$\pm T_b, \pm 2T_b, ..$

Also the size of the side lobes decrease as the time increases as shown in Figure 3.4 [38].

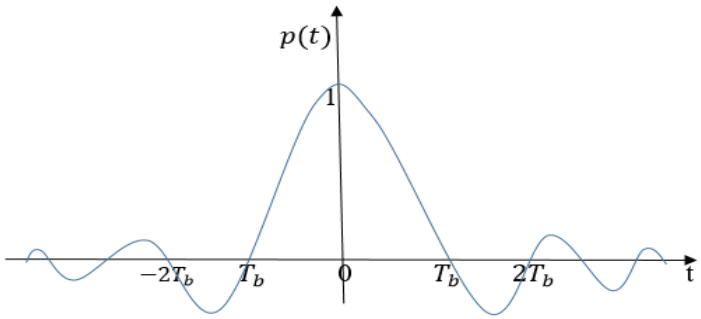


Figure 3.4: Impulse response of an ideal low pass filter [15].

Using Fourier transform, the function $p(t)$ in time domain becomes $P(f)$ in frequency domain which shows a rectangular pulse of magnitude $\frac{1}{2B_0}$ and bandwidth $2B_0$ .

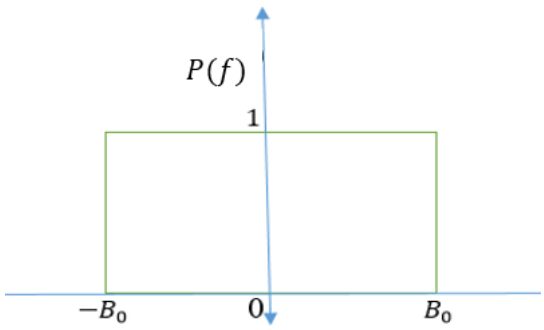


Figure 3.5: Frequency response of an ideal low pass filter [7].

The function $P(f)$ has a discontinuity at $\pm B_0$. This shows the frequency response of an ideal low pass filter and mathematically it is represented as

$$P(f) = \begin{cases} \frac{1}{2B_0} \ , & |f| < B_0 \\ 0 \ , & |f| > B_0 \end{cases} \tag{3.14}$$

The $sinc$ function in time domain $p(t) = 0$ at integer multiples of $T_b$ as depicted in Figure 3.4,

$$p(t - T_b) = sinc[2B_0(t - kT_b)] \tag{3.15}$$

where $k$ is an integral multiple and the negative sign shows the delay time [12], [13]. The area under the rectangular pulse is unity denoted by $\int_{-\infty}^{\infty} P(f)\, df = 1$ as shown in Figure 3.5. In baseband transmission of binary data, the modified PAM signal is approximately given by

$$y(t) = \mu \sum_{-\infty}^{\infty} a_k p(t - kT_b) \tag{3.16}$$

Where $\mu$ is a constant. To get zero interference $y(t)$ is sampled at $t = 0, \pm T_b, \pm 2T_b, \ldots$ .To get an ideal solution in time domain, it follows that;

$$p(t) = sinc(2B_0 t) \tag{3.17}$$

Which gives

$$y(t) = \mu \sum_{-\infty}^{\infty} a_k sinc(2B_0(t - kT_b))$$

$$= \mu \sum_{-\infty}^{\infty} a_k sinc(2B_0 t - 2kB_0 T_b) \tag{3.18}$$

Since Nyquist bandwidth is $\beta_0 = \frac{1}{2T_b}$ then $2B_0 T_b = 1$. The modified $y(t)$ becomes

$$y(t) = \mu \sum_{-\infty}^{\infty} a_k sinc(2B_0 t - k) \tag{3.19}$$

Where $\mu$ denotes a constant. Consider timing error $\Delta(t)$ which causes ISI due to inaccurate synchronisation of the clock in the receiver sampling circuit. Let $t = \Delta(t)$ we consider $\Delta(t)$ to be a small error for ISI [21].

$$\begin{aligned} y(t) &= \mu \sum_{-\infty}^{\infty} a_k sinc(2B_0\Delta(t) - k \\ &= \mu \sum_{-\infty}^{\infty} \frac{a_k \sin(2B_0\pi\Delta(t) - \pi k)}{\pi(2B_0\Delta(t) - k)} \\ &= \mu \sum_{-\infty}^{\infty} \frac{a_k[sin(2B_0\pi\Delta(t)) \cos(\pi k) - cos(2B_0\pi\Delta(t)) sin(\pi k)]}{\pi(2B_0\Delta(t) - k)} \end{aligned} \tag{3.20}$$

Considering Bessel function of first order $cos\pi k = (-1)^k$ and $\sin(\pi k) = 0$ , [6, 47], then

$$y(t) = \mu \sum_{-\infty}^{\infty} \frac{a_k(-1)^k sin(2B_0\pi\Delta(t))}{\pi(2B_0\Delta(t) - k)} \tag{3.21}$$

When $k = 0$ the desired symbol $A$ is obtained and when $k \neq 0$ the ISI caused by timing error $\Delta(t)$ decays slowly at the rate $\frac{1}{\Delta(t)}$, due to discontinuity of $P(f)$ $at$ $\pm B_0$.

$$y(t) = \frac{\mu a_0}{2B_0\Delta(t)} \sin(2B_0\Delta(t)) + \sum_{-\infty}^{\infty} \frac{\mu a_k(-1)^k sin(2B_0\pi\Delta(t))}{\pi(2B_0\Delta(t) - k)} \tag{3.22}$$

Let the desired symbol be A

$$A = \frac{\mu a_0}{2B_0\pi\Delta(t)} \sin(2B_0\pi\Delta(t)) \tag{3.23}$$

And let the ISI be the $Z$ term

$$Z = \sum_{-\infty}^{\infty} \frac{\mu a_k(1)^{-1} sin(2B_0\pi\Delta(t))]}{\pi(2B_0\Delta(t) - k)} \tag{3.24}$$

### 3.4.2 Physical realization of Nyquist channel

It has been established that it is not possible to have data rate being higher than capacity of a communication channel [6]. The channel capacity of a communication channel as Shannon puts it, gives the upper limit and Nyquist formulae defines the number of signal levels used. To make it realizable with desirable features, modification is implemented. This section explains the physical realization of a Nyquist channel.

The bandwidth of a Nyquist channel is depicted in Figure 3.5. The modified filter function $P(f)$ is called the raised cosine filter in which there is a flat portion in the passband and roll-off portion in the stopband shown below in Figure 3.7.

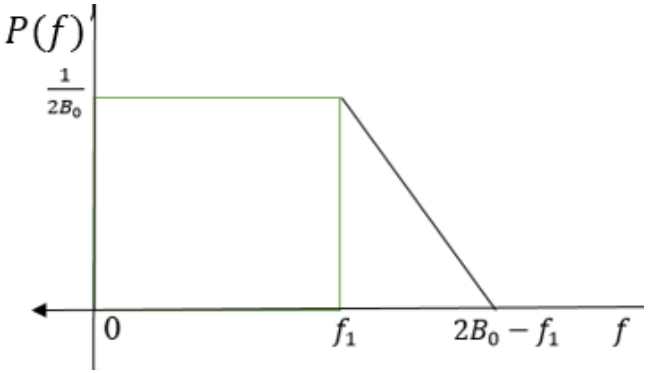


Figure 3.6: Ideal amplitude response [6].

The abrupt discontinuity is converted to the roll-off portion from Figure 3.6 to $2B_0 - f_1$ having a magnitude of $\frac{1}{2B_0}$ for the flat portion in the passband from zero to $f_1$. This characteristic is called raised cosine roll-off filter $P(f)$ and it is practically realizable. It corresponds to the low pass filter. The roll-off portion introduces a parameter $\alpha$ called the roll-off factor. Roll-off is the relation between $f_1$ and the Nyquist bandwidth $B_0$ [21].

$$\alpha = 1 - \frac{f_1}{B_0} \tag{3.25}$$

The roll-off factor is the relationship between frequency $f_1$ and $B_0$ the Nyquist bandwidth. When $\alpha = 0$ then the value of $f_1 = B_0$ which represents the ideal low pass amplitude response with

transmission bandwidth value $B_T = B_0\ (minimum)$ which is minimum and it is the Nyquist bandwidth. When $\alpha = 1$ then the value of $f_1 = 0$ which represents the full cosine roll-off characteristic response with transmission bandwidth value $B_T = 2B_0\ (twice\ ideal)$ which is minimum and it is the Nyquist bandwidth. To move to time domain analysis, inverse Fourier Transform of $P(f)$ is considered resulting in $p(t)$ where the roll-off factor is $\alpha$ and $B_0$ denotes the Nyquist bandwidth. The $sinc(2B_0t)$ corresponding to the ideal solution shows zero crossing of function $p(t)$ at $= 0, \pm T_b, \pm 2T_b, \ldots$ , when $\alpha = 0$ and for $\alpha = 1$ for zero crossings at $t = \pm 1.5T_b, \pm 2.5T_b$ ... which is depicted in Figure 3.7.

$$P(f) = \begin{cases} \dfrac{1}{B_0} & , \quad |f| < f_1 \\ \dfrac{1}{4B_0}\left[1 + \cos\left(\dfrac{\pi|f| - f_1}{2B_0 - 2f_1}\right)\right] & , f_1 \le |f| < 2B_0 - f_1 \\ 0 & , \quad |f| \le 2B_0 - f_1 \end{cases} \tag{3.26}$$

$$P(f) \xrightarrow{IFFT} \boxed{p(t) = sinc(2B_0t)\frac{\cos(2\pi\alpha B_0 t)}{1 - 16\alpha^2 {B_0}^2 t^2}} \tag{3.27}$$

The factor values $t^2$ reduces as $t$ increases accordingly the $t$ factor reduces the tail of the sinc function which is the side lobe hight as compared to the Nyquist solution and which reduces the sampling errors.

### 3.4.3 Time response of a sinc function

In digital signal processing, an ideal filter such as a sinc filter removes frequency elements that are above a certain cut-off frequency, having a linear phase response, and not affecting the lower frequency elements. The sinc function time response is given in Figure 3.7.

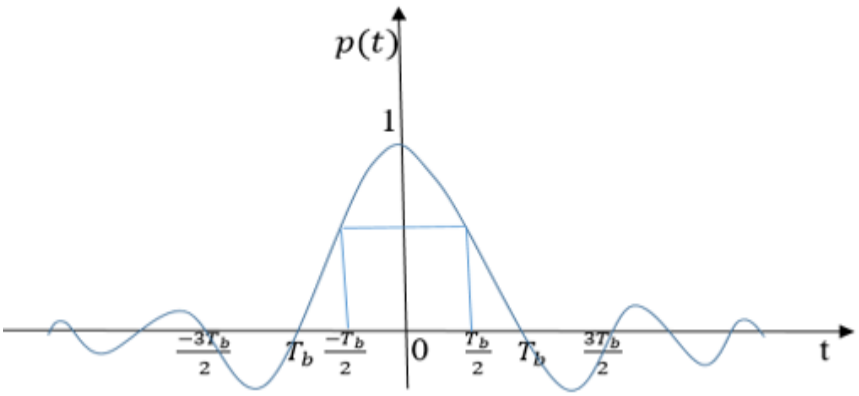


Figure 3.7: Sinc function time response with high roll-off factor [21].

Figure 3.7, [23] depicts a sinc function response of the filter with decaying side lobes At $\alpha = 0$ then $p(t)$ has zero crossing at $t = 0, \pm T_b, \pm 2T_b, \ldots$. At $\alpha = 1$ then $p(t)$ has zero crossing at $\frac{T_b}{2}$ and $\frac{3T_b}{2}$ etc as shown in Figure 3.7 including crossings at

$$t = \pm T_b, 2T_b \ldots \tag{3.28}$$

At $T_b = 0$ then $p(t) = 1$. Which means the physical realisation of Nyquist channel for zero ISI at $\alpha = 1$. When $\alpha = 1$ then

$$1 = 1 + \frac{f_1}{B_0} \tag{3.29}$$

And when $f_1 = 0$ for

$$P(f) = \begin{cases} \frac{1}{4B_0}\left[1 + \cos\left(\frac{\pi|f|}{2B_0}\right)\right] & 0 < |f| \leq 2B_0 \\ 0 & |f| \geq 2B_0 \end{cases} \tag{3.30}$$

After taking the Inverse Fourier Transform then

$$p(t) = \frac{sinc(4B_0 t)}{1 - 16x^2 {B_0}^2 t^2} \tag{3.31}$$

Therefore $p(t)$ is the raised cosine filter which is physically realizable.

### 3.4.4 Raised cosine filter bandwidth requirements

The bandwidth requirements for raised cosine filter is given by

$$B_T = 2B_0 - f_1 \tag{3.32}$$

Figure 3.7 depicts the raised cosine filter bandwidth requirements whereby the Nyquist bandwidth becomes

$$f_1 = B_0(1-\alpha) \tag{3.33}$$

$$B_T = 2B_0 - B_0(1-\alpha) \tag{3.34}$$

When $\alpha = 0$ therefore $B_T = B_0$ which is minimum. When $\alpha = 1$ then $B_T = 2B_0$ which is twice the ideal solution. The term $\alpha B_0$ is the transmission bandwidth requirement of raised cosine spectrum. It is the excess bandwidth. The ratio of excess bandwidth to Nyquist bandwidth gives the roll-off factor [4]. In practical case When $\alpha = 1$ provides basis for synchronizing the receiver and the transmitter and this is physically realisable.

### 3.4.5 Finite Impulse Response windowing design

Assume that a filter has linear phase finite impulse response (FIR) filter and the order (m) is even. The frequency response

$$H\left(e^{jw}\right) = \sum_{k=0}^{m} h(k)e^{-jk\omega}$$

$$= A(\omega)e^{-\frac{j\omega m}{2}} \tag{3.35}$$

The factor $A(\omega)$ is a real value. Assume that it is linear phase with phase factor $e^{-\frac{j\omega m}{2}}$. Consider minimising the mean square error.

$$\min_{h[k]} \frac{1}{2\pi} \int_{-\pi}^{\pi} \left| H_d\left(e^{j\omega}\right) - H(e^{j\omega}) \right|^z d\omega \tag{3.36}$$

The term $H_d\left(e^{j\omega}\right)$ is the desired filter response and the term $H(e^{j\omega})$ is the actual filter response. The magnitude of the difference of the desired filter and the actual filter is squared. Then let

$$H_d\left(e^{j\omega}\right) = A_d(\omega) e^{-\frac{j\omega m}{2}} \tag{3.37}$$

The negative complex term is the group delay term. The phase factor terms are then taken out of the mean squared error expression to get an expression as

$$\min_{h[k]} \frac{1}{2\pi} \int_{-\pi}^{\pi} |A_d(\omega) - A(\omega)|^2 d\omega \tag{3.38}$$

Assume a shift to the left corresponding to the phase factor $e^{-\frac{j\omega m}{2}}$ is equal to the coefficients $a[k]$ which has discrete Fourier transform of $A(\omega)$;

$$h\left(k + \frac{m}{2}\right) = a[k] \tag{3.39}$$

Which has a discrete Fourier transform $A(\omega)$. Parseval's theorem states that

$$\min_{a[k]} \int_{-\pi}^{\pi} |a_d(k) - a(k)|^2 dk \tag{3.40}$$

Where $a_d(k)$ is non zero for $-\frac{m}{2} \leq k \leq \frac{m}{2}$ [7]. Then $a_d(k)$ has discrete Fourier transform of $A_d(\omega)$. Parseval's theorem is then expanded to get

$$\min_{a[k]} \sum_{-\frac{m}{2}}^{\frac{m}{2}} |a_d(k) - a(k)|^2 + \sum_{k=-\infty}^{-\frac{m}{2}-1} |a_d(k)|^2 + \sum_{k=\frac{m}{2}+1}^{\infty} |a_d(k)|^2 \tag{3.41}$$

Then it becomes trivial to identify solutions to this optimisation problem. Then values of $a(k)$ are taken such that this magnitude goes to zero by setting $a(k) = a_d(k)$.

$$a(k) = a_d(k) \qquad -\frac{m}{2} \leq k \leq \frac{m}{2} \tag{3.42}$$

To get $a_d(k)$, consider the inverse discreet Fourier transform (IDFT) of the desired response. This minimises the average squared error between $A_d(\omega) - A(\omega)$. Taking from $a_d(k)w(k)$ then

$$A(\omega) = A_d(\omega) * we^{j\omega} \tag{3.43}$$

The actual response $A(\omega)$ is the result of the desired response convolved with the window function. In this case the window function is the rectangular window that minimises the minimum square error (MMSE) [4, 7].

## 3.5 OFDM Simulation

A system model for OFDM is created in this work, based upon the simulation in MATLAB performed with BER calculations for digital modulations BPSK, QPSK, 8QAM, 16QAM, 32QAM and 64QAM. Channel noise is modelled by adding a white Gaussian noise (AWGN) and an AWGN multipath fading channel noise. The channel noise variance decreases with an increase in signal to noise ratio (SNR). In MATLAB, a picture was used as the input signal to identify the OFDM modulation scheme with the lowest bit error rate (BER) per input SNR For 10dB and 20dB input SNR, and the OFDM signal was sent through the channel. The received signal was demodulated for each SNR level, and the obtained data were compared to the original information to evaluate the performance. The results of the simulation may be seen in the Bit Error Rate plot compared to SNR, which gives system performance information.. From 0dB to 10dB SNR, a change in BER is noticeable. AT 20dB SNR to values beyond 20dB SNR, the BER remains constant leading to the choice made for the experiments of 10dB as the low SNR and 20dB as the high SNR values for the input signal.

The OFDM signal was sent through the AWGN channel, and then the experiment was repeated in an AWGN multipath fading channel. The received signal was demodulated for each SNR level and the obtained data were compared to the original information to evaluate the performance. The

results of the simulation may be seen in the Bit Error Rate plot compared to SNR, which gives system performance information. This achieves the first objective of this study.

Eb/N0 (energy per bit to noise power spectral density ratio) is a normalised signal-to-noise ratio (SNR) metric, often known as the "SNR per bit" in digital communication or data transfer. It is notably handy for evaluating the bit error rate (BER) performance of different digital modulation methods without accounting for bandwidth.

Table 3.1: Parameters of OFDM simulation

| **Properties** | **Values** |
|---|---|
| FFT Length, the maximum number of subcarriers in the OFDM system | 64 |
| Number of the fast Fourier transform points | 64 |
| cyclic prefix size | 16 |
| Input SNR in decibels | 10dB and 20 dB |
| Modulation method | BPSK, 8PSK, QPSK, 32QAM and 64QAM |
| Number of OFDM symbols | 10000 |
| Number of bits per OFDM symbol | 26 |
| Number of data sub-carriers | 26 |
| Number of data sub-carriers after coding | 52 |
| OFDM symbol | 80 (64 +16) |

Performance evaluation of OFDM modulation method was simulated using parameters for simulations in Table 3.1 with multipath fading effects, but channel estimation methods were not

analysed for an ideal channel because the effects of multipath fading do not exist in an ideal communication system. Further experiments on the OFDM communication system were simulated in a noisy channel without channel estimation for a particular OFDM modulation scheme. Another set of experiments were conducted for OFDM modulation scheme for the implementation of channel estimation methods in a noisy channel for the removal of multipath fading effects.

The OFDM system simulations made use of parameters in Table 3.1. A cyclic prefix extension of length 16 was used. The modulation order returns a vector that contains linear indices of the nonzero elements in the array that contains a logical 1 or true when data is found in methods of modulation parameter. An image file command was used to fetch the image from the computer file that was specified by the input parameter thereby inferring the file format from its contents. The image file was then converted to a binary stream data format. A stream of binary data bits were shifted to parallel blocks by a serial to parallel shifter. Then the parallel blocks of data, using a suitable modulation scheme, were mapped into symbols. An inverse fast Fourier transformation was then used to change the data stream from frequency domain to the time domain. The signal was shifted to serial data in time domain, followed by the addition of a cyclic prefix to the OFDM signal for orthogonality and combating ISI. Cyclic prefix was removed in the receiver and the data stream was then shifted to parallel blocks for signal processing. Fast Fourier transform was then used for shifting the data stream into the frequency domain. The data stream was then demodulated and was shifted from symbols to bits and finally the bit stream was shifted from the parallel blocks to serial binary data stream thereby recovering the image message signal.

### 3.5.1 Experiment 1a: BPSK in an ideal channel

In experiment 1a, BPSK modulation scheme simulation was performed using the parameters in Table 3.1 for an ideal OFDM communication system.

### 3.5.2 Experiment 1b: BPSK in a noisy channel with Channel estimation

In experiment 1b, BPSK modulation scheme in a noisy channel simulation was performed using the parameters in Table 3.1 for an OFDM system with channel estimation implemented.

### 3.5.3 Experiment 2a: 8PSK in an ideal channel

In experiment 2a, 8PSK modulation scheme was simulated using the parameters in Table 3.1.

### 3.5.4 Experiment 2b: 8PSK in a noisy channel with Channel estimation

In experiment 2b, 8PSK modulation scheme in a noisy channel simulation was performed using the parameters in Table 3.1 for an OFDM system with channel estimation implemented.

### 3.5.5 Experiment 3a: QPSK in an ideal channel

In experiment 3a, QPSK modulation scheme simulation was performed using the parameters in Table 3.1 for an ideal communication system.

### 3.5.6 Experiment 3b: QPSK in a noisy channel with Channel estimation

In experiment 3b, QPSK modulation scheme in a noisy channel simulation was performed using the parameters in Table 3.1 for an OFDM system with channel estimation implemented.

### 3.5.7 Experiment 4a: 16QAM in an ideal channel

In experiment 4a, the 16QAM modulation scheme simulation was performed using the parameters in Table 3.1 for an ideal OFDM communication system.

### 3.5.8 Experiment 4b: 16QAM in a noisy channel with Channel estimation

In experiment 4b, 16QAM modulation scheme in a noisy channel simulation was performed using the parameters in Table 3.1 for an OFDM system with channel estimation implemented.

### 3.5.9 Experiment 5a: 32QAM in an ideal channel

In experiment 5a, 32QAM modulation scheme simulation was performed using the parameters in Table 3.1 for an ideal OFDM communication system.

### 3.5.10 Experiment 5b: 32QAM in a noisy channel with Channel estimation

In experiment 5b, a 32QAM modulation scheme in a noisy channel simulation was performed using the parameters in Table 3.1 for an OFDM system making use of channel estimation method.

### 3.5.11 Experiment 6a: 64QAM in an ideal channel

In experiment 6a, 64QAM modulation scheme simulation was performed using the parameters in Table 3.1 for an ideal OFDM communication system.

### 3.5.12 Experiment 6b: 64QAM in a noisy channel with Channel estimation

In experiment 6b, a 64QAM modulation scheme in a noisy channel simulation was performed using the parameters in Table 3.1 for an OFDM system and channel estimation was implemented.

## 3.6 FBMC Simulation

This Section describes the experiments that were done for FBMC simulations using different modulation parameters for communications systems to achieve the objectives set in Chapter 1. These experiments were conducted in an ideal communication system and repeated in multipath fading channels. The values 0, 0.6, and 2 represent no impairment, mild impairment (rarely cause symbol error recovery) and harsh impairments (which causes symbol errors) respectively. The second prompt was used for the selection of multipath interference: none, mild, and harsh. In the cases of mild and harsh conditions, three copies of a signal that is transmitted get summed at the receiver with each having a different amplitude and delay. This was implemented by passing transmitted signals through a filter. The next pair of simulation prompts concern the FBMC communication system transmitter and receiver oscillators. FBMC receiver system assumes the phase of the oscillator at transmitter module is zero at time of arrival of first sample of the message signal. This assumption is true in an ideal system, however mismatch that occurs between phase of the oscillator at the transmitter and the phase at receiver section is unavoidable. The user was then prompted for carrier phase offset in radians and this was then added to the phase of the

oscillator at the transmitter and it was not added at the receiver. Frequency offset was specified as a percentage of the carrier frequency scaling the carrier frequency at the transmitter, but not scaling the receiver.

Table 3.2: Parameters of an FBMC ideal channel

| **Properties** | **Values** |
|---|---|
| channel noise gain | 0 |
| channel multipath | 0 |
| transmitter mixer frequency offset in percent | 0 |
| transmitter mixer phase offset in radians | 0 |
| baud timing offset as percent of symbol period | 0% |
| symbol period offset | 0 |

### 3.6.1 Experiment 7a: FBMC modulation in an ideal channel

The ideal channel parameters that were used for simulation in an FBMC communication system are as shown in Table 3.2. Transmitter mixer frequency offset, transmitter mixer phase offset, timing offset, symbol period offset, channel noise gain and channel multipath fading parameters were taken to be nil to have a perfect communication system.

### 3.6.2 Experiment 7b: Additive Channel Noise Impairments

Communication impairments are encountered in a real transmission system such that they deviate the system from ideal conditions and these impairments include multipath fading channel. A range of interference and synchronisation impairments that make a violation of the idealized communication system were studied.

Table 3.3: Parameters for mild conditions with additive channel noise impairments

| **Properties** | **Values** |
|---|---|
| channel noise gain | 0.6 |
| channel multipath | 1 |
| transmitter mixer frequency offset in percent | 0 |
| transmitter mixer phase offset in radians | 0.7 |
| baud timing offset as percent of symbol period | 20% |
| symbol period offset | 0 |

Symbol error occurs when the channel noise exceeds half the gap that is in-between symbols that are adjacent in a source constellation. Broadband noise was simulated using the noise gain factor parameter for FBMC modelling. Noise gain factor of 0.6 was implemented and a cluster variance was expected with error free symbols. Noise gain of 2 was implemented in the simulations and expected to lead to a cluster variance of 0.2 with an approximate of 2% of the symbol errors. 10% of errors was expected to result in the received message signal being undecipherable. Performance of the communication system was expected to degrade when there was an increase in noise. Table 3.3 shows the parameters for mild conditions with additive channel noise impairments.

### 3.6.3 Experiment 7c: FBMC modulation in a harsh impairment multipath fading channel

The multipath impairments and additive channel noise impairments that were added in the simulations as given in Table 3.4. The message signal was expected to be unrecoverable when the impairments were high.

Table 3.4: Parameters for harsh impairments multipath fading channel

| **Properties** | **Values** |
|---|---|
| channel noise gain | 2 |
| channel multipath | 2 |
| transmitter mixer frequency offset in percent | 0.01 |
| transmitter mixer phase offset in radians | 0.9 |
| baud timing offset as percent of symbol period | 30% |
| symbol period offset | 1 |

## 3.7 FBMC and OFDM Spectral Efficiency Modelling

Spectral efficiency of FBMC and OFDM was implemented in MATLAB. The length of the filters used were assumed to be equal for OFDM and FBMC modulation schemes. Simulations adjustments on the burst from 0ms up to 30ms were implemented for FBMC and OFDM in MATLAB.

Experiment 8: Spectral Efficiency Modelling

The multicarrier communication systems of FBMC and OFDM were modelled in MATLAB using the parameters given in Table 3.5 to observe the spectral efficiency. The plots were simulated by making adjustments on the duration of the burst from 0ms up to 30ms. Number of cyclic prefix extension and length of the filters used were assumed to be equal thereby making OFDM and FBMC to vary over given bursts. The cyclic prefix size for OFDM was chosen to be 16 and the number of symbols overlapping was minimised to 4 to prevent ISI if the number of symbols overlapping increased. Four bits per subcarrier were used for the simulations.

Table 3.5: Parameters of Spectral efficiency modelling

| **Properties** | **Values** |
|---|---|
| bits per each subcarrier | 4 |
| K represents the symbols that are overlapping | 4 |
| cyclic prefix size | 16 |
| Filter length | 64 |
| Number of the Fast Fourier Transform points | 64 |
| Modulation Methods | FBMC against OFDM |

## 3.8 Chapter Summary

Chapter 3 presented a full description of how the design methodology was done in the OFDM and FBMC modelling using MATLAB simulations. The research methodology was structured in such a way as to answer the research objectives and also answering the research questions given in Chapter 1. MATLAB software was used for the simulations of OFDM using different modulation schemes in this case BPSK, 8PSK, QPSK, 32QAM, and 64QAM. FBMC simulations using MATLAB using PAM modulation scheme for CMT multicarrier modulation technique in an ideal channel and repeated in a multipath fading channel. Various impairments were implemented for FBMC communication system to simulate an ideal and a multipath fading channel. Channel estimation was implemented in an OFDM communication system and experiments were conducted for varying channel impairments. Spectral efficiency was simulated for OFDM against FBMC. A structure for the spectral efficiency modelling of the communication systems of OFDM and FBMC was developed and performance analysis was done to check on which modulation scheme performed better than the other to ensure a good recommendation for future communications.

# Chapter 4

# Results and Discussion

## 4.1 Introduction

This Chapter presents the results which were achieved throughout the OFDM and FBMC simulations in MATLAB and a discussion of the results. Simulation experiments were done for BER performance of AWGN channel and the experiments were repeated for BER performance of AWGN multipath fading channel of OFDM modulation schemes, BPSK, QPSK, 8QAM, 16QAM, 32QAM and 64QAM. FBMC modulation scheme simulations were carried out in an AWGN channel and repeated in an AWGN multipath fading channel. A comparison of Eb/No and SNR is presented to show the effects of increase in SNR on the decrease in BER for theoretical calculations and experimental differences. This is then evaluated against the experimental outcomes of this study for OFDM modulation systems in AWGN channels and AWGN multipath fading channels.

## 4.2 OFDM Modelling Results

Simulations on various OFDM digital modulation schemes were examined using measured input SNR values of 10dB and 20dB in an AWGN channel and repeated in an AWGN multipath fading channel. Noisy channel simulations were examined first without channel estimation method and repeated using least squares channel estimation method.

### 4.2.1 Experiment 1a Results: BPSK in an ideal channel

This section presents the results which were obtained after a BPSK modulation scheme simulation was examined in an ideal channel. In this study, an input SNR of 10dB was examined and the received image had a BER of 0.013 as depicted in Figure 4.1(a). Further increase in input SNR to 20dB resulted in BER of 0.0019 as shown in Figure 4.1(b). BPSK consists of two points on an in phase axis opposite the quadrature axis which maps one bit to one symbol.

Transmitted and recovered images in an ideal communication system were the same because BER was low. Bit error rate remained at 0.0019 when input SNR was increased from 20dB.

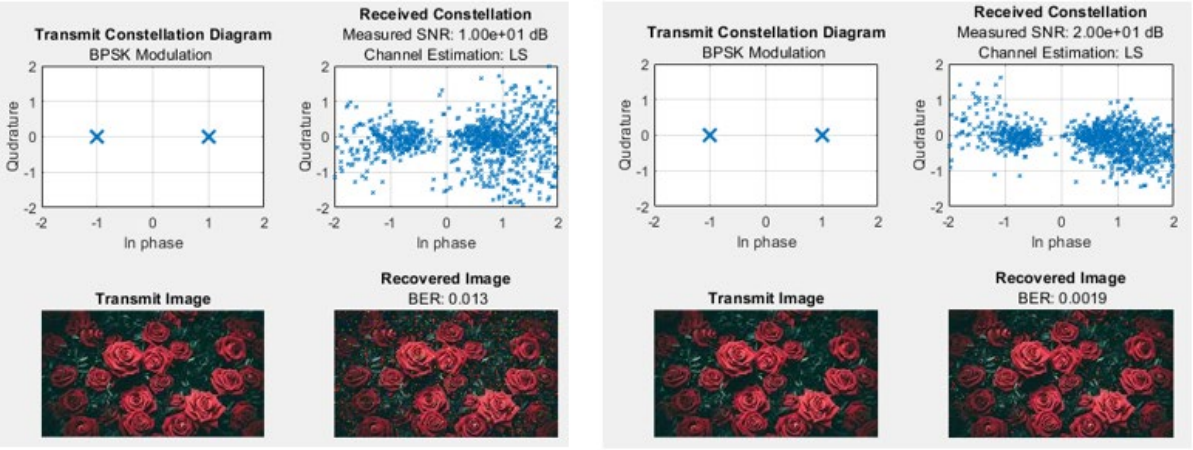


(a) (b)

Figure 4.1 BER performance of AWGN channel for BPSK at input (a) 10dB SNR (b) 20dB SNR

## 4.2.2 Experiment 1b Results: BPSK in a Multipath fading channel

BPSK modulation scheme had 2 points in the transmit constellation on the In Phase axis opposite the quadrature axis and maps one bit to one symbol as shown in Figure 4.2.

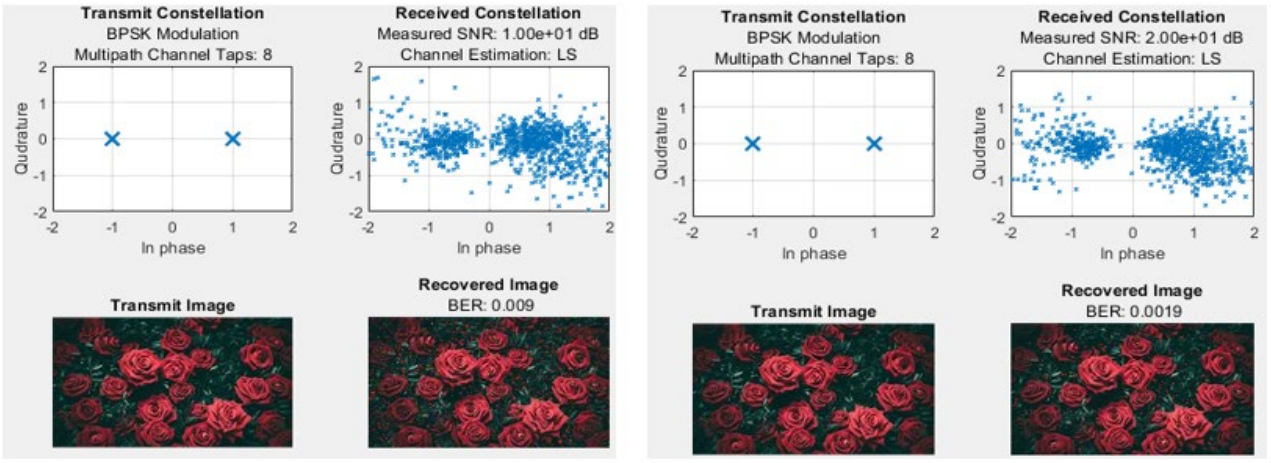


(a) (b)

Figure 4.2: BER performance of AWGN multipath fading channel for BPSK at (a) 10dB SNR (b) 20dB SNR

Least squares channel estimation method was used in the simulation. Input SNR of 10dB resulted in a BER of 0.009 as depicted in Figure 4.2(a). Further increase of input SNR to 20dB resulted in a low BER of 0.0019. The recovered images in Figure 4.2 were similar to the transmitted images.

### 4.2.3 Experiment Results Discussion for BPSK

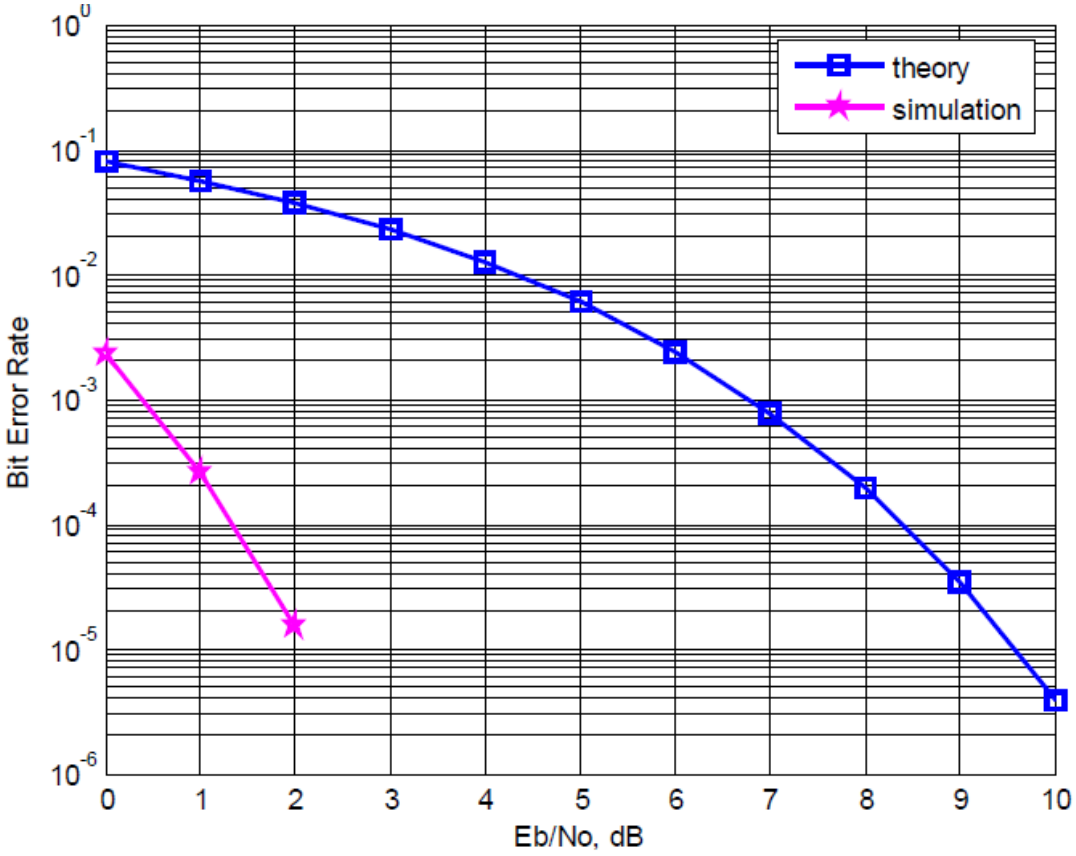


Figure 4.2.1: Bit error rate against Eb /No for BPSK [48].

Fig 4.2.1 depicts plots between BER and Eb/No for BPSK in an OFDM system. When the BER is set between $10^{-4}$ and $10^{-5}$, the simulated Eb/No (db) is 1.4 to 2 and the theoretical Eb/No (db) is 8.4 to 9.6, indicating that the BER for the simulated model is better than the theoretical model for noisy channels. As a result, in a noisy channel, the simulated BPSK model performs better. Even under the worst channel conditions, i.e. for Eb/No dB of 0 to 2 dB. The simulated BPSK model does not allow BER between $10^{-1}$and $10^{-2}$ in [48]. As shown in [48], a 10dB value of SNR results

in BER between $10^{-5}$ and $10^{-6}$. A 20 dB SNR used in the study for BPSK results in a low BER and this agrees with [48].

### 4.2.4 Experiment 2a Results: 8PSK in an ideal channel

The results of experiment 2a which were obtained after an 8PSK modulation scheme was simulated in a noiseless communication system for 8PSK modulation scheme are shown in Figure 4.3. 8PSK expands QPSK by doubling the number of unit points on the unit circle on the In Phase axis opposite the quadrature axis and maps 3 bits to 1 symbol.

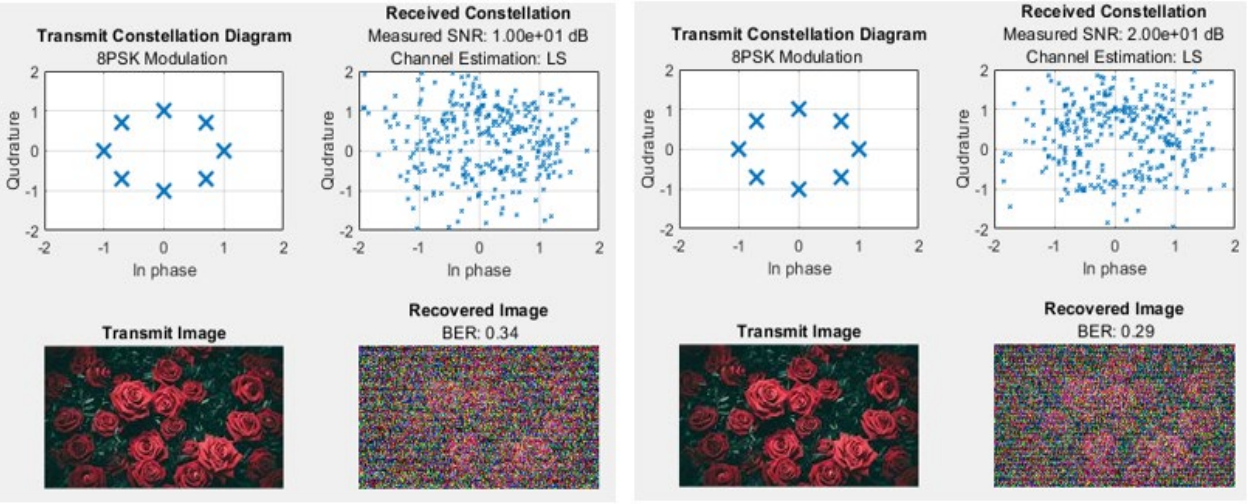


Figure 4.3: BER performance of AWGN channel for 8PSK at input (a) 10dB SNR (b) 20dB SNR

10dB input SNR resulted in achieving a BER of 0.34. The transmit image and the received image were different due to high BER of 0.34 shown in Figure 4.3(a). Input SNR of 20dB resulted in a BER of 0.29. The received image had a high BER leading to loss of recovered image quality. High input SNR beyond 20dB resulted in recovered image having a BER of 0.29.

### 4.2.5 Experiment 2b Results: 8PSK in a noisy channel

8PSK modulation scheme in a multipath channel had 4 unit points on the unit circle on the in phase axis opposite the quadrature axis. As depicted in Figure 4.4(a), a 10dB input SNR resulted in the

received image BER of 0.33. Figure 4.4(b) shows that 10dB input SNR resulted in 0.33 BER as depicted in Figure 4.4 (b).

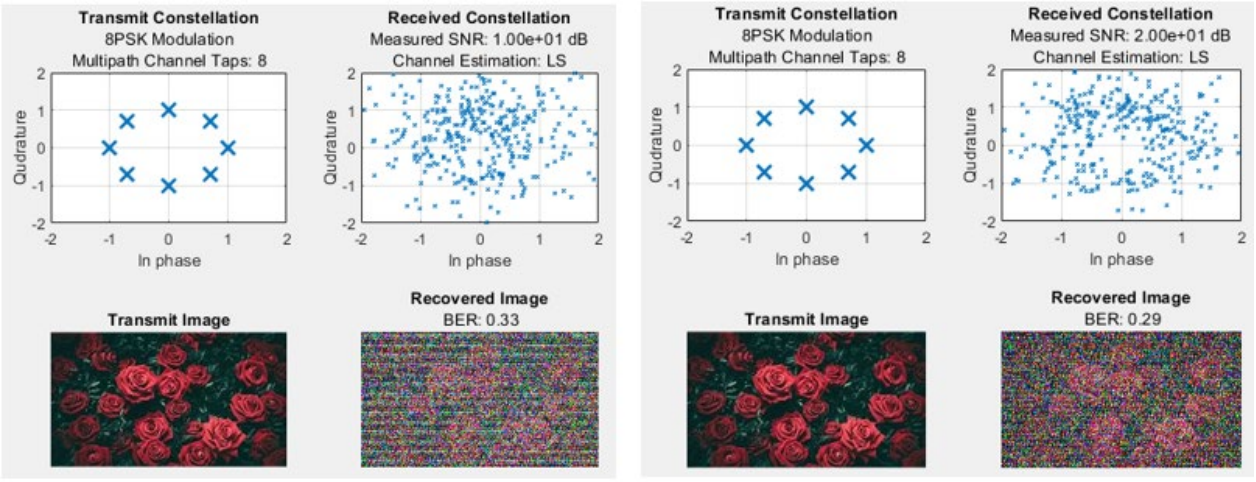


Figure 4.4: BER performance of AWGN multipath channel for 8PSK at input (a) 10dB SNR (b) 20dB SNR

The received image BER was high at 0.33 when a high input SNR of 10dB was used, but a further increase in input SNR to 20dB resulted in decreasing the BER to 0.29 leading to refinement of the recovered image.

### 4.2.6 Experiment 3a Results: QPSK in an ideal channel

Figure 4.5 shows that QPSK has four points on the transmit constellation diagram. QPSK maps 2 bits to 1 symbol. Figure 4.5(a) depicts that an input SNR of 10dB resulted in a BER of 0.075 and an input SNR of 20 dB resulted in a BER of 0.024. QPSK modulation scheme in an ideal communication system had results of higher BER than achieved in an ideal BPSK modulation scheme. Further increase in input SNR above 20dB resulted in the BER of 0.024.

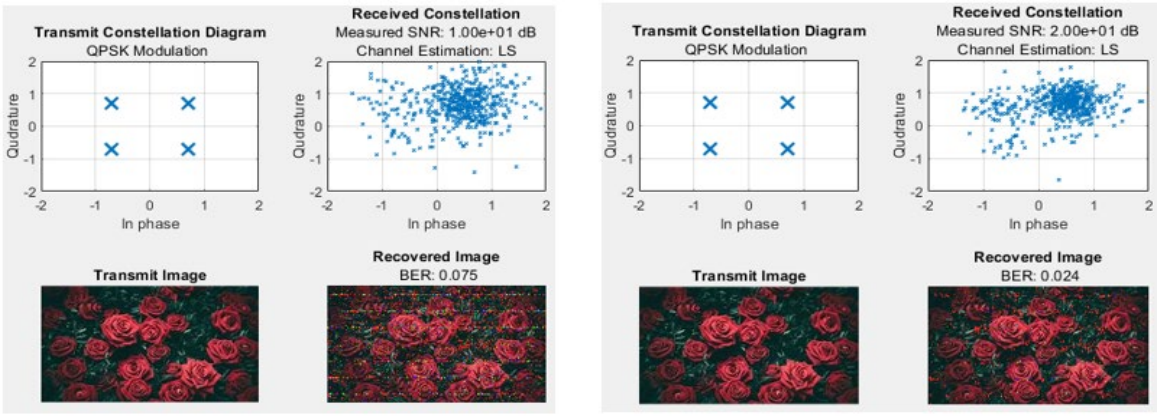


(a) (b)

Figure 4.5: BER performance of AWGN channel for QPSK at (a) 10dB SNR (b) 20dB SNR

The recovered image in QPSK modulation scheme had a BER of 0.024 which was higher than BPSK modulation scheme BER at 20dB SNR.

### 4.2.7 Experiment 3b Results: QPSK in a noisy channel

QPSK has 4 points in the transmit constellation. Least squares estimation method was used.

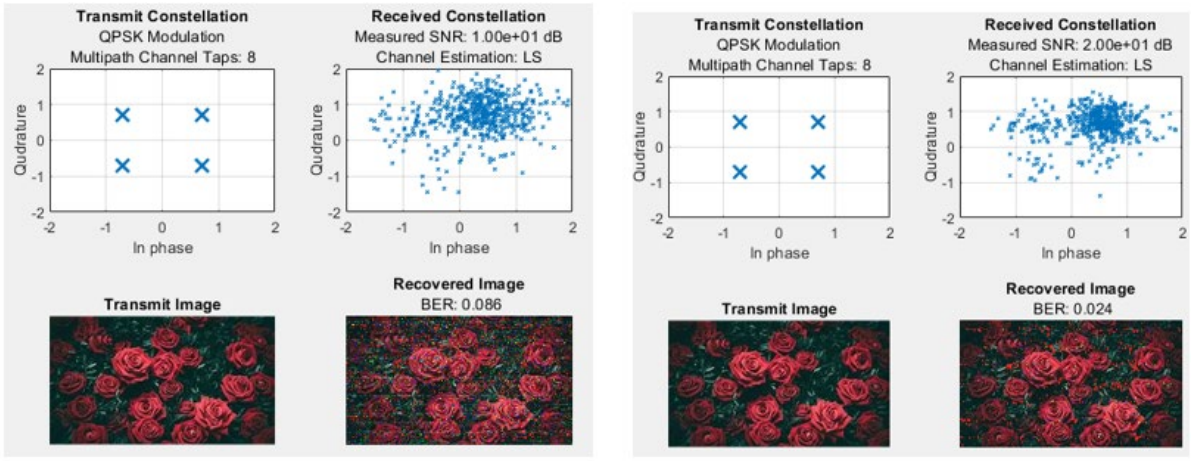


(a) (b)

Figure 4.6: BER performance of AWGN multipath channel for QPSK at (a) 10dB SNR (b) 20dB SNR

The received message signal was recovered with a very BER of 0.086 for a 10dB input SNR shown

in Figure 4.6(a). The BER was decreased to 0.024 by the increase of input SNR to 20dB in Figure 464(b).The recovered image was readable.

### 4.2.8 Experiment Results Discussion for QPSK.

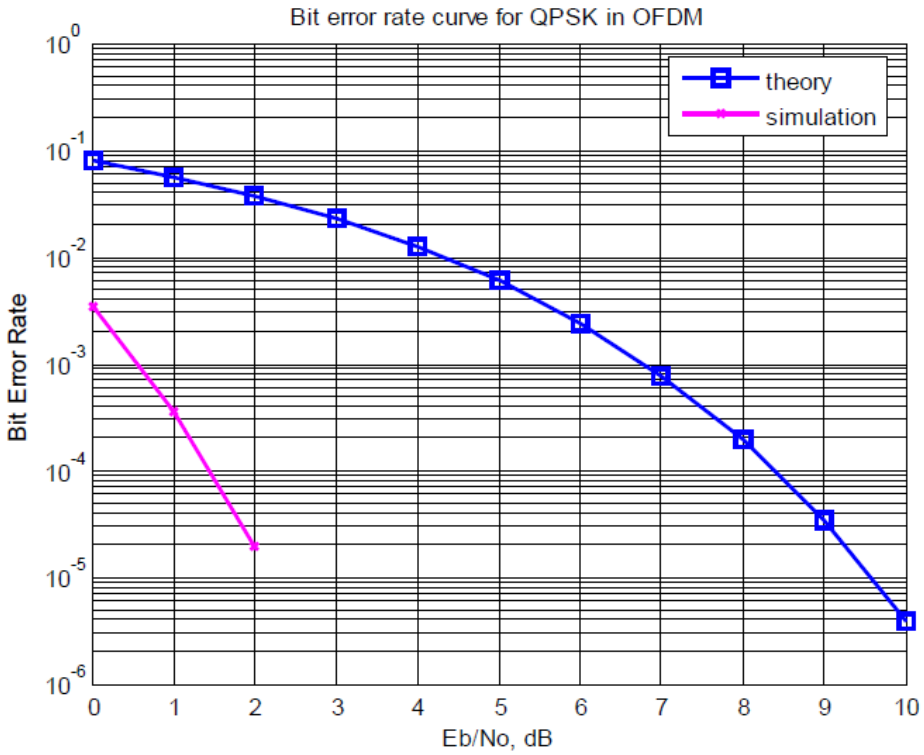


Figure 4.6.1: Bit error rate against Eb /No for QPSK [48].

Figure. 4.2.1 depicts the Simulated Plots between BER and Eb/No for QPSK in an OFDM system as shown in [48]. when the BER is set to $10^{-4}$ or $10^{-5}$, the simulated Eb /No(dB) is 1.5 to 2 while the theoretical Eb /No (dB) is 8.4 to 9.6, indicating that the BER for the simulated model is better than the theoretical model for noisy channel. As a result, the simulated model performs optimally in noisy channels. Even under the worst channel conditions, i.e. for Eb /No (dB) of 0 to 2 dB, the simulated model does not enable BERs between $10^{-1}$ and $10^{-2}$. In this study, a 10dB value of SNR results in 0.086 BER which is in contrast to [48] where the BER is between $10^{-5}$ and $10^{-6}$. A 20 dB SNR used in the study for BPSK results in a low BER and this agrees with [48].

### 4.2.9 Experiment 4a Results: 16QAM in an ideal channel

Figure 4.7 shows that 16QAM has 16 points in the transmit constellation. 16QAM mapped 4 bits to 1 symbol. The recovered image in Figure 4.7(a) had a BER of 0.31 for an input SNR of 10dB.

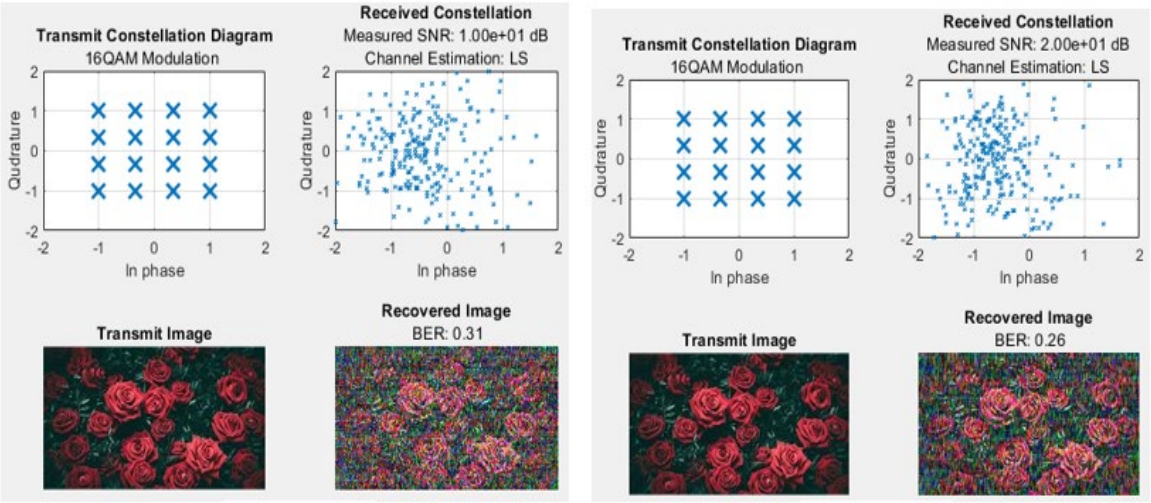


(a) (b)

Figure 4.7: BER performance of AWGN channel for 16QAM at (a) 10dB SNR (b) 20dB SNR

An increase in input SNR to 20dB produced a BER of 0.26 as depicted in Figure 4.7(b). Increase in input SNR resulted in lowering the output BER.

### 4.2.10 Experiment 4b Results: 16QAM in a multipath fading channel.

The transmit constellation plot received in 16QAM had 32 points. 16QAM mapped 8 bits to 1 symbol as shown in Figure 4.8. An input SNR of 10dB resulted in a BER of 0.3 depicted in Figure 4.8(a) and an increase in input SNR to 20dB resulted in a BER of 0.27 depicted in Figure 4.8(b).

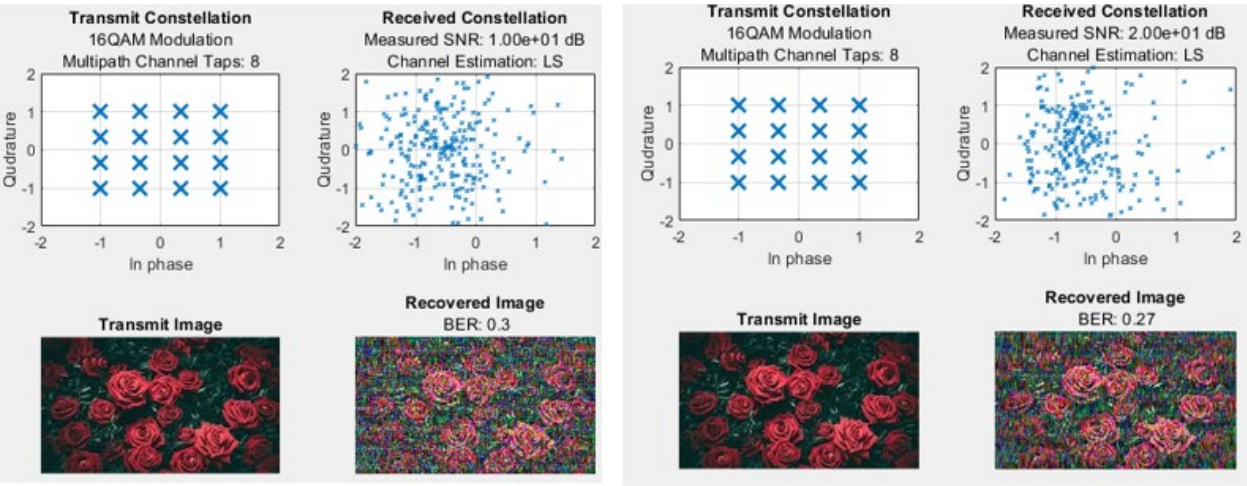


(a) (b)

Figure 4.8: BER performance of AWGN multipath channel for 16QAM at (a) 10dB SNR (b) 20dB SNR

QPSK modulation scheme in a multipath fading system produced bit error rates which are higher to those produced in BPSK modulation scheme.

## 4.2.11 Experiment Results Discussion for 16QAM.

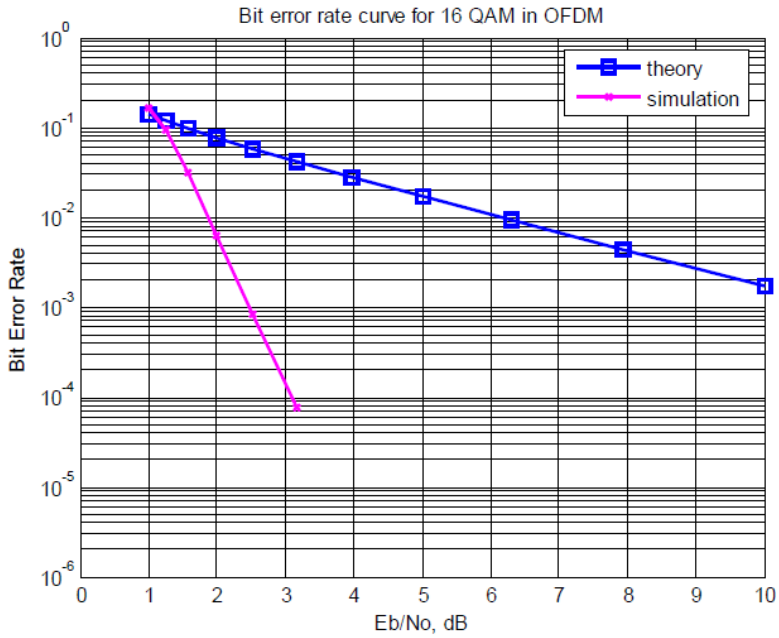


Figure 4.8.1: Demonstrates plot of Bit error rate against Eb /No for 16QAM [48].

Figure 4.2.1 depicts the Simulated Plots between BER and Eb/No for 16 QAM in an OFDM system. When the BER is fixed between $10^{-3}$ and $10^{-4}$, the simulated Eb /No (dB) is 2.5 to 3.1 while the theoretical Eb /No (dB) is 11 to 18, indicating that the BER for the simulated model is better than the theoretical model for noisy channel. As a result, the simulated model performs optimally in noisy channels. The 16 QAM modulation scheme does not support BER values between $10^{-4}$ and $10^{-5}$. In this study, a 10dB value of SNR results in 0.3 BER, which is in contrast to [48], where theoretically 10dB SNR results in $10^{-3}$ BER is shown in Figure 4.8.1. A 20 dB SNR used in the study for BPSK results in a 0.27 BER, and this differs from the theoretical model in [48].

### 4.2.12 Experiment 5a Results: 32QAM in an ideal channel

The results that were obtained after a simulation on a 32QAM modulation scheme in a noiseless communication system are presented in Figure 4.9.

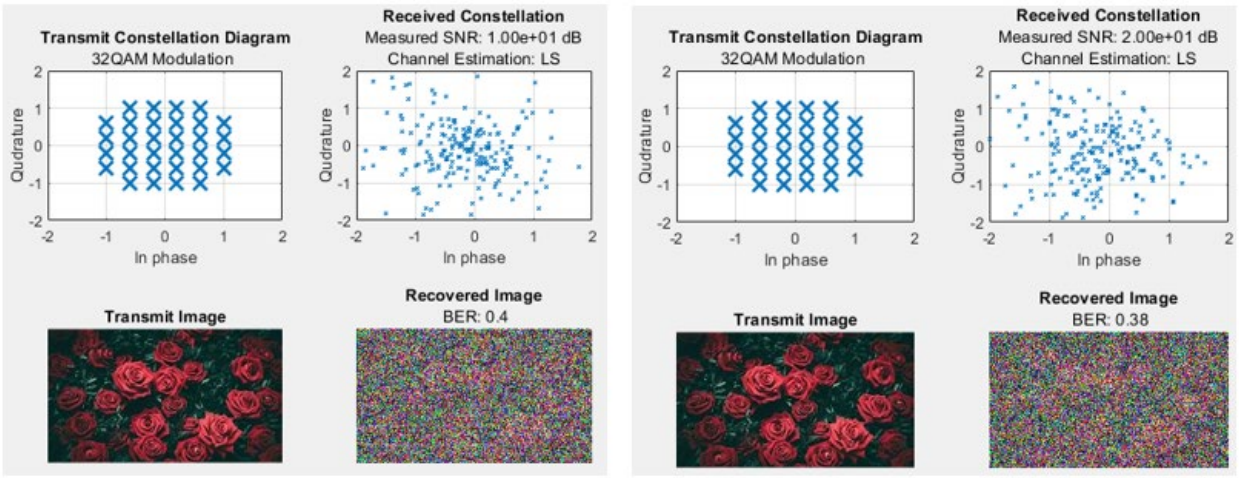


Figure 4.9: BER performance of AWGN channel for 32QAM at (a) 10dB SNR (b) 20dB SNR.

When 10dB input SNR was used, the recovered image had a BER of 0.4 which is shown in Figure 4.9(a). An increase to input SNR to 20dB gave a BER of 0.38 as shown in Figure 4.9(b).

### 4.2.13 Experiment 5b Results: 32QAM in a noisy channel with Channel estimation

The transmit constellation for 32QAM had 16 points in the transmit constellation for a multipath fading channel with least squares estimation method implemented. Figure 4.10(a) shows that an input SNR of 10dB resulted in 0.39 BER.

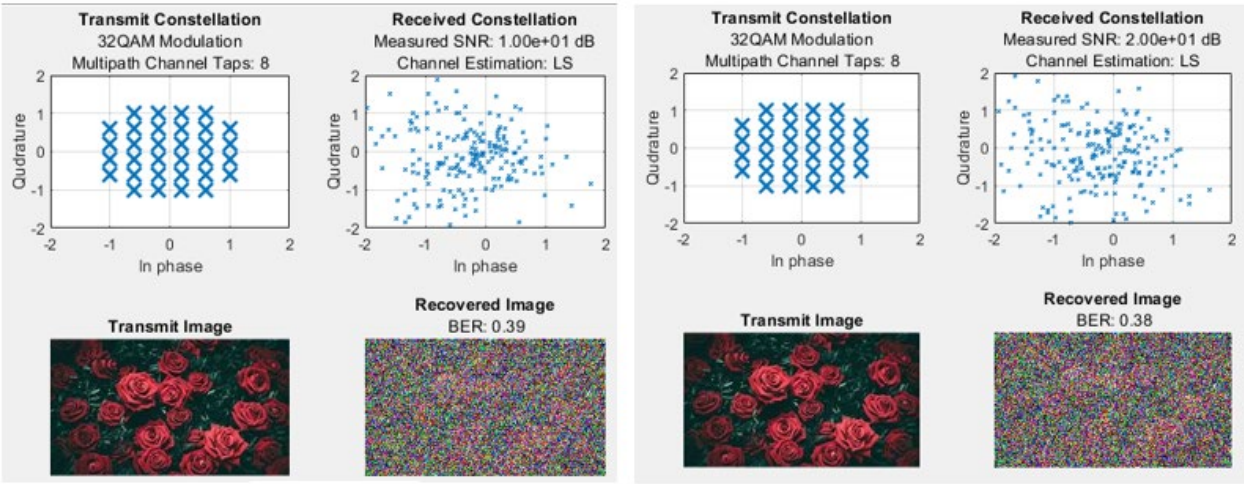


(a) (b)

Figure 4.10: BER performance of AWGN multipath channel for 32QAM at (a) 10dB SNR (b) 20dB SNR

Figure 4.10(b) demonstrates that when an SNR of 20 dB is used, a BER of 0.38 is produced.

### 4.2.14 Experiment Results Discussion for 32QAM.

According to [48], Figure. 4.10.1 depicts the simulated plots between BER and Eb/No for 32 QAM in an OFDM system. When the BER is fixed between $10^{-4}$ and $10^{-5}$, the simulated Eb /No (dB) is 4.9 to 6.1. The theoretical Eb /No (dB) is 32 to 44, indicating that the BER for the simulated model is better than the theoretical model for noisy channels. As a result, the simulated model performs optimally in noisy channels. The simulated model produces an extremely low BER of $10^{-5.5}$ at an Eb /No (dB) ratio of 6.3. In this study, a 10dB value of SNR results in 0.39 BER, which is in contrast to [48], where theoretically 10dB SNR results in $10^{-2.2}$ BER as shown in Figure 4.8.1.

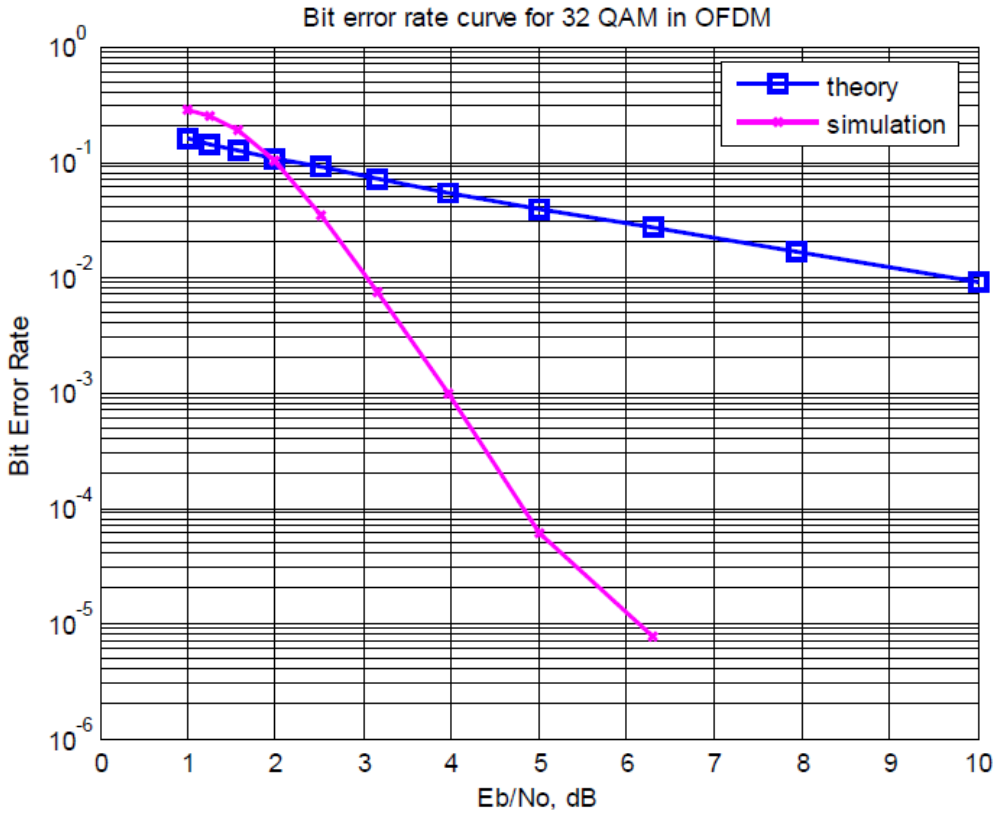


Figure 4.10.1: Demonstrates plot of Bit error rate against Eb /No for 32QAM [48].

A 20 dB SNR used in the study for BPSK in a AWGN multipath fading channel results in a 0.38 BER, which differs from the theoretical model in [48].

### 4.2.15 Experiment 6a Results: 64QAM in an ideal channel.

64QAM had 64 points in the transmit constellation and 64QAM mapped 16 bits to 1 symbol as depicted in Figure 4.11. A 10dB input SNR resulted in a 0.37 BER on the recovered image as shown in Figure 4.11(a). A 20dB input SNR resulted in 0.34 BER as depicted in Figure 4.11(b).

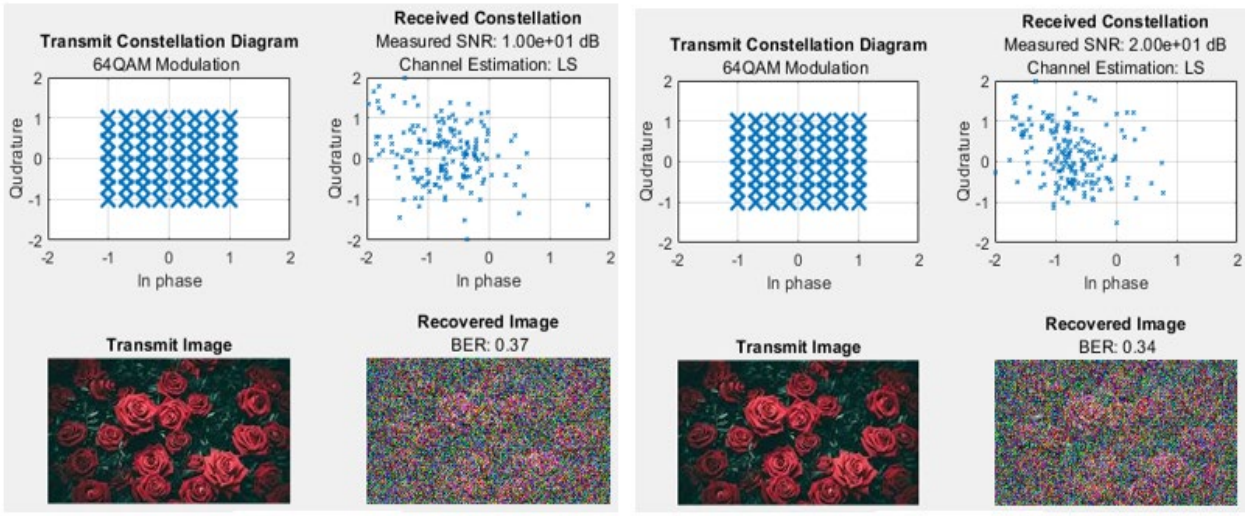


(a) (b)

Figure 4.11: 64QAM in an ideal communication system at input (a) 10dB SNR (b) 20dB SNR

64QAM modulation scheme had a high BER in comparison to BPSK modulation scheme.

## 4.2.16 Experiment 6b Results: 64QAM in a multipath fading channel

64QAM has 64 points in the transmit constellation as shown in Figure 4.12.

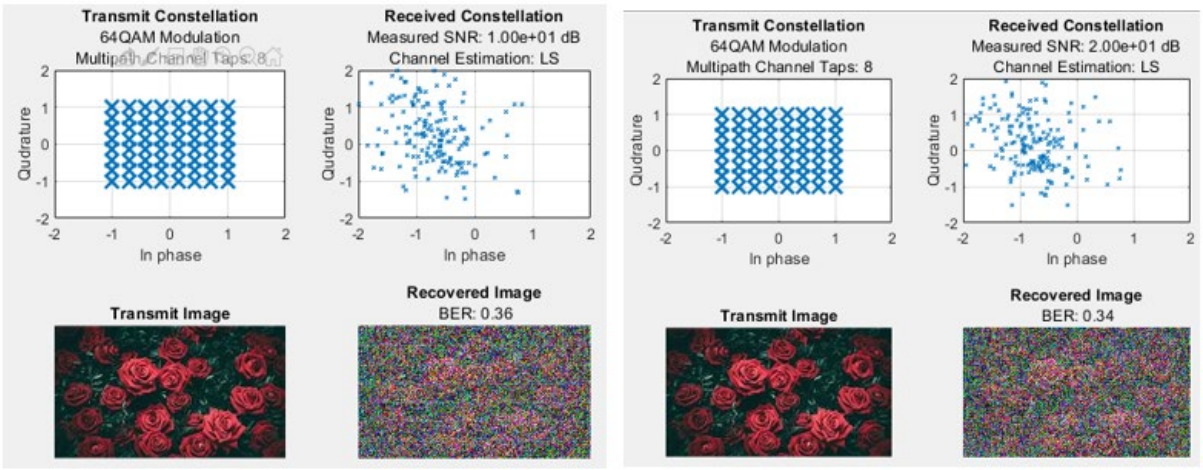


(a) (b)

Figure 4.12: BER performance of AWGN multipath channel for 64QAM at (a) 10dB SNR (b) 20dB SNR

An input SNR of 10dB resulted in 0.36 BER as shown in Figure 4.8(a) and an input SNR of 20 dB resulted in 0.34 BER as depicted in Figure 4.12(b).

### 4.2.17 Experiment Results Discussion for 64QAM.

Figure 4.12.1shows that for 64 QAM, the simulated Eb/No (dB) is 8 to 10 and the theoretical Eb/No (dB) is 45 to 60 when the BER (Bit Error Rate) is fixed between 10-4 and 10-5, indicating that the BER for the simulated model is better than the theoretical model for noisy channel.

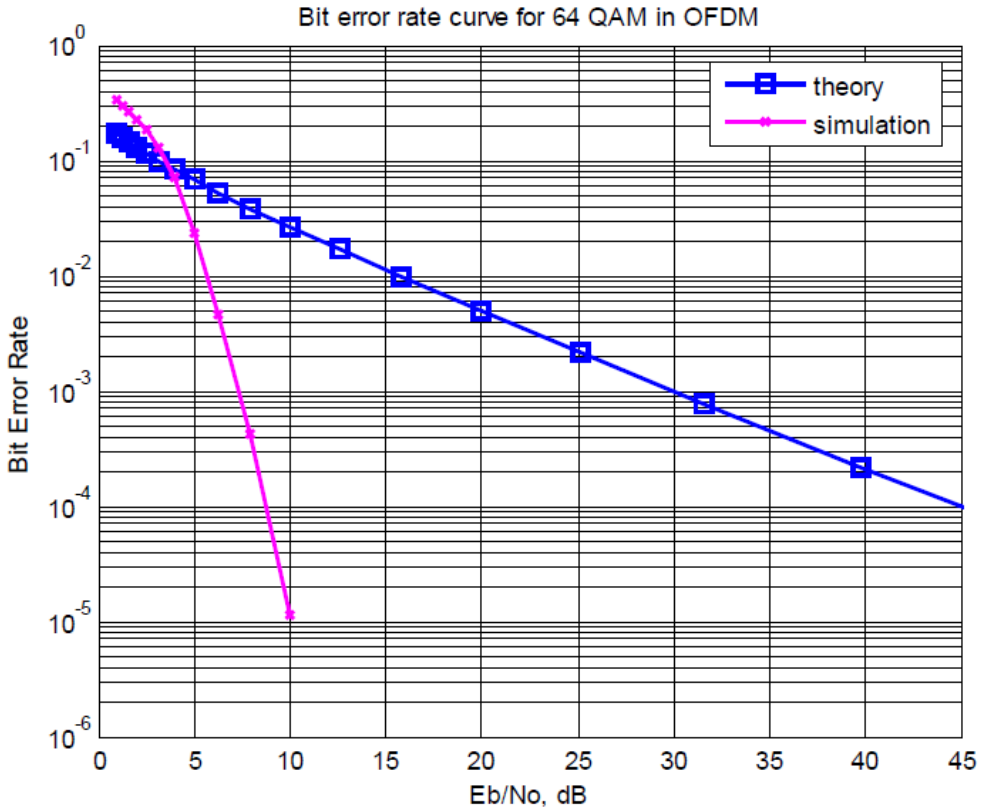


Figure 4.12.1: Demonstrates plot of Bit error rate against Eb /No for 64QAM [48].

As a result, in a noisy channel, the simulated model performs better. At Eb/No (dB) = 10, the simulated model yields an extremely low BER of 10-5. In this study, a 10dB value of SNR results in 0.36 BER, which is identical to BER in [48], where theoretically 10dB SNR results in $10^{-1.8}$ BER as shown in Figure 4.12.1. A 20 dB SNR used in the study for BPSK in an AWGN multipath fading channel results in a 0.34 BER, which differs from the theoretical model in [48].

## 4.3 FBMC Modelling Results

Simulations of the FBMC modulation scheme were carried out in an ideal communication channel and repeated in a multipath fading channel. Frequency and phase offsets were also considered for the implementation of a noisy channel for modelling the FBMC communication system.

### 4.3.1 Experiment 7a Results: FBMC modulation scheme in an ideal Channel

This section presents the results which were obtained after an FBMC modulation scheme simulation was done in a noiseless channel with no multipath fading effects, no frequency and phase offsets. The results of an ideal communication system are shown in Figure 4.13.

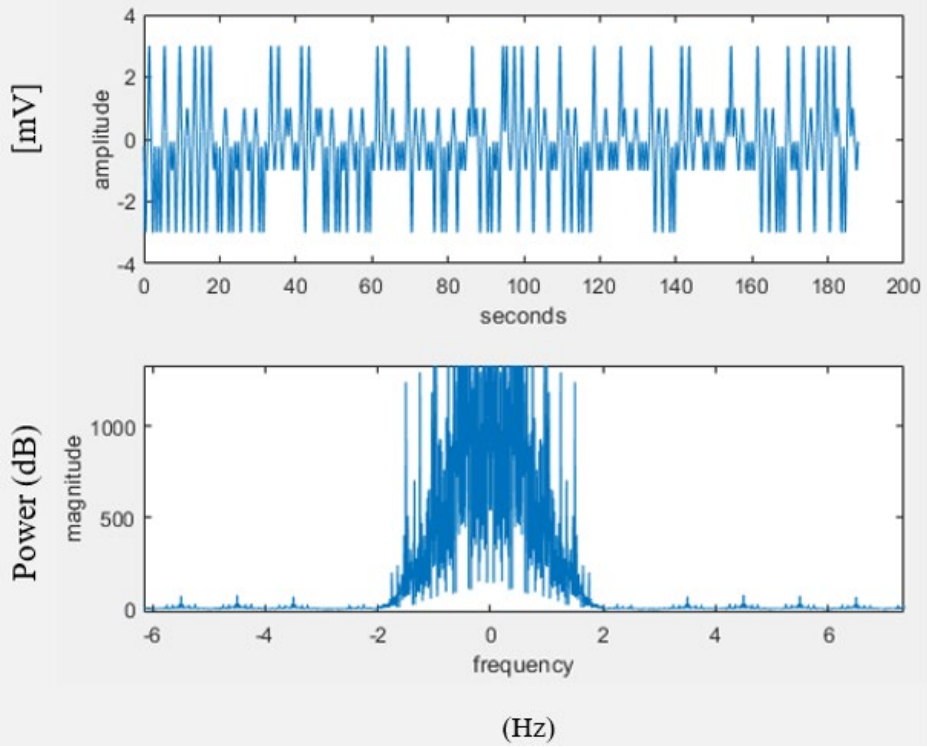


Figure 4.13: FBMC Received signal x3 is identical to the baseband transmitted.

The time interval between the symbols $T$ and the oversampling factor $M$ in which the simulation operates. Oversampling factor is the speed at which the analogue portion of the system evolves. The change from character string to a four-level $T$-spaced sequence mimicking the sequence of $\frac{T}{M}$ spaced pulse filter outputs and its magnitude spectrum are depicted in Figure 4.13. Each pulse was

one time unit long such that successive pulses were initiated without any overlap. For a pulse frequency of 1 kHz, the unit duration of pulses were milliseconds. The magnitude spectrum bandwidth of Figure 4.13 had little apparent energy outside the bandwidth $2Hz$.

The oversampled waveform was up converted by being multiplied with a sinusoid. The transmitted message passband signal and its bandwidth spectrum are depicted in Figure 4.14. The carrier frequency was $f_c = 20$. The Nyquist sampling of a received signal occurred as long as sample frequency $\frac{1}{\frac{T}{M}} = M$ for $T = 1$ is twice the highest frequency in the received signal which was the carrier frequency added to the baseband signal bandwidth of 2Hz.

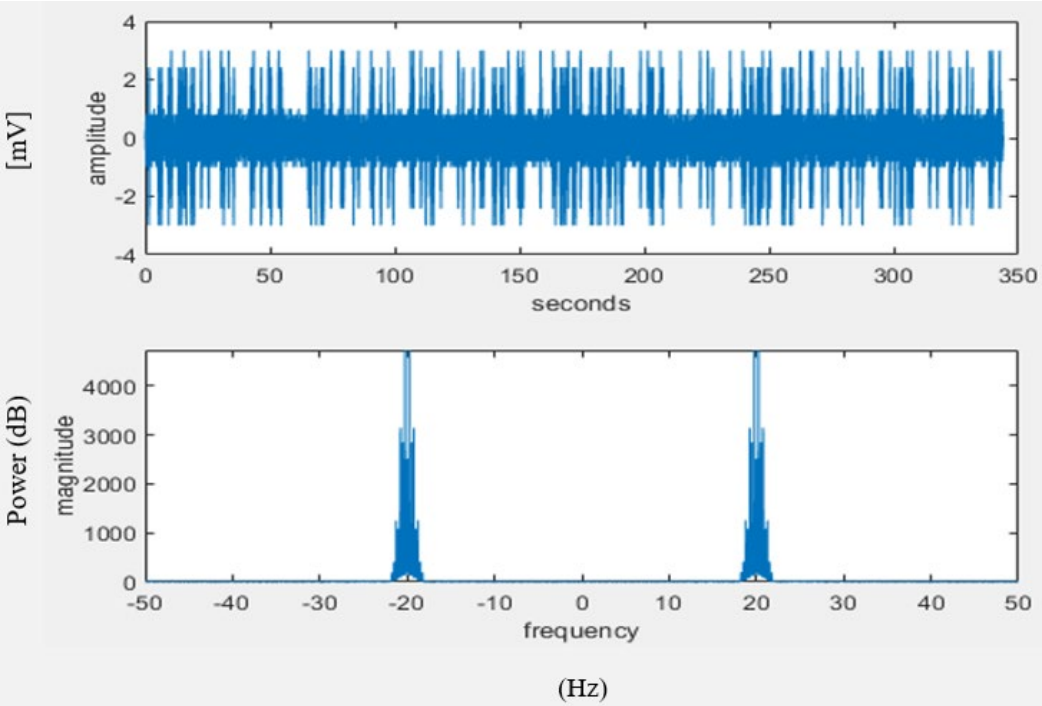


Figure 4.14: The spectrum $X(f)$ and the FBMC Received signal after up conversion.

For the prevention of aliasing of the received signal, $M$ was deduced to be greater than 44. This allowed for the reconstruction of the analogue received signal at the desired points and that proved to be valuable for the times that the samples were taken were not synchronised with the received pulses.

The first $4M$ samples of the resulting message signal had three samples -3, 3 and -3 and it was best taking the samples at the indices $125 + kM$. The delay which was experienced initially corresponded to the half-length of the low-pass filter in addition to the length of the correlator filter added to half the symbol period thereby accounting for the delay which was experienced at

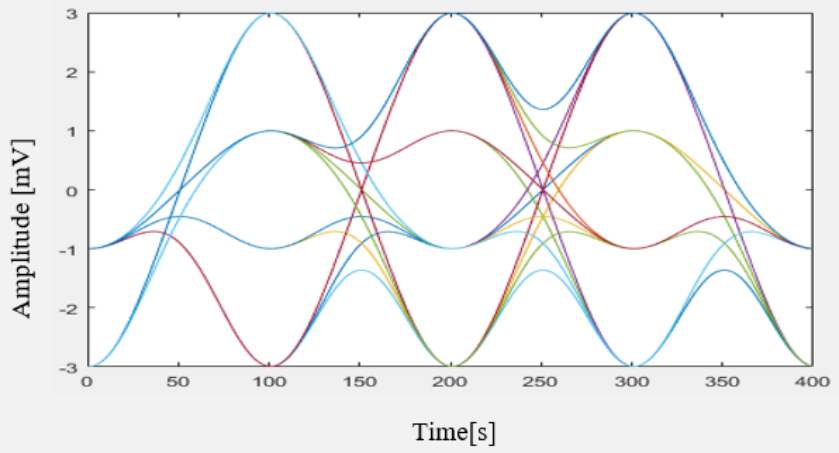


Figure 4.15: The eye diagram of an FBMC ideal communication system.

the start of each of the pulses to its peak. The selection of this delay together with the associated down-sampling was accomplished by simulation in which the MATLAB code recovered the $T$-spaced samples. With reference to Figure 4.15, the parameter for down-sampling was 125. A revealing idea of plotting the oversampled waveform for a complete transmission in order to see subsequent peaks due to the pulses occurs at regular intervals that are precisely on the source alphabet symbol values. For small messages, squeezing such a figure onto one graph is not possible in order to make detailed visual examination of the signal peaks. Plotting the next four symbol periods on top of those first four which was done by shifting the start of a next second block to the time zero. Continuation of that approach over the entire data record triggered the same points in each symbol group. This was implemented in MATLAB for FBMC simulation by first determining maximum number of groups of the samples that fitted in the vector from the $Ith$ sample. A reshape command was used for the formation of a matrix that had $4 * M$ rows and $I$ columns. This was plotted in Figure 4.15 and this type of figure is called the eye diagram which is used for troubleshooting.

### 4.3.1 Decisions and Error Measures

In an analogue communication system, transmitted waveforms attain any values, but however in digital communication systems the message which was transmitted should be one of a small number of the values that are defined by the symbol alphabet. This results in the received waves in the analogue system attaining any value, but in digital communication system implementation the message signal that was recovered was meant to be one of a small number of values which were from a source alphabet. Consequently, when the signal was demodulated to a symbol and when it did not belong to the alphabet, the difference between the demodulated value which was called a soft decision and that nearest element of that alphabet (the hard decision) have a provision to provide the information that shows the performance of the system. When the transmitted message signal differs from the received signal, then errors would have occurred during transmission. The quality of the system was measured by symbol recovery errors. The difference between the message signal and the quantized output of the receiver was used to measure the "hard-decision error".

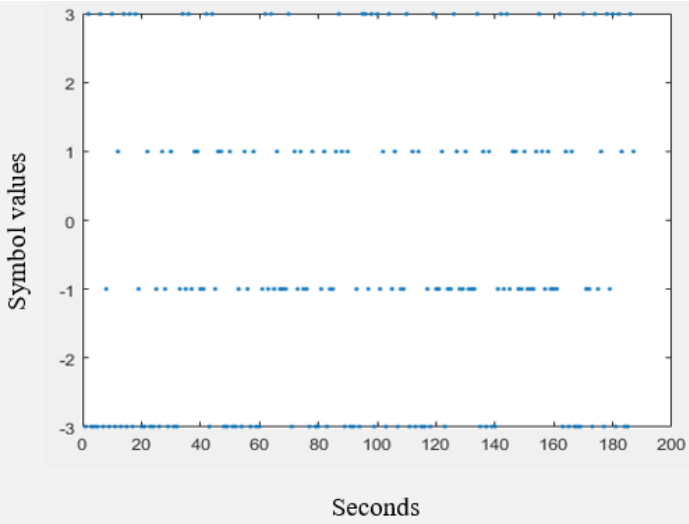


Figure 4.16: Time history of the FBMC constellation diagram.

A vector that contains estimates of the decoded symbols and the commands that produce a time history of the output of the down-sampler as depicted in Figure 4.16. This is called a time history of a constellation diagram where the dots are meant to be near the allowable symbol values. The

points in Figure 4.16 cluster tightly about alphabet values $\pm 1$ and $\pm 3$. How tightly these points cluster was quantified by the use of cluster variance, which is of the square of the difference between decoded symbol values (the soft decisions) in down sampled to symbol rate value and the nearest member of the alphabet( the hard decision). Hard decisions were converted back to a text string which then reproduced the original message. The flaw that existed was that the last symbol of the message signal was lost due to delay of low pass filtering and the pulse-shape correlation. Since four symbols were needed for the single character to be decoded successfully, the loss of the last symbol resulted in loss of character.

### 4.3.2 Experiment 7b Results: Additive Channel Noise Impairments

The channel noise gain parameter was used as a factor that was associated with the Gaussian noise which was added at the received message signal. The FBMC simulation used the suggested values 0, 0.6, and 2 to represent the no impairments, mild impairments and the harsh impairments respectively. Mild impairments rarely caused symbol recovery errors, but the harsh impairments caused multiple symbol errors. Symbol error occurred when the channel noise was greater than half the gap that existed between adjacent symbols that were in the source constellation. In the simulation constellation of $\pm 1s$ and $\pm 3s$, when there was a noise sample with a magnitude which was larger than 1, the output of the quantizer became erroneous.

The received signal is jittery as depicted in figure 4.17. The noise gain factor that was chosen as 0.6 resulted in the cluster variance of 0.02 and no symbol errors. The noise gain factor of 2 resulted in a cluster variance 0.2 which gave an approximately 2% symbol errors. When there were 10% symbol errors, the text that was reconstructed became undecipherable. As was expected that the performance of an FBMC communication degrades as the noise was increased. The eye diagram of a received signal that is noisy is depicted in Figure 4.18.

The noisy eye diagrams show that it is difficult to decode correctly the symbols that are directly from this signal.

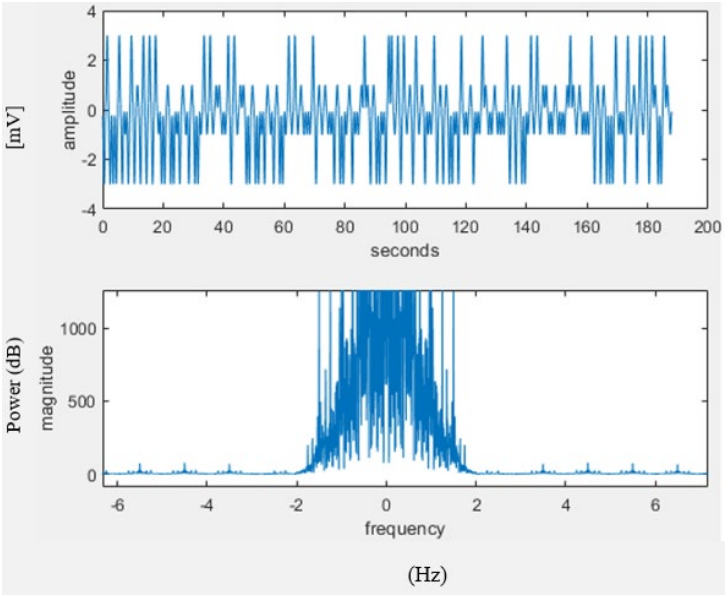


Figure 4.17: Non-zero noise floor exists when noise is added for FBMC.

The correlation filter reduces noise significantly as depicted in Figure 4.17 and Figure 4.14. Comparing Figure 4.17 and Figure 4.14 closely, we observed that whole of Figure 4.17 was shifted in time by 50 samples. This was caused by the time delay of a correlator filter, which is half the length of the filter. It was clear that Figure 4.17 was blurred than Figure 4.11.

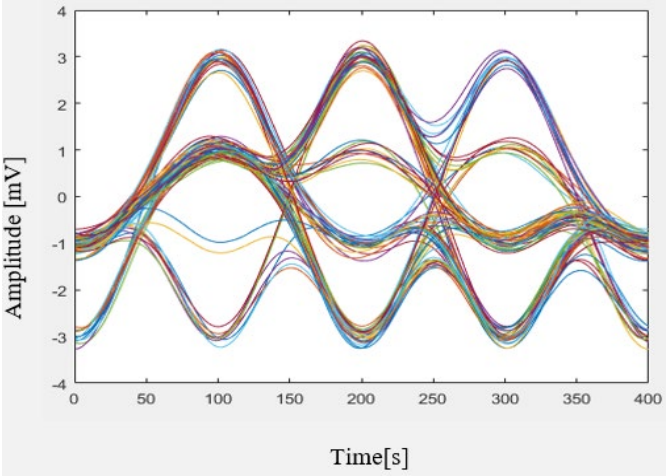


Figure 4.18: FBMC received signal eye diagram for mild additive channel noise

The received signal eye diagram after correlation filter is shown in Figure 4.18. Mild channel noise had no significant effects. The channel noise had no significant effects as the received message could be readable.

Symbol error occurred when the channel noise exceeded half the gap that was in-between symbols that were adjacent in a source constellation. Broadband noise was simulated using the noise gain factor parameter for FBMC modelling. Noise gain factor of 0.6 was implemented and a cluster variance of 0.02 was expected with error free symbols. Noise gain of 2 was expected to lead to a cluster variance of around 0.2 with an approximate of 2% of the symbol errors.

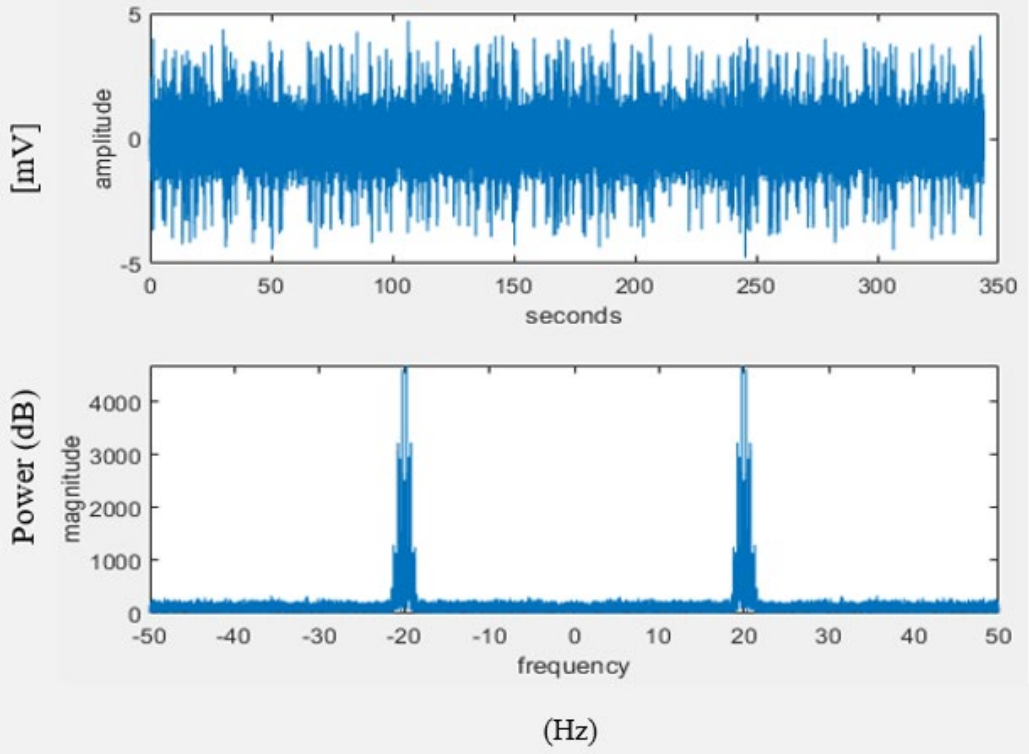


Figure 4.19: FBMC mild additive channel noise is added.

10% of errors results in the received message signal being undecipherable. Performance of the communication system was expected to degrade when there was an increase in noise. Figure 4.19 shows the frequency spectrum attained a noise floor that appeared noticeable.

The received message signal jittery due to the additive channel noise.

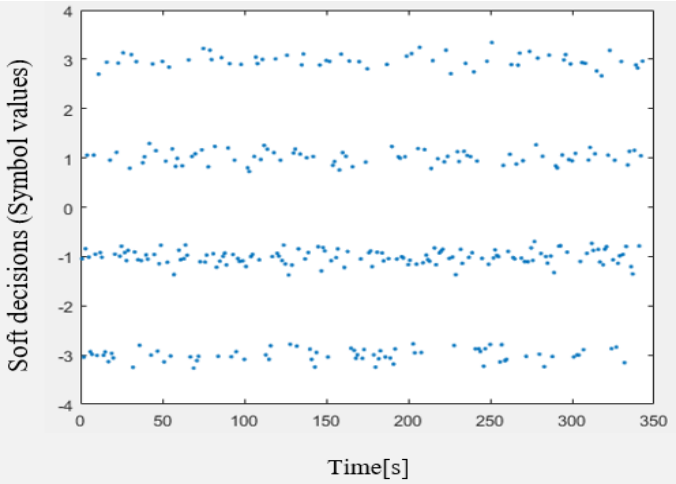


Figure 4.20: FBMC soft decisions for mild additive channel noise

Due to mild additive channel noise, soft decisions were segregated into stripes that corresponded to four symbols as shown in Figure 4.20. The stripes could easily be distinguished.

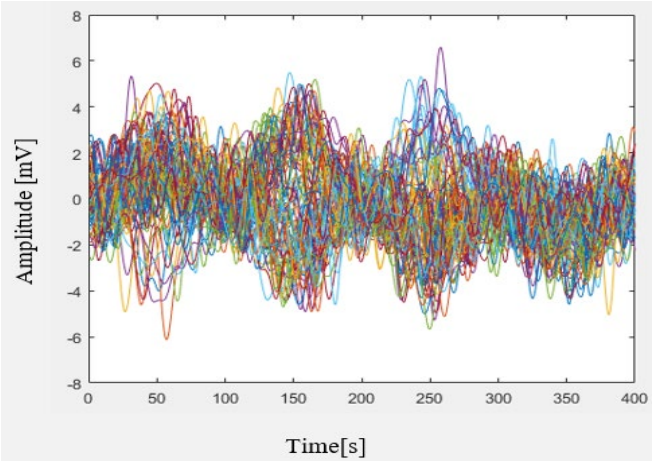


Figure 4.21: FBMC received signal eye diagram for harsh additive channel noise

The received signal eye diagram after correlation filter is shown in Figure 4.21, overlays repeatedly the four symbol wide segments. The channel noise had significant effects as the received message could not be readable. The recovered message was distorted.

### 4.3.3 Experiment 7c Results: multipath fading channel impairments

The results that were obtained when the channel noise gain was 0.6 and the multipath harsh impairments of 2 with the frequency and phase offsets being set to zero are given in Figure 4.22.

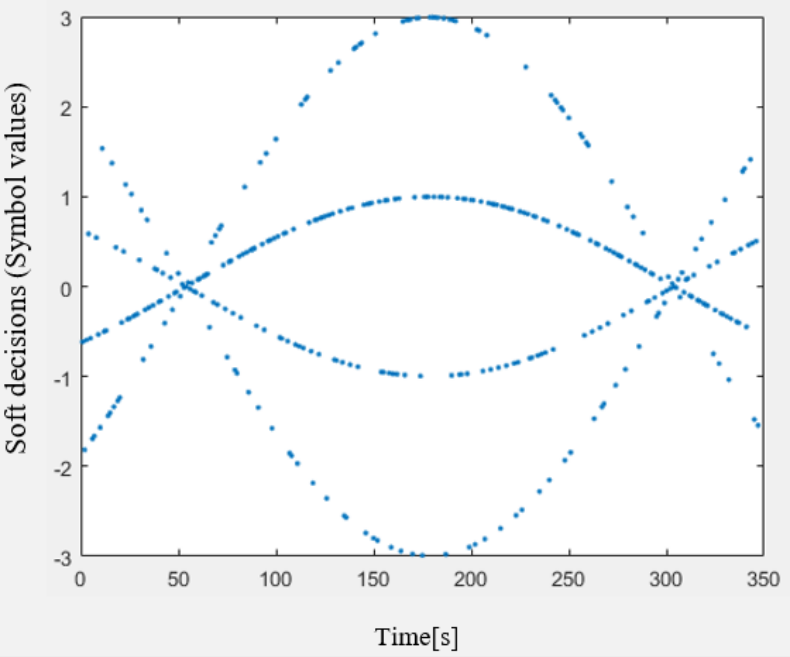


Figure 4.22: FBMC soft decisions for 0.01 frequency offset and 0.9 phase offset

Figure 4.22 shows that any chosen symbol values led to symbol errors. These results show that the receiver frequency and phase offset simulations needed to be adjusted for it to track the frequency and phase of the transmitter.

Figure 4.23 shows effects of mild multipath impairments. Smear soft decision line into stripes, but with harsh multipath fading impairments, the soft decisions were smeared all over and it was impossible to distinguish visually the four stripes which represent four symbol values. Harsh impairments on multipath fading channel had three taps between the receiver and the transmitter.

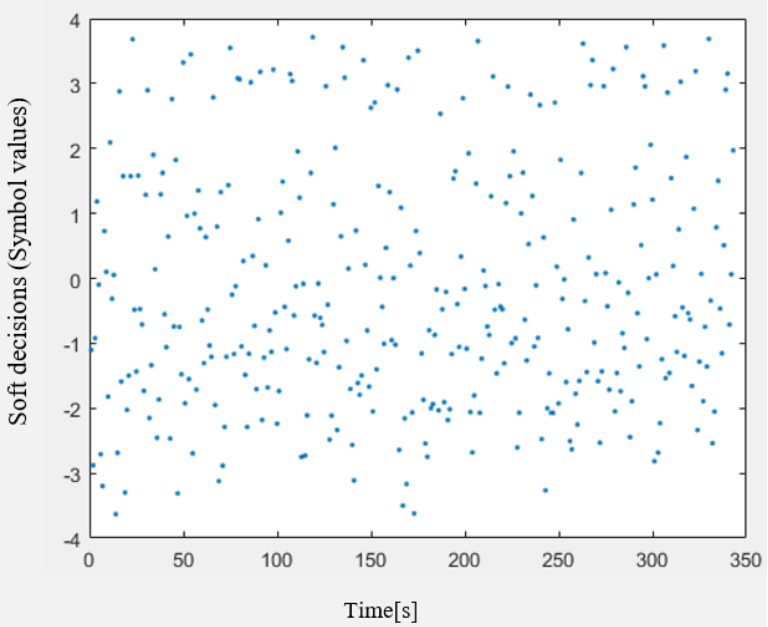


Figure 4.23: FBMC soft decisions smearing for harsh multipath impairments

The channel frequency response had peaks to about +4 dB and down to -8 dB which resulted in the effects being more severe. The received message became unreadable.

## 4.4 FBMC and OFDM Spectral Efficiency Modelling Results

### 4.4.1 Experiment 8: Spectral Efficiency Modelling Results

Figure 4.24 depicts spectral efficiency of FBMC and OFDM. The plot was simulated by making adjustments on the duration of the burst from 0ms up to 30ms. Number of cyclic prefix extension and length of the filter used are equal, OFDM and FBMC vary over 30ms. It was observed that FBMC CMT's spectral efficiency made an increase as the duration of the bursts increased from 0ms to 30ms. The experiment was examined for a duration of 30ms. When the duration increased from 0ms to 2ms FBMC spectral efficiency increased from 0 bps/Hz to 2.35 bps/Hz when the duration was 5ms.

During this transition OFDM remained constant at 3.2 bps/Hz. At 14ms the spectral efficiency of OFDM and FBMC were equal at 3.2 bps/Hz.

An increase in the duration led to the spectral efficiency of FBMC to be higher than spectral efficiency of OFDM as depicted in Figure 4.24

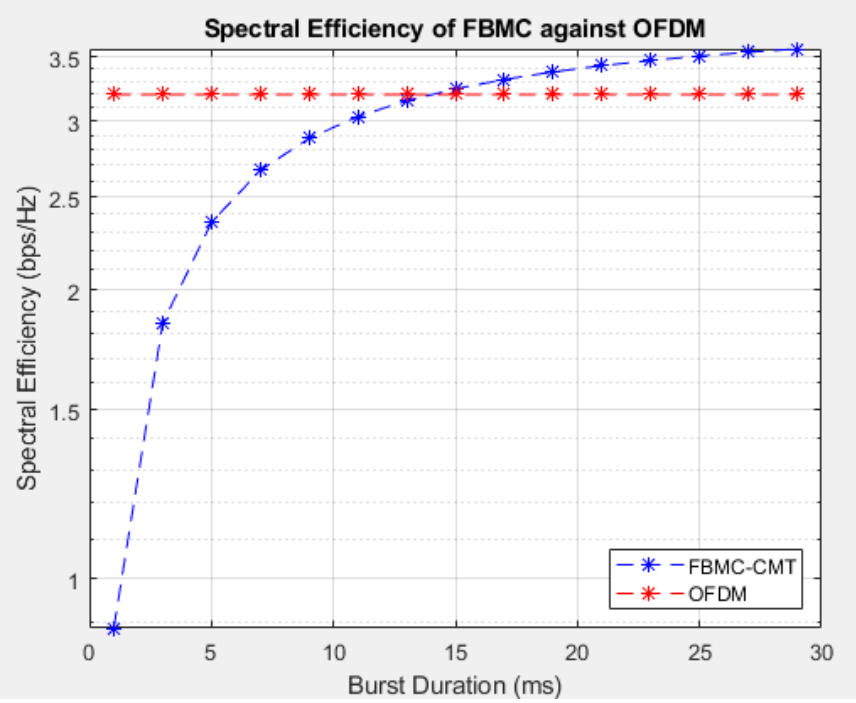


Figure 4.24: Spectral Efficiency of FBMC CMT against OFDM

When the duration got above 14ms the FBMC spectral efficiency gets higher spectral efficiency than OFDM. For lower than 14ms duration OFDM spectral efficiency was higher than FBMC spectral efficiency.

## 4.5 Discussion

The first objective was to evaluate BER of OFDM modulation scheme using BPSK, QPSK, 16QAM, 64QAM at input SNR values of 0dB and 20dB. This objective had the research requirement R2 stated in the research requirements section. This was examined in experiment 1a for BPSK modulation scheme in an ideal system. The results showed that for an input SNR of 10dB in an ideal system, a BER of 0.013 was obtained and a BER of 0.0019 was achieved for

20dB input SNR. BPSK modulation scheme in a multipath fading channel resulted in a BER of 0.09 for input SNR of 10dB and for input SNR of 20dB resulted in a BER of 0.0019.

8PSK modulation scheme was examined in an ideal and multipath fading system with input SNR of 10dB and 20dB. 10dB input SNR resulted in 0.34 BER and 20dB input SNR resulted in 0.29BER in an ideal communication system. In a multipath fading channel, a 10dB input SNR achieved output BER of 0.33 and input SNR of 20dB achieved an output BER of 0.29.

The third experiment was on QPSK modulation scheme whereby in an ideal communication system, a 10dB input SNR resulted in 0.075 BER and 20dB SNR resulted in 0.024BER. In a multipath fading channel, an input of 10dB SNR resulted in 0.086BER and 20dB input SNR resulted in recovered image with 0.024 BER.

The fourth experiment examined 16QAM modulation scheme. In an ideal system, an input of 10dB SNR resulted in 0.31 BER and a 20dB SNR input resulted in 0.26 BER. In a communication system with multipath fading channel, 10dB input SNR resulted in 0.3 BER and 20dB SNR resulted in 0.27 BER.

An experiment on 32 QAM modulation scheme was examined for an ideal and multipath fading channel systems. In an ideal communication system a 10dB SNR input resulted in 0.4 BER and a 20dB SNR resulted in 0.38 BER. For 32QAM modulation scheme with a multipath fading channel, an input SNR of 10dB resulted in 0.39 BER and 20dB SNR resulted in 0.38 BER.

The sixth experiment was on 64QAM modulation scheme for an ideal communication system and a multipath fading channel system. For an ideal communication system, an input SNR of 10dB resulted in 0.39 BER and an input SNR of 20dB resulted in 0.38 BER. The lowest BER was achieved using BPSK modulation scheme.

Simulations in an ideal channel were done and repeated in a multipath fading channel and frequency and phase offsets were also considered for implementation of a noisy channel for modelling the FBMC communication system. In experiment 7a, FBMC modulation scheme simulation was done in an ideal communication system. The received signal eye diagram after correlation filter was plotted and the constellation diagrams depicting the soft decisions were obtained in the plot of a constellation diagram time history. There was no channel noise implemented. In experiment 7b, the frequency spectrum attained a noise floor that appeared noticeable. The received message signal appeared jittery due to the additive channel noise that was added. The received signal eye diagram after correlation filter showed mild channel noise. The channel noise had no significant effects as the received message could be readable. Due to mild additive channel noise, soft decisions were segregated into stripes that corresponded to four symbols. The stripes could easily be distinguished. The received signal eye diagram after correlation filter overlays repeatedly the four symbol wide segments. The channel noise had no significant effects as the received message could be readable. In experiment 7c, the results that were obtained when the channel noise gain was 0.6 and the multipath harsh impairments of 2 with the frequency and phase offsets being set to zero. The soft decisions for 0.01 frequency offset and 0.9 phase offset results show that the receiver frequency and phase offset simulations needed to be adjusted in order to track the frequency and phase of the transmitter. Soft decisions for harsh multipath impairments were smeared and it was impossible for distinguishing visually of the four stripes which represent four symbol values. Harsh impairments on multipath fading channel had three taps/paths between the receiver and the transmitter. The channel frequency response had peaks to about +4 dB and down to -8 dB which resulted in the effects being more severe. The received message became unreadable.

The third objective was to evaluate the spectral efficiency of OFDM modulation scheme in comparison with FBMC modulation scheme and it addressed the requirement R3 that was set in the main requirements. In experiment 8 for spectral efficiency modelling, the simulations were examined for a burst duration of 30ms. When the burst duration increased from 0ms to 2ms FBMC

spectral efficiency increased from 0 bps/Hz to 2.35 bps/Hz when the burst duration was 5ms. During this transition OFDM remained constant at 3.2 bps/Hz. At 14ms burst duration the spectral efficiency of OFDM and FBMC were equal at 3.2 bps/Hz. A further increase in the burst duration led to the spectral efficiency of FBMC to be higher than spectral efficiency of OFDM.

## 4.6 Chapter Summary

Chapter 4 presents the results of the simulations of OFDM and FBMC modulation system in an ideal channel and repeated in a multipath fading channel. Simulations were done for 0dB and 20dB input SNR for OFDM modulation scheme. The results for ideal channel, multipath fading channel without channel estimation methods were implemented and repeated using a multipath fading channel with channel estimation methods in the receiver module. The results were shown for different input parameters of an ideal channel simulation and a multipath fading channel simulations of OFDM and FBMC modulation techniques. As the modulation order increased, the constellation became dense and a high SNR was needed to preserve the BER. Results on spectral efficiency for a range of 30 bursts for OFDM against OFDM are obtained and shown. Ideal communication system is not possible in a realistic communication system. Impairments result in bit error rates in a communication system.

# Chapter 5

# Conclusion And Future Work

The first step for this research was identifying a research area in communications that had a need in enhancements in multicarrier modulation techniques. OFDM and FBMC modulation techniques were chosen for analysis between them. After the identification of a possible research area, the aims and objectives to be studied on were established. A methodology to be implemented was then designed to achieve the goals set in order to obtain the stated research questions and objectives. All evaluations were possible to be implemented in software in this case MATLB modelling software was used. The next step was deciding on how the simulations were to be done. MATLAB code snippets were then formulated to achieve the desired objectives. OFDM modelling using different modulation schemes in this case 16QAM, BPSK, 8PSK, QPSK, 32QAM, 64QAM, were implemented in MATLAB and FBMC using the PAM modulation scheme in CMT was also implemented in MATLAB. Spectral efficiency of OFDM against FBMC was simulated. A literature review was done for the study and then design methodology was implemented.

This Chapter deals with the discussion of the results that were obtained and presented in the previous chapter in chapter 4.

## 5.1 Conclusion

The research objectives which were set for this simulation project were examined and the results were obtained. The results are presented in the order in which the research objectives were set.

QPSK modulation scheme in a multipath fading system produced bit error rates which are higher to BER produced in BPSK modulation scheme. 8PSK modulation scheme produced a higher BER

compared to BER of BPSK modulation scheme at the same input SNR. As the modulation order increased the BER increased with 64QAM having the highest BER. Frequency and Phase offsets resulted in symbol error rate increasing as the impairment increased in FBMC. Spectral Efficiency of OFDM is higher than FBMC spectral efficiency at low burst durations. AT high burst durations, FBMC spectral efficiency is higher than OFDM spectral efficiency.

FBMC modulation scheme has high spectral efficiency at high burst durations such that it is recommended that FBMC be used in MIMO communications for spatial modulation. Further increase in spectral efficiency should be accompanied by a high energy efficiency communication system such that this area should be researched for green communication. High spectral efficiency leads to high consumption of power leading to high PAPR which results in low energy efficiency in communication systems.

## 5.2 Recommendations

This research project has provided valuable insight on the OFDM and FBMC modulation techniques. Further research in these areas is of paramount importance such that multipath fading effects can be efficiently and accurately compensated for, if not entirely eradicated for a system with very dense multipath fading effects. There are other techniques which can be of significant use in research in the implementation of OFDM and FBMC to be done using a massive multiple input multiple output techniques. Use of pilot symbols should also be taken into account for OFDM modelling and FBMC modelling to check on the performance evaluations of the two modulation schemes. Modelling of OFDM and FBMC to achieve a low peak to average power ratio which is a much-needed aspect I development of future communications.

From the results obtained in this research project, it is hoped that a further research into this area be taken up for future communications to be innovated and come up with efficient modulation methods for future communications modulation methods. Research can be taken up to implement FBMC using the golden code spatial modulation.

# References


[1] M. Agiwal, A. Roy, and N. Saxena, "Next generation 5G wireless networks: A comprehensive survey," *IEEE Communications Surveys & Tutorials,* vol. 18, pp. 1617-1655, 2016.

[2] Y. Cai, Z. Qin, F. Cui, G. Y. Li, and J. A. McCann, "Modulation and multiple access for 5G networks," *IEEE Communications Surveys & Tutorials,* vol. 20, pp. 629-646, 2017.

[3] B. Sklar, *Digital communications: fundamentals and applications*, 2001.

[4] M. Sauter, *From GSM to LTE-advanced Pro and 5G: An introduction to mobile networks and mobile broadband*: John Wiley & Sons, 2017.

[5] T. Seki, N. Taga, and S. Okita, "OFDM transmission/reception system and transmitting/receiving apparatus," ed: Google Patents, 1997.

[6] J. G. Proakis and M. Salehi, *Digital communications* vol. 4: McGraw-hill New York, 2001.

[7] F.-L. Luo and C. J. Zhang, *Signal processing for 5G: algorithms and implementations*: John Wiley & Sons, 2016.

[8] A. Ibrahim and M. Abdullah, "The potential of FBMC over OFDM for the future 5G mobile communication technology," in *AIP Conference Proceedings*, 2017, p. 020001.

[9] R. Van Nee and A. De Wild, "Reducing the peak-to-average power ratio of OFDM," in *VTC'98. 48th IEEE Vehicular Technology Conference. Pathway to Global Wireless Revolution (Cat. No. 98CH36151)*, 1998, pp. 2072-2076.

[10] C. R. Johnson Jr, W. A. Sethares, and A. G. Klein, *Software receiver design: build your own digital communication system in five easy steps*: Cambridge University Press, 2011.

[11] P. Kansal and A. K. Shankhwar, "FBMC vs OFDM waveform contenders for 5G wireless communication system," *Wireless Engineering and Technology,* vol. 8, pp. 59-70, 2017.

[12] T. S. Rappaport, *Wireless communications: principles and practice* vol. 2: prentice hall PTR New Jersey, 1996.

[13] L. Thibault and M. T. Le, "Performance evaluation of COFDM for digital audio broadcasting. I. Parametric study," *IEEE Transactions on broadcasting,* vol. 43, pp. 64-75, 1997.

[14] Y. Wu and B. Caron, "Digital television terrestrial broadcasting," *IEEE Communications Magazine,* vol. 32, pp. 46-52, 1994.

[15] W. Henkel, G. Taubock, P. Odling, P. O. Borjesson, and N. Petersson, "The cyclic prefix of OFDM/DMT-an analysis," in *2002 International Zurich Seminar on Broadband Communications Access-Transmission-Networking (Cat. No. 02TH8599)*, 2002, pp. 22-22.

[16] J. Jose, A. Ashikhmin, T. L. Marzetta, and S. Vishwanath, "Pilot contamination problem in multi-cell TDD systems," in *2009 IEEE International Symposium on Information Theory*, 2009, pp. 2184-2188.

[17] H. Rohling and R. Grunheid, "Performance of an OFDM-TDMA mobile communication system," in *Proceedings of Vehicular Technology Conference-VTC*, 1996, pp. 1589-1593.

[18] T. Jiang and G. Zhu, "OFDM peak-to-average power ratio, reduction by complement block coding scheme and its modified version," in *IEEE 60th Vehicular Technology Conference, 2004. VTC2004-Fall. 2004*, 2004, pp. 448-451.

[19] S. H. Muller and J. B. Huber, "OFDM with reduced peak-to-average power ratio by optimum combination of partial transmit sequences," *Electronics letters,* vol. 33, pp. 368-369, 1997.

[20] E. Dahlman, S. Parkvall, and J. Skold, *4G, LTE-advanced Pro and the Road to 5G*: Academic Press, 2016.

[21] B. Farhang-Boroujeny, *Signal processing techniques for software radios* vol. 2: Lulu publishing house, 2008.

[22] A. Farhang, A. Aminjavaheri, N. Marchetti, L. E. Doyle, and B. Farhang-Boroujeny, "Pilot decontamination in CMT-based massive MIMO networks," in *2014 11th International Symposium on Wireless Communications Systems (ISWCS)*, 2014, pp. 589-593.

[23] L. W. Couch, *Digital & Analog Communication Systems*: Pearson Higher Ed, 2012.

[24] H. Zarrinkoub, *Understanding LTE with MATLAB: from mathematical modelling to simulation and prototyping*: John Wiley & Sons, 2014.

[25] R. O'neill and L. Lopes, "Envelope variations and spectral splatter in clipped multicarrier signals," in *Proceedings of 6th International Symposium on Personal, Indoor and Mobile Radio Communications*, 1995, pp. 71-75.

[26] M. H. Rehmani and R. Dhaou, *Cognitive Radio, Mobile Communications and Wireless Networks*: Springer, 2019.

[27] M. Rupp, "Training and synchronization sequences for wireless systems with multiple transmit and receive antennas used in CDMA or TDMA systems," ed: Google Patents, 2007.

[28] D. Wulich and L. Goldfeld, "Reduction of peak factor in orthogonal multicarrier modulation by amplitude limiting and coding," *IEEE Transactions on Communications,* vol. 47, pp. 18-21, 1999.

[29] L. Cimini, "Analysis and simulation of a digital mobile channel using orthogonal frequency division multiplexing," *IEEE transactions on communications,* vol. 33, pp. 665-675, 1985.

[30] L. Hanzo, Y. Akhtman, J. Akhtman, L. Wang, and M. Jiang, *MIMO-OFDM for LTE, WiFi and WiMAX: Coherent versus non-coherent and cooperative turbo transceivers*: John Wiley & Sons, 2011.

[31] N. Hassan and X. Fernando, "Massive MIMO wireless networks: An overview," *Electronics,* vol. 6, p. 63, 2017.

[32] L. Lin and B. Farhang-Boroujeny, "Cosine-modulated multitone for very-high-speed digital subscriber lines," *EURASIP Journal on Advances in Signal Processing,* vol. 2006, p. 019329, 2006.

[33] C. Lim, T. Yoo, B. Clerckx, B. Lee, and B. Shim, "Recent trend of multiuser MIMO in LTE-advanced," *IEEE Communications Magazine,* vol. 51, pp. 127-135, 2013.

[34] Y. Mostofi, D. C. Cox, and A. Bahai, "ICI mitigation for mobile OFDM receivers," in *IEEE International Conference on Communications, 2003. ICC'03.*, 2003, pp. 3351-3355.

[35] W. Saad, M. Bennis, and M. Chen, "A vision of 6G wireless systems: Applications, trends, technologies, and open research problems," *IEEE network,* vol. 34, pp. 134-142, 2019.

[36] !!! INVALID CITATION !!!

[37] Y.-C. Wang and Z.-Q. Luo, "Optimized iterative clipping and filtering for PAPR reduction of OFDM signals," *IEEE Transactions on communications,* vol. 59, pp. 33-37, 2010.

[38] B. Farhang-Boroujeny, "OFDM versus filter bank multicarrier," *IEEE signal processing magazine,* vol. 28, pp. 92-112, 2011.

[39] B. D. Tensubam and S. Singh, "A review on FBMC: An efficient multicarrier modulation system," *International Journal of Computer Applications,* vol. 98, 2014.

[40] J. Zhang, M. Xu, J. Wang, F. Lu, L. Cheng, H. Cho*, et al.*, "Full-duplex quasi-gapless carrier aggregation using FBMC in centralized radio-over-fiber heterogeneous networks," *Journal of Lightwave Technology,* vol. 35, pp. 989-996, 2017.

[41] R. S. Yarrabothu and L. I. Pasala, "Performance Analysis of 5G Waveform-Pruned DFT Spread FBMC with Real Time Fading Conditions," in *2019 25th Asia-Pacific Conference on Communications (APCC)*, 2019, pp. 136-141.

[42] J. G. D. Forney and R. G. Gallager, "Signal structures for double side band-quadrature carrier modulation," ed: Google Patents, 1975.

[43] H.-H. Lu, "CSO/CTB performances improvement by using optical VSB modulation technique," *IEEE Photonics Technology Letters,* vol. 14, pp. 1478-1480, 2002.

[44] I. H. Choi, Y. M. Gu, K. W. Kang, and K. Y. Kwak, "VSB transmission system," ed: Google Patents, 2008.

[45] D. J. Higham and N. J. Higham, *MATLAB guide*: SIAM, 2016.

[46] A. Doufexi, S. Armour, M. Butler, A. Nix, D. Bull, J. McGeehan*, et al.*, "A comparison of the HIPERLAN/2 and IEEE 802.11 a wireless LAN standards," *IEEE Communications magazine,* vol. 40, pp. 172-180, 2002.

[47] E. Kreyszig, K. Stroud, and G. Stephenson, "Advanced engineering mathematics," *Integration,* vol. 9, p. 4, 2008.

[48] Manjit Sandhu, Jaipreet Kaur, and Hardeep Kaur. Comparison of ber in the ofdm system for various digital modulation schemes.International Journal of Advanced Research in Electronics and Communication Engineering, 5(4), 2016.